

# Investigation of Unsteady Flow Conditions at Dam Bottom Outlet Works Due to Air Entrainment During Gate Closure

## VOLUME I: PHYSICAL MODELLING

Eddie Bosman & Gerrit Basson (Editors)



TT 528/12

# INVESTIGATION OF UNSTEADY FLOW CONDITIONS AT DAM BOTTOM OUTLET WORKS DUE TO AIR ENTRAINMENT DURING GATE CLOSURE

## Volume I: Physical Modelling

EDDIE BOSMAN & GERRIT BASSON (Editors)



Report to the  
**Water Research Commission**

by  
Institute for Water and Environmental Engineering  
Department of Civil Engineering  
University of Stellenbosch

**WRC Report No. TT 528/12**  
**July 2012**

## **OBTAINABLE FROM**

Water Research Commission  
Private Bag X03  
Gezina, 0031  
Republic of South Africa

[orders@wrc.org.za](mailto:orders@wrc.org.za) or download from [www.wrc.org.za](http://www.wrc.org.za)

The publication of this report emanates from a project entitled *Hydraulic Testing of the Outlet Works of the Berg River Dam* (WRC Project No. K5/1914//1).

This report forms part of a series of two reports. The other report in the series is *Investigation of unsteady flow conditions at dam bottom outlet works due to air entrance during gate closure: Computational Modelling*. (WRC Report No. TT 529/12)

### **DISCLAIMER**

This report has been reviewed by the Water Research Commission (WRC) and approved for publication. Approval does not signify that the contents necessarily reflect the views and policies of the WRC, nor does mention of trade names or commercial products constitute endorsement or recommendation for use.

**ISBN 978-1-4312-0286-7**  
**Set No. 978-1-4312-0288-1**  
**Printed in the Republic of South Africa**

**© WATER RESEARCH COMMISSION**

## SYNOPSIS

The Berg River Dam is equipped with the first multi-level draw off environmental flood release outlet in South Africa and can release flows of up to 200 m<sup>3</sup>/s. The outlet is controlled by a radial gate and is protected by a vertical emergency gate. Commissioning tests of the emergency gate in 2008 found that large volumes of air were expelled from the air supply shaft designed to reduce expected negative pressures in the conduit during emergency gate closure.

In 2009 Stellenbosch University was first commissioned by the WRC to investigate this phenomenon. The 2009 study, comprising of tests on a 1:40 scale physical model and a two-dimensional numerical computational fluid dynamics (CFD) analysis, was inconclusive on the cause of the large air releases. This report (Volume I) covers subsequent study using a 1:14.066 scale physical model. The accompanying Volume II covers a study using three-dimensional CFD analyses.

Simulations of continuous gate closure on the as-built physical model of the Berg River Dam outlet showed predominant inflow of air into the airshaft during emergency gate closure with short high speed air releases while the emergency gate was between 35% and 25% open. The problem was determined to be one of air blowback in the air shaft rather than continuous air release.

The cause of the blowback was found to be the constriction of flow at the radial gate chamber.

A number of modified model configurations were tested and recommendations were made for future design. The most crucial of these is that flow in high headed outlets should not be constricted.



## ACKNOWLEDGEMENTS

The research in this report emanated from a project funded by the SA Water Research Commission entitled:

### INVESTIGATION OF UNSTEADY FLOW CONDITIONS AT DAM BOTTOM OUTLET WORKS DUE TO AIR ENTRAINMENT DURING GATE CLOSURE

The Reference Group responsible for this project consisted of the following persons:

Mr W Nomquphu	WRC (chairperson)
Mr L Furstenburg	Knight Piésold
Mr S Malan	Goba/BRC
Prof G Pegram	University KwaZulu-Natal
Dr P Roberts	SANCOLD/Consultant
Dr M Shand	Aurecon
Mr T Tente	TCTA
Dr P Wessels	DWA

The following persons also attended a Reference Group meeting and contributed towards a better understanding of what happened during the 2008 commissioning tests at Berg River Dam:

Mr R Fraser	Aurecon/BRC
Mr J Metcalf	Goba
Mr L Mills	Knight Piésold /BRC

The financing of the project by the Water Research Commission and TCTA, and the contribution of the members of the Reference Group are gratefully acknowledged.

This report was edited by Mr Eddie Bosman and Prof Gerrit Basson of the University of Stellenbosch.

Co-authors of this report were Ms R Kime and Ms A Vos of the University of Stellenbosch. Co-workers on this project, all from the University of Stellenbosch, were Ms D Pulle, Mr J Calitz, Mr W Kamish, Mr H Schwedhelm, Ms L Schulze, Mr D van den Heever and Mr C Visser.

## TABLE OF CONTENTS

<b>Synopsis.....</b>	<b>iii</b>
<b>Acknowledgements.....</b>	<b>iv</b>
<b>Table of Contents .....</b>	<b>v</b>
<b>List of Figures .....</b>	<b>viii</b>
<b>List of Tables .....</b>	<b>x</b>
<b>List of Abbreviations .....</b>	<b>xi</b>
<b>1. Introduction .....</b>	<b>1</b>
1.1 Berg Water Project.....	1
1.2 Berg River Dam .....	1
1.3 Background to the Project.....	5
1.4 Report Outline.....	6
<b>2. Objectives and Scope of Physical Model Study.....</b>	<b>8</b>
2.1 Objectives .....	8
2.2 Extent of Model Study .....	8
<b>3. Literature Study.....</b>	<b>9</b>
3.1 Model Scale Effects .....	9
3.1.1 Introduction .....	9
3.1.2 Hydraulic Similarity.....	9
3.1.3 Conformance with Similarity Laws .....	12
3.1.4 Governing Similarity Law of the Berg River Dam Model .....	18
3.2 Cavitation .....	18
3.3 Bottom Outlet Conduits.....	19
3.3.1 Introduction .....	19
3.3.2 The Need for Air Vents.....	20
3.3.3 Flow Under Gates .....	21
3.3.4 Air Entrainment .....	28
3.3.5 Functions and Features of Air Vents.....	34
3.3.6 Air Demand ( $\beta$ ).....	35
3.3.7 Recent Studies.....	44
3.3.8 Air Vent Dimensioning.....	45
<b>4. Physical Model of the Berg River Dam Outlet .....</b>	<b>50</b>

---

4.1	General Description .....	50
4.2	Model Scale .....	52
4.3	Parameters Recorded and Instruments Used.....	53
4.3.1	Pressure Measurements .....	54
4.3.2	Air Velocity Measurements and Direction Indicator .....	55
4.3.3	Water Discharge Measurements.....	55
4.4	Experimental Controls.....	56
4.4.1	Water Supply.....	56
4.4.2	Water Levels .....	56
4.4.3	Selector Gates .....	57
4.4.4	Emergency Gate .....	57
4.4.5	Radial Gate .....	58
4.5	Experimental Procedure .....	58
4.5.1	Stationary Emergency Gate Opening Simulations.....	58
4.5.2	Transient Gate Closing Simulations.....	59
4.5.3	Vortex Formation Test with 100% Open Gate .....	61
<b>5.</b>	<b>Results .....</b>	<b>62</b>
5.1	Air Flow Recordings from Commissioning Test on As-built Prototype .....	62
5.2	As-Built Outlet.....	63
5.2.1	Stationary Emergency Gate Opening Tests.....	63
5.2.2	Continuously Closing Emergency Gate Tests.....	65
5.2.3	Vortex Formation Test.....	72
5.2.4	Conclusions from Tests on As-built Model of Outlet .....	72
5.3	Modified Model Configurations.....	73
5.3.1	Removal of Ski Jump and Second Bend.....	74
5.3.2	Removal of the Radial Gate Chamber .....	75
5.3.3	Provision of Extra Air Vent at the Radial Gate Constriction .....	77
5.3.4	Conclusions from Tests on Modified Model Configurations .....	79
<b>6.</b>	<b>Further Discussion of Results .....</b>	<b>80</b>
6.1	Air Blowback .....	80
6.2	Comment on Air Transient Pressures Waves in Conduit .....	80
6.3	Air Demand (Aeration Ratio) .....	81
<b>7.</b>	<b>Conclusions.....</b>	<b>82</b>
<b>8.</b>	<b>Recommendations .....</b>	<b>83</b>
8.1	Configuration.....	83
8.2	Berg River Dam Operation.....	84

---

8.3 Further Studies .....	85
<b>9. Guidelines for the Design of Future Bottom Outlets .....</b>	<b>86</b>
<b>10. References.....</b>	<b>87</b>
<i>Appendix A: As-Built Drawings of Berg River Dam Outlet Works .....</i>	<i>90</i>
<i>Appendix B: Commissioning Test on Berg River Dam – June 2008.....</i>	<i>100</i>
<i>Appendix C1: Photos of the 1:14.066 Berg River Dam Model .....</i>	<i>106</i>
<i>Appendix C2: Photos of the Berg River Dam (Prototype).....</i>	<i>111</i>
<i>Appendix D: Air Velocity Graphs .....</i>	<i>117</i>
<i>Appendix E: Pressure Graphs.....</i>	<i>124</i>
<i>Appendix F: Stage Discharge Curve.....</i>	<i>149</i>
<i>Appendix G: Extra Test Results .....</i>	<i>151</i>
<i>Test 1: Radial Gate Test.....</i>	<i>152</i>
<i>Test 2: Vortex Formation Test .....</i>	<i>156</i>
<i>Test 3: Extra Air Vent.....</i>	<i>161</i>



## LIST OF FIGURES

Figure 1-1: Scheme layout .....	2
Figure 1-2: Berg River Dam .....	2
Figure 1-3: Cross-section of Berg River Dam intake tower (a) and outlet structure (b) .....	4
Figure 1-4: Commissioning test of 2008.....	5
Figure 3-1: Hydraulic configuration of bottom outlet.....	19
Figure 3-2: Origin of aeration .....	22
Figure 3-3: Classification of flow types in bottom outlets without bottom aerators .....	23
Figure 3-4: Definition sketch for free flow .....	25
Figure 3-5: Coefficient of discharge for free and submerged flow under a vertical gate .....	27
Figure 3-6: Photos of Vortices ( (Rindles & Gulliver, 1983).....	28
Figure 3-7: Gordon's curve of minimum submergence (USACE, 1980) .....	29
Figure 3-8: Vertical structure of highly turbulent flows (Falvey, 1980) .....	30
Figure 3-9: Numerical model output showing air entrainment at a hydraulic jump (the colours indicate volume fraction of air) (Hirt, 2003) .....	31
Figure 3-10: Airflow above a water surface.....	31
Figure 3-11: Bubble motion in closed conduits flowing full (Falvey, 1980).....	32
Figure 3-12: Long section of Owyhee Dam outlet (Lowe, 1944) .....	33
Figure 3-13: Outlet at Rangipo Hydropower Station, 300 mm extra vent proposed as preventative measure for future blowback (Webby, 2003) .....	34
Figure 3-14: Schematic layout of parameters influencing air entrainment .....	36
Figure 3-15: $(1+\beta)$ versus $(A_0/A_T)$ for different Froude numbers.....	40
Figure 3-16: Comparison between the various calculation formulas.....	42
Figure 3-17: Air demand versus gate opening ( $G_O$ ) (Sharma, 1976) .....	43
Figure 3-18: Comparison of measured aeration versus gate opening with 3D numerical model and two empirical equations .....	44
Figure 4-1: Photograph of Physical Model .....	50
Figure 4-2: Line sketch of physical model layout (prototype dimensions given) .....	51
Figure 4-3: Location of Measuring Instruments in the Model .....	53
Figure 4-4: Top view of water tank.....	56
Figure 4-5: Model inlet pipe and valves.....	57
Figure 5-1: Air Velocity versus Gate Opening for Commissioning Test on Berg River Dam Prototype .....	62

---

Figure 5-2: Flow Patterns at the End of an Air Shaft.....	63
Figure 5-3: Air velocity versus Gate Opening for Stationary Gate Openings .....	64
Figure 5-4: Pressure versus Gate Opening for Stationary Gate Openings .....	64
Figure 5-5: Air Velocity versus Gate Opening for Closing Gate Simulations at the Commissioning Water Level.....	66
Figure 5-6: Pressure versus Gate Opening for Simulation of 20 minute Closure at the Commissioning Water Level.....	66
Figure 5-7: Air Velocity versus Gate Opening for Closing Gate Simulations at the Full Supply Water Level .....	67
Figure 5-8: Pressure versus Gate Opening for Simulation of 20 minute Closure at the Full Supply Level.....	68
Figure 5-9: Air Velocity versus Gate Opening for Closing Gate Simulations at the Lower Water Level .....	68
Figure 5-10: Pressure versus Gate Opening for Simulation of 20 minute Closure at the Lower Water Level .....	69
Figure 5-11: Sketches of Flow Patterns for Closing Gate Simulations.....	71
Figure 5-12: Modified Model Configurations .....	74
Figure 5-13: Air Velocity versus Gate Opening for Tests on Conduit with Ski-jump and Radial Gate Chamber Removed (Modification 4).....	76
Figure 5-14: Pressure versus Gate Opening for Tests on Conduit with Ski-jump and Radial Gate Chamber Removed (Modification 4).....	76
Figure 5-15: Sketches of Flow Patterns for As-Built Conduit and Modified Conduit with Radial Gate and Ski-jump Removed .....	77
Figure 5-16: Extra Air Vent Configuration Tested .....	78
Figure 5-17: Examples of Other Possible Configurations for an Extra Air Vent .....	78
Figure 6-1: Aeration Ratio ( $\beta$ ) versus Gate Opening.....	81
Figure 8-1: Possible radial gate configuration to prevent blowback .....	83
Figure 8-2: Failed radial gate chamber .....	84

**LIST OF TABLES**

Table 3-1: Scalar Relationships for Models (Reynolds & Froude laws) .....16

Table 3-2: K-coefficients.....39

Table 4-1: Pressure Transducers.....54

Table 4-2: Water Levels .....60

Table 5-1: Description of Flow Patterns for Closing Gate Simulations.....70

## LIST OF ABBREVIATIONS

A	Area ( $\text{m}^2$ )
B	Gate width (m)
BWP	Berg Water Project
CFD	Computational fluid dynamics
D	Conduit diameter or height
DWA	Department of Water Affairs
$F_r$	Froude number
$Fr_c$	Froude number at vena contracta
g	Gravitational constant ( $\text{m/s}^2$ )
G	Percentage of gate opening
h	Full size of gate opening
Hz	Hertz
km	Kilometre
L	Tunnel length
m	Metre
$\text{m}^2$	Metre square
mA	Milli-ampere
masl	Meters above sea level
mm	Millimetre
p	Prototype
$Q_a$	Air flow ( $\text{m}^3/\text{s}$ )
$Q_w$	Water flow ( $\text{m}^3/\text{s}$ )
$Re$	Reynolds number
s	Seconds
T	Top width of flow passage (m)
TCTA	Trans-Caledon Tunnel Authority
V	Mean flow velocity (m/s)
V	Volt
$\nu$	Kinematic viscosity of water
$W_e$	Webber number
y	Flow depth
$y_e$	Effective flow depth (m)
$\beta$	Air demand ratio
$\Omega$	Ohm
$\gamma_w$	Water specific weight



$\Delta P$	Sub-atmospheric pressure after gate
$\rho_w$	Water density

# 1. INTRODUCTION

## 1.1 Berg Water Project

Water is of critical importance to protect and maintain healthy ecosystems, as well as to provide for basic human needs. It also supports South Africa's mines, power generation and industries, and it is used for recreational purposes. Water is the key to development and a good quality of life.

The Berg Water Project (BWP) is the result of a 14-year strategic integrated planning process carried out by the Department of Water Affairs (DWA) to identify suitable measures to address the increasing water demand in the Greater Cape Town region. The BWP includes the Berg River Dam (previously known as the Skuifraam Dam) and supplement scheme. The supplement scheme pumps a portion of the winter high flows from downstream tributaries back into the Berg River Dam to augment the water from the Berg River as an additional water supply to the Greater Cape Town region and to supply environmental requirements. The Berg River Dam is situated in the La Motte plantation, about 6 km west of Franschhoek, and the supplement scheme is located approximately 10 km downstream of the dam (TCTA, 2008).

## 1.2 Berg River Dam

The Berg River Dam on the Berg River forms the major part of the Berg Water Project. The dam is operational alongside the Theewaterskloof Dam, situated in the Breede River catchment. The Riviersonderend inter-basin transfer tunnel, constructed through the Franschhoek Mountain range, links the two dams to provide water to the Greater Cape Town area (**Figure 1-1**) (TCTA, 2008).

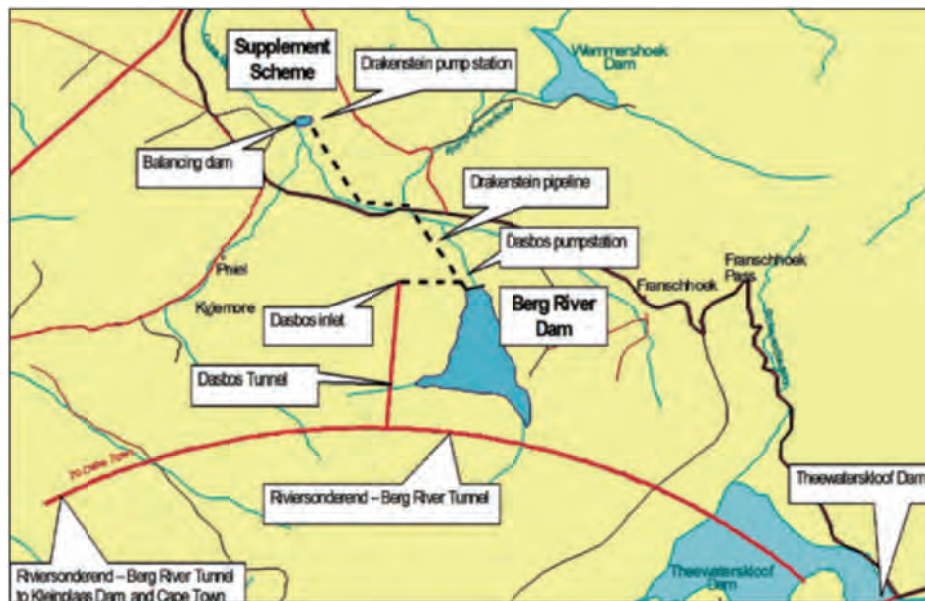


**Figure 1-1: Scheme layout**

The Berg River Dam is a concrete-faced rockfill embankment, approximately 65 m high and 990 m wide, with a base width of 220 m, and is shown in **Figure 1-2** (TCTA, 2008). It has a gross storage capacity of 130 million m<sup>3</sup>.



**Figure 1-2: Berg River Dam**

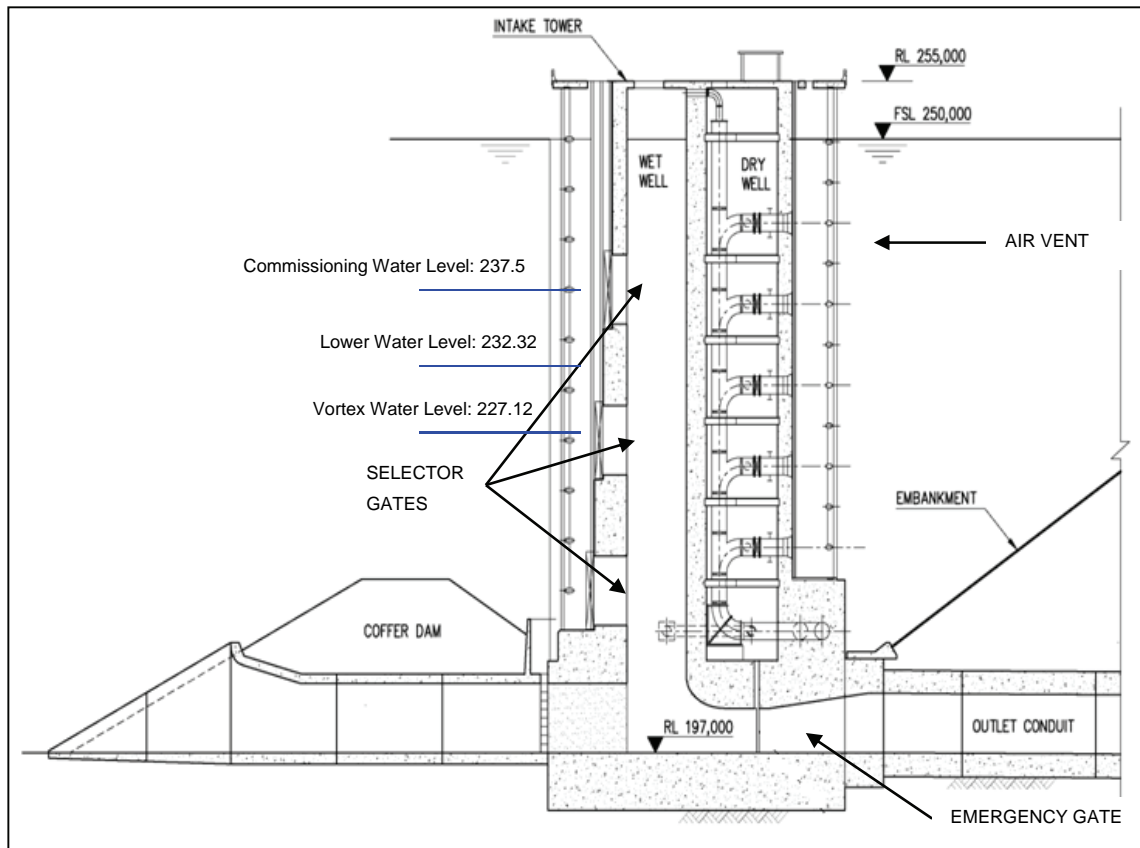
The Berg River Dam is the first of its kind in South Africa, comprising structures that permit the release of both low and high flows, the latter up to  $200 \text{ m}^3/\text{s}$ . The Ecological Reserve water release, downstream of the dam, had been determined beforehand for the BWP, which ensures that the aquatic ecosystems downstream of the dam are protected. This reserve prescribes low and high flow releases, as well as the quality of the water released (TCTA, 2006).

The Berg River Dam was designed to inter alia cater for the Ecological Reserve, and this is made possible by the intake tower (Figure 1.3). The intake tower is divided into a north and south section. The north section is a dry well equipped with multi-level inlets, pipes and valves, which enable the facilities for extracting water from the dam into the supply system to the Greater Cape Town region, as well as making provision for low flow environmental releases (less than  $12 \text{ m}^3/\text{s}$ ). The southern section of the intake tower is an open vertical wet well with multi-level gates designed to draw water from the dam for high flows, which imitate the occurrence of natural flood events (up to  $200 \text{ m}^3/\text{s}$ ). The wet well is connected to the concrete bottom outlet underneath the dam embankment. This system, for releasing high floods, is a requirement of the Ecological Reserve and is unique to the Berg River Dam. Surplus water spills over the 40 m side spillway with modified Roberts splitters and flows down the concrete chute to the ski-jump (TCTA, 2006). **Figure 1-3** shows a cross-sectional view of the intake tower of the Berg River Dam.

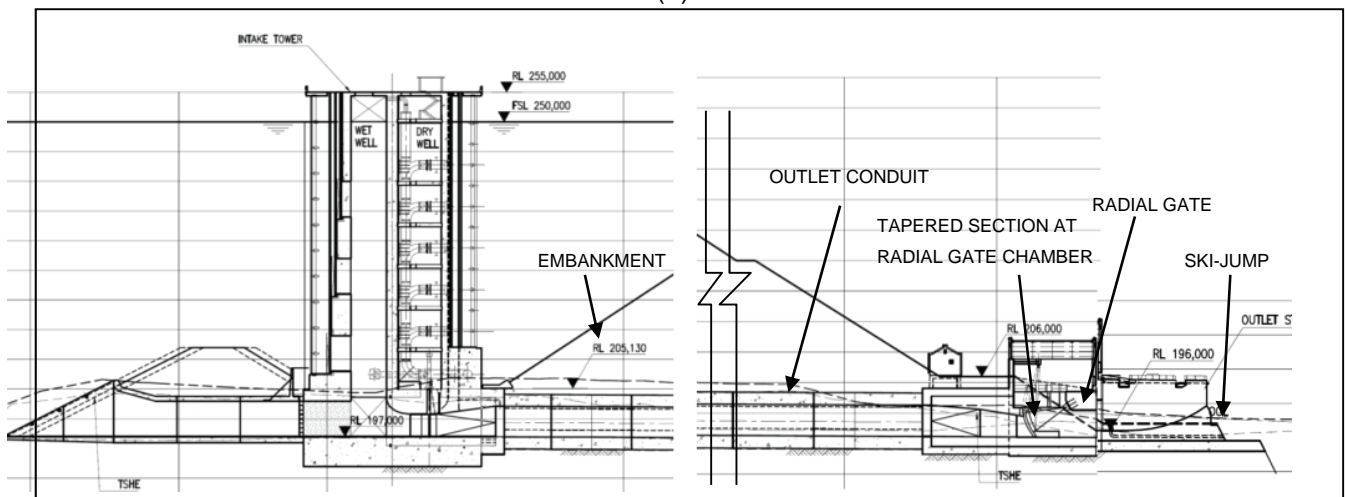
The outflow for the environmental flood release is controlled by a radial gate at the end of the outlet conduit. If this gate should fail, the dam would empty, giving rise to hazardous conditions as a result of downstream river bank erosion. An emergency gate therefore is provided that can close under its own weight if the radial gate fails. The design speed of this closure is 12 minutes (Van Vuuren, 2003).

The Berg River Dam and its appurtenant structures were the first large water resource infrastructure project in South Africa to be subjected to the National Water Act of 1998 (Act 36) and the World Commission on Dams (WCD) Report of 2000 (Abban et al., 2008). It is anticipated that a prerequisite for future dam-related projects in South Africa will be that they have to make provision for ecological or environmental flow releases to maintain the integrity of the rivers and to ensure a healthy ecosystem. Therefore it is fundamental that lessons learned from the BWP are shared with the engineering industry.





(a)



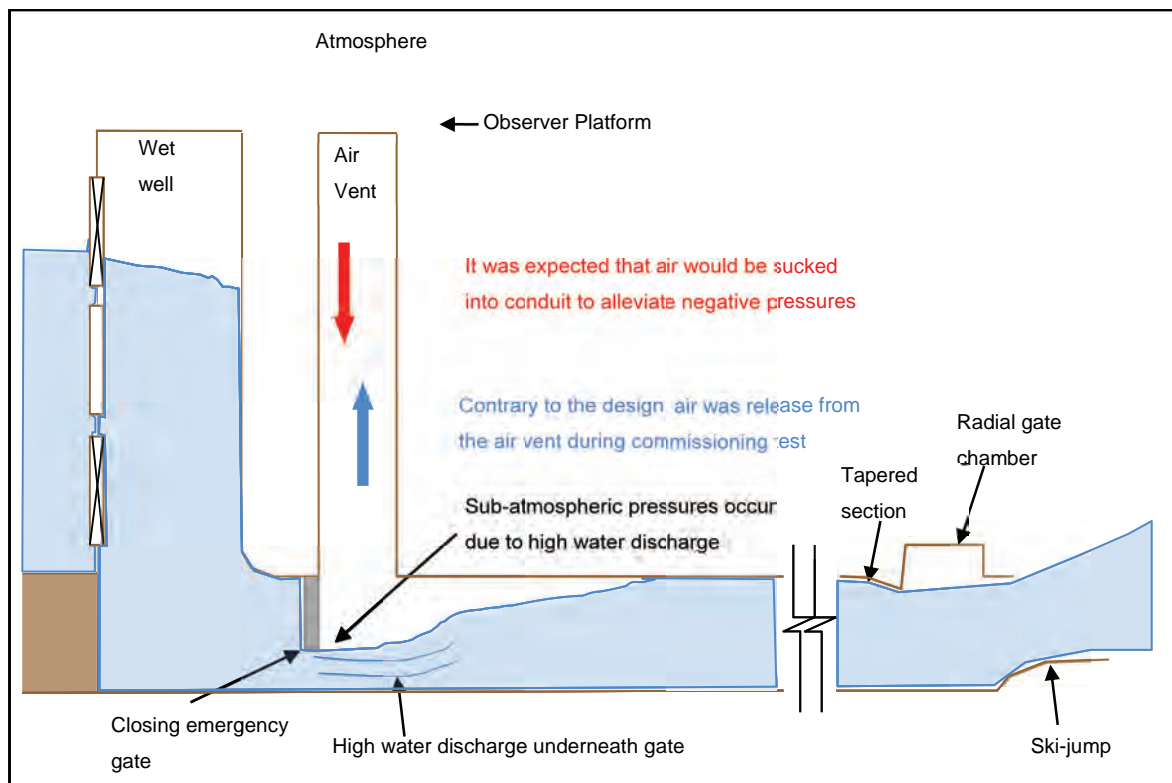
(b)

**Figure 1-3: Cross-section of Berg River Dam intake tower (a) and outlet structure (b)**

### 1.3 Background to the Project

Commissioning closure of the emergency gate **Figure 1-4** of the Berg River Dam was undertaken by the TCTA on 12 June 2008. An air shaft, downstream of the emergency gate was designed to introduce air downstream of the gate to counteract the negative pressures that were expected in the conduit during emergency gate operations. Contrary to the theoretical design, manual field observations during commissioning indicated that, while the emergency gate was closing, very large volumes of air were released in a surging manner from the 1.8 m<sup>2</sup> air shaft, commencing when the gate was about 30% closed (i.e. 70% open), (refer to **Appendix B** for a report on the record of the manual observations during the commissioning test on the Berg River Dam in June 2008).

The 1.8 m<sup>2</sup> Mentis grid cover on top of the shaft was blown off and lifted to a height of about 3 to 4 m, tipping the observer off the shaft top and against the upstream concrete wall.



In this thesis the full-scale structure under investigation is referred to as the prototype (p), and the smaller version of the prototype as the model (m). In 2003 a 1:18.966 scale model of the

Berg River Dam was tested by Sinotech in Pretoria, and this test formed part of the detailed design process of the BWP. The study was specifically carried out to test the bottom outlet and concluded that air would be drawn down the shaft and that no visible vortex formed at the intake in the reservoir. Emergency gate operations/ closure were not simulated, since, as it was accepted that air would be drawn into the air vent to alleviate the negative pressures that form downstream of the gate (Van Vuuren, 2003).

Guidelines for the design and operation of bottom outlet works with emergency gate closure were investigated, analysed and developed by the University of Stellenbosch in 2009. This project was commissioned by the South African Water Research Commission (WRC), who appointed the University of Stellenbosch to undertake the work. The University initially investigated the air vent operation by means of a physical 1:40 scale model (originally used for the 2003 detailed design of the outlet works) and a two-dimensional computational fluid dynamics (CFD) analysis. The study provided inconclusive results regarding air release from the air vent, as observed during the June 2008 commissioning test. The study concluded that the flow of air through the air vent and the potential for formation of vortices at the intake shaft on the physical model would not be as proficient as they would be in the prototype and, hence, that the entrainment of air could not be analysed accurately on the 1:40 scale model, as the model was too small. It also concluded that a three-dimensional CFD analysis would be required for reliable computer simulation of the problem.

In this study a 1:14.066 (undistorted scale) physical model of the outlet works and air shaft of the Berg River Dam was constructed and 3 dimensional CFD model was created.

## 1.4 Report Outline

The physical modelling aspects of this study are covered in **Volume I**, and the computational modelling aspects are covered in **Volume II**.

The objective and scope of the physical and computational components of the study are given in Chapter 2 of Volume I and II respectively.

All the literature review is contained in **Volume I** (Chapter 3), while background to computational fluid dynamics (CFD) modelling of flows is given in Chapter 3 of **Volume II**.

**Volume I** further contains the physical model setup and measuring equipment (Chapter 4), the methodology used to analyse water and air flow conditions during gate closure (Chapter 5), the results (Chapter 6) and an evaluation thereof (Chapter 7), and conclusions from the physical model study (Chapter 8). The Volume ends with design guidelines and recommendations in Chapter 9.

The computational modelling part, covered in **Volume II**, consists of two consecutive studies or stages. Chapters 4 to 6 cover the first stage which involves simulation of static gate openings with steady-state solutions, and Chapters 7 to 11 cover the second stage in which the model was modified to simulate a continuously closing gate. Final conclusions and recommendations are made in Chapter 12.



## 2. OBJECTIVES AND SCOPE OF PHYSICAL MODEL STUDY

### 2.1 Objectives

The objectives of the model study were as follows:

- Determine reasons for the release of very large volumes and fluctuating positive and negative air flow from the air vent shaft, as observed during the commissioning test closure of the emergency gate on 12 June 2008.
- Provide a solution to mitigate the excessive airflow.

### 2.2 Extent of Model Study

The physical model included a distance of 101.51 m (prototype) upstream of the emergency gate to 214.58 m (prototype) downstream of the emergency gate. This incorporated the wet well, the bottom outlet conduit, the emergency gate chamber, the air vent, the radial gate chamber and the ski-jump. The total length of the model was 316.09 m (prototype length). The scale of the model was 1:14.066.

**It should be noted that the parameters recorded in the model study and presented in this report has been transformed to reflect the values as would have been observed in the prototype, unless stated otherwise.** Elevations of both the prototype and the model were reduced to meters above sea level (masl).

## 3. LITERATURE STUDY

### 3.1 Model Scale Effects

#### 3.1.1 Introduction

In various aspects of engineering, physical models can often prove to be more efficient than computer or numerical analysis to solve fluid hydraulic problems, due to the intricate characteristics of the physics and boundaries of the flow. Under these circumstances, laboratory-controlled models provide an advantage and give proven accurate results (Webber, Fluid Mechanics for Civil Engineers, S.I. Edition, 1971).

It is critical that the model must accurately represent the behaviour of the prototype, which requires that the layout of the prototype should be modelled correctly. It is essential that the phenomenon to be studied are understood clearly so that the results from the model are interpreted correctly. The *laws of hydraulic similarity* govern the relationship between the prototype and the performance of the model. Simultaneous compliance with all the laws is impossible, thus some discrepancies are inevitable when extrapolating the results from the model to the full scale, which is known as scale effects. The scale effects can be minimised by ensuring that the model is large enough, or by taking necessary compensatory steps (Webber, Fluid Mechanics for Civil Engineers, S.I. Edition, 1971).

The expected performance of the prototype can be verified with hydraulic models. Models indicate the necessary modifications to the design, which saves a significant amount of construction cost and usually depicts the best design from an economical point of view.

#### 3.1.2 Hydraulic Similarity

The behaviour of the model under examination must be sufficiently similar to the behaviour of the prototype for accurate prototype conditions to be obtained. The two flow systems must be hydraulically similar in order to transfer the results from the model to the prototype. This entails that geometric similarity of boundaries be retained and that dynamic and kinematic similarity be established by assuring that the forces having an impact on the motion of the water particles in the model and prototype be of constant ratio to each other.

Thus, the water particles in the model and prototype must flow in similar geometrical patterns in proportional times (USACE, 1980).

### 3.1.2.1 Geometric Similarity

Geometric similarity indicates similarity of shape and is obtained if the model is constructed in an undistorted manner according to the linear scale adopted. This is achieved if the ratio of any two dimensions of the model is the same as the corresponding ratio of the prototype. The scale ratio can be expressed as follows (USACE, 1980):

$$\frac{(L_1)_m}{(L_2)_m} = \frac{(L_1)_p}{(L_2)_p}$$

**Equation 3.1**

where

$L_m$ : linear dimensions of the undistorted model (m)

$L_p$ : linear dimensions of the prototype (m)

The area and volume ratios are the square and cube of the linear scale ratio respectively. Therefore, if the scale of the linear model is 1:x, then the scalar relationship for the area and volume can be represented as 1:x<sup>2</sup> and 1:x<sup>3</sup> respectively (USACE, 1980).

To obtain complete geometric similarity, the boundary roughness of the model and prototype should have a corresponding ratio. If  $k$  is defined as the sand grain diameter, the scalar roughness ratio  $k_m:k_p$  at corresponding positions on the surface of the model and prototype must be 1:x. The reproduction of the boundary roughness to this high level of conformity is not always possible, because of the irregular nature of the material finishes (Webber, Fluid Mechanics for Civil Engineers, S.I. Edition, 1971). In prototypes with boundaries with smooth surfaces (e.g. well-finished concrete or metal) it is impossible to achieve the additional degree of smoothness required for the surface of the model.

Bearing in mind the discrepancies in geometric similarity as described above, it should be remembered that it is most important that the hydraulic behaviour of the flow arising from the boundary conditions is of a similar ratio for the model and the prototype. Therefore, some geometric dissimilarity is unavoidable and tolerable (Webber, Fluid Mechanics for Civil Engineers, S.I. Edition, 1971).

### 3.1.2.2 Kinematic Similarity

Fulfilment of the requirements of kinematic similarity requires a consideration of the motion of the fluid. Kinematic similarity is satisfied if the velocities and acceleration at congruent points at congruent times in the both systems have the same ratio. The homologous direction of the motion in the two systems must also be the same. The ratio to comply with kinematic similarity is given by the following formula (Webber, Fluid Mechanics for Civil Engineers, S.I. Edition, 1971):

$$\frac{(v_1)_m}{(v_2)_m} = \frac{(v_1)_p}{(v_2)_p} \text{ and } \frac{(a_1)_m}{(a_2)_m} = \frac{(a_1)_p}{(a_2)_p}$$

**Equation 3.2**

where

$v_m$ : velocity of fluid in model (m/s)

$v_p$ : velocity of fluid in prototype (m/s)

$a_m$ : acceleration of fluid in model (m/s<sup>2</sup>)

$a_p$ : acceleration of fluid in prototype (m/s<sup>2</sup>)

It must be noted that geometric similarity of the surface boundaries is an important prerequisite to obtain similar flow patterns in order to achieve kinetic similarity.

### 3.1.2.3 Dynamic Similarity

The forces capable of influencing the motion of the fluid at homologous points in the model and prototype system must have the same ratio and act in the same direction to achieve dynamic similarity. The ratio to comply with dynamic similarity is given by the following formula (Webber, Fluid Mechanics for Civil Engineers, S.I. Edition, 1971):

$$\frac{(F_1)_m}{(F_2)_m} = \frac{(F_1)_p}{(F_2)_p}$$

### Equation 3.3

where

$F_m$ : forces acting on fluid in the model (kN)

$F_p$ : forces acting on fluid in the prototype (kN)

The forces acting on the fluid in both systems are gravity, surface tension, elasticity and fluid viscosity. The regime of the flow can be defined by dimensionless numbers known as Froude (gravity), Reynolds (viscosity), Webber (surface tension) and Euler (elasticity), which are specific combinations of the abovementioned forces. The regime of the flow is governed by the forces acting on the fluid particles, consequently geometric and kinematic similarity must also be obtained if dynamic similarity must exist throughout the two systems (Webber, Fluid Mechanics for Civil Engineers, S.I. Edition, 1971).

### 3.1.3 Conformance with Similarity Laws

The connotations of the various similarity laws as discussed in Section 3.1.2 are as follows:

#### 3.1.3.1 Euler's Law

The basic relationship between velocity ( $V$ ) and pressure ( $p$ ) is depicted by the Euler equation ( $E = V/\sqrt{2\Delta p/\rho}$ ) [Equation 3.4]. The Euler number is of particular significance in enclosed fluid system models where the turbulence of the fluid is fully developed, resulting in the viscous forces being irrelevant in relation to inertia forces acting on the fluid particles. Evidently, gravity and surface tension forces are completely absent. Thus, the applied pressure forces are the controlling factor and act as an independent variable. However, this is contrary to most fluid phenomena, in which the pressure force is a dependent variable, as it is consequential upon the motion of the fluid (Webber, Fluid Mechanics for Civil Engineers, S.I. Edition, 1971).

Euler's Law can be integrated into the corresponding model and prototype velocities as follows (Webber, Fluid Mechanics for Civil Engineers, S.I. Edition, 1971):

$$\frac{V_p}{V_m} = \frac{\Delta p_p^{1/2}}{\Delta p_m^{1/2}} \times \frac{\rho_m^{1/2}}{\rho_p^{1/2}}$$

**Equation 3.5**

where

V: velocity (m/s)

p: pressure (kN/m<sup>2</sup>)

ρ: density (kg/litre)

It can be observed from the above equation that the relationship between the velocity and pressure is nonlinear and universally applicable whenever inertia forces are of great significance. The operating speed (or controlling pressure) will be within the researcher's judgment, provided that the model is large enough to ensure that all forces except pressure remains trivial (Webber, Fluid Mechanics for Civil Engineers, S.I. Edition, 1971).

### 3.1.3.2 Froude's Law

Gravity and inertia are the dominant forces that influence the motion of the fluid in systems where a free surface gradient is present, particularly those in open channels, spillways, weirs, rivers, etc. Dynamic similitude is achieved by designing the model according to Froude's Law. In other words, the Froude number in the model and prototype must be equal. The Froude number is defined as follows (USACE, 1980):

$$F_r = \frac{V}{\sqrt{gL}}$$

**Equation 3.6**

where

F<sub>r</sub>: Froude number (dimensionless)

V: velocity (m/s)

g: acceleration of gravity (9.81 m/s<sup>2</sup>)

L: characteristic linear dimension (m)

The corresponding velocities in the two systems must be of similar ratio to comply with Froude's Law (Webber, Fluid Mechanics for Civil Engineers, S.I. Edition, 1971)

$$\frac{V_p}{V_m} = \frac{(L_p)^{1/2}}{(L_m)^{1/2}} = x^{1/2}$$

**Equation 3.7**

Velocities that occur in models are less than those that occur in the prototype, which is beneficial, as improved measuring instruments are available in the laboratory, whereas pumping capacity is a limiting factor (Webber, Fluid Mechanics for Civil Engineers, S.I. Edition, 1971).

The discharge characteristics of models subjected to Froude's Law can generally be predicted within  $\pm 5\%$ , which is adequate for hydrometric purposes (Webber, Fluid Mechanics for Civil Engineers, S.I. Edition, 1971).

### 3.1.3.3 Reynolds Law

A real fluid has viscosity, therefore the potential influence of viscous shear drag on the fluid needs consideration. The Darcy-Weisbach coefficient as a function of the Reynolds number ( $Re$ ) is used to reproduce the conduit surface irregularities affecting the motion of the fluid.

According to the Reynolds law ( $Re = VL/\nu$ ) [**Equation 3.8**], the corresponding velocities in the model and prototype must be related as follows (Webber, Fluid Mechanics for Civil Engineers, S.I. Edition, 1971):

$$\frac{V_p}{V_m} = \frac{v_p L_m}{v_m L_p} = \frac{v_p}{v_m} \frac{1}{x}$$

**Equation 3.9**

where

$V$ : velocity (m/s)

$L$ : length of homologous sections in model and prototype (m)

$\nu$ : kinematic viscosity ( $m^2/s$ ) =  $1.13 \times 10^{-6} m^2/s$

The equation above indicates that, if the same fluid at the same temperature is utilised in both systems, the prototype velocity must be  $x$  times greater than that of the model (Webber, Fluid Mechanics for Civil Engineers, S.I. Edition, 1971).

Viscous forces are generally a secondary influence on the fluid in the prototype because of the low viscosity of water. They are, however, important considering their influence on boundary frictions and their role as the origin of turbulence in fluids (Webber, Fluid Mechanics for Civil Engineers, S.I. Edition, 1971).

The model and prototype cannot be satisfied by both Froude's and Reynolds' laws at the same time. Variation in the Reynolds number is not of great importance, provided that both the prototype and the model have high Reynolds numbers ( $Re > 100\,000$ ) and have similar roughness-to-diameter ratios. Under these conditions, the head loss will be a function of the square of the velocity in both systems. If the Reynolds number of the model approaches the transition zone where the flow changes from turbulent to laminar flow, laminar flow might occur in the model, whereas turbulent flow will occur in the prototype. This can be avoided by choosing a minimum Reynolds number where the model must be operated. Models of pipelines often operate in this "transition zone" category, where the energy grade line dictates the motion of the fluid and not the pipeline slope (Lewin, 2001).

Under full-scale conditions, the Reynolds number of the prototype will be greater than in the model, but the overall friction factor will be less. Consequently, for fluids other than water, the model conduit must be shortened from the length required to comply with geometric similarity in order to artificially reproduce the loss that will occur through the conduit (USACE, 1980).

The derived scalar relationships according to Froude's and Reynolds' laws are summarised in **Table 3-1** below.



**Table 3-1: Scalar Relationships for Models (Reynolds & Froude laws)**

Hydraulic Similarity	Quantity	Dimensions	Reynolds law	Froude law	
			Natural scale 1:x	Natural scale 1:x	Distorted scales 1:x horiz.; 1:y vert
Geometric	Length	L	x	x	x (horiz.) y (vert.)
	Area	L <sup>2</sup>	x <sup>2</sup>	x <sup>2</sup>	x <sup>2</sup> (plan) xy (sect.)
	Volume	L <sup>3</sup>	x <sup>3</sup>	x <sup>3</sup>	x <sup>2</sup> y
Kinematic	Time	T	x <sup>2</sup> /v <sub>r</sub>	x <sup>1/2</sup>	xy <sup>1/2</sup>
	Velocity	L/T	v <sub>r</sub> /x	x <sup>1/2</sup>	xy <sup>1/2</sup> (horiz.) y <sup>3/2</sup> /x (vert.)
	Acceleration	L/T <sup>2</sup>	v <sub>r</sub> <sup>2</sup> /x <sup>3</sup>	1	y/x (horiz.) y <sup>2</sup> /x <sup>2</sup> (vert.)
	Discharge	L <sup>3</sup> /T	v <sub>r</sub> x	x <sup>5/2</sup>	xy <sup>3/2</sup>
Dynamics	Pressure	M/LT <sup>2</sup>	ρ <sub>r</sub> v <sub>r</sub> <sup>2</sup> /x <sup>2</sup>	ρ <sub>r</sub> x	ρ <sub>r</sub> y (sect.)
	Force	M/LT <sup>2</sup>	ρ <sub>r</sub> v <sub>r</sub> <sup>2</sup>	ρ <sub>r</sub> x <sup>3</sup>	ρ <sub>r</sub> xy <sup>2</sup> (sect.)
	Energy	M <sup>2</sup> /LT <sup>2</sup>	ρ <sub>r</sub> v <sub>r</sub> <sup>2</sup> x	ρ <sub>r</sub> x <sup>4</sup>	ρ <sub>r</sub> xy <sup>3</sup> (sect.)
	Power	M <sup>2</sup> /LT <sup>3</sup>	ρ <sub>r</sub> v <sub>r</sub> <sup>3</sup> /x	ρ <sub>r</sub> x <sup>7/2</sup>	ρ <sub>r</sub> y <sup>7/2</sup> (sect.)

### 3.1.3.4 Weber's Law

Surface tension is only of importance when an air-water boundary exists and the linear dimensions of the model are small. However, it is of great importance to study the influence of surface tension on the fluid in models, with very low weir heads, air entrainment, spray or splash (Webber, Fluid Mechanics for Civil Engineers, S.I. Edition, 1971).

The corresponding velocities in the prototype and model must relate as follows to comply with Webber's Law ( $W = V/\sqrt{\sigma/L\rho}$ ) [Equation 3.10]:

$$\frac{V_p}{V_m} = \frac{\sigma_p^{1/2} \rho_m^{1/2} L_m^{1/2}}{\sigma_m^{1/2} \rho_p^{1/2} L_p^{1/2}} = \frac{\sigma_p^{1/2} \rho_m^{1/2}}{\sigma_m^{1/2} \rho_p^{1/2}} \frac{1}{x^{1/2}}$$

**Equation 3.11**

where

V: velocity (m/s)

L: length of homologous sections in model and prototype (m)

$\sigma$ : stress (kN/m<sup>2</sup>)

$\rho$ : density (kg/litre)

The above equation indicates that the velocity in the prototype will be  $x^{1/2}$  times greater than the velocity in the model.

Generally, surface tension has very little or no influence on the behaviour of fluid in the prototype. By ensuring that the model is large enough, the surface tension will still be insignificant at model scale, therefore it will be practical to abstain from complying with this law (Webber, Fluid Mechanics for Civil Engineers, S.I. Edition, 1971).

Sub-atmospheric pressures are another scalar discrepancy that requires attention. The model and prototype are both operated under atmospheric conditions, ensuring that pressures relative to atmospheric pressures are modelled to scale. On the contrary, absolute pressures are not reproduced to scale. The vaporisation of water is initiated when the pressure falls within a metre of absolute zero pressure. However, dissolved air is released from solution before this stage is reached. This phenomenon will occur at an earlier stage in the prototype than in the model, as pressures are lowered at the reduced scale. Judgement on the part of the modeller with regard to the interpretation of the results from the model is required to prevent incorrect predictions about the discontinuity of the flow and cavitation. Pressures of up to 5 m below atmospheric pressure are acceptable because a tolerable margin of dissimilarity of surface roughness, vorticity and/or turbulence may exist, which can create a temporary lowering of pressures in the prototype. Operating the model in a vacuum container is one solution to overcome the

pressure relationship problem, but this is not always feasible, as attendant experimental complications are unavoidable (Webber, Fluid Mechanics for Civil Engineers, S.I. Edition, 1971).

### 3.1.4 Governing Similarity Law of the Berg River Dam Model

A free surface gradient is present in the outlet conduit when the largest volumes of air are released from the air shaft when the emergency gate is about 40% to 30% open. Gravitational and inertial forces are thus the dominant forces that influence the motion of the fluid in the system, therefore the **Froude's Law** is the criterion.

In this model study the gravity and inertia forces are dominant. However, the accurate modelling of the two phase, air water flow require that viscosity and surface tension also be simulated. This implies that the Froude, Reynolds and Weber similarity laws would have to be fulfilled simultaneously. Therefore, if Froude law is used, the scale should be sufficiently large to minimise the scale effects due to not fulfilling the Reynolds and Weber laws.

According to Speerli (1991) a Froude-scale model of a bottom outlet should be larger than 1:20. Therefore a scale of 1:14 was selected for the Berg River model.

## 3.2 Cavitation

Given the high velocities and varying pressures in dam outlet structures, cavitation is a very common occurrence in their operation. Cavitation occurs whenever the pressure in the flow of water drops to the value of the pressure of the saturated water vapour and cavities filled by vapour, and partly by gases excluded from the water as a result of the low pressure are formed. When these 'bubbles' are carried by the water into regions of higher pressure, the vapour quickly condenses and the bubbles implode, the cavities being filled suddenly by the surrounding water. Not only is this process noisy with disruption in the flow pattern, but more importantly, if the cavity implodes against a surface, the violent impact of the water particles acting in quick succession at very high pressures, if sustained for long periods of time can cause substantial damage to the surface, which can lead to a complete failure in the structure. (Novak P. et al, 2007). Thus cavitation corrosion (pitting) and the often accompanying vibration is a phenomenon that has to be taken into account in the design of hydraulic structures, and prevented whenever possible. (Knapp, Daily and Hammit, 1970).

### 3.3 Bottom Outlet Conduits

#### 3.3.1 Introduction

Bottom outlets are used primarily for the emergency drawdown of reservoirs. They are also used for sediment flushing or to regulate the water level in the reservoir. In recent years, bottom outlets connected to multi-level intake towers have been designed for drawing water from the reservoir, as required by the Ecological Reserve downstream of dams.

A bottom outlet must be designed to cater for all the flow release systems for which it was planned. Generally, the system is designed with two control gates, the emergency gate, which is either open or closed, and the service gate, with a variable opening. **Figure 3-1** below illustrates the hydraulic configuration of a bottom outlet (Vischer & Hager, 1998).

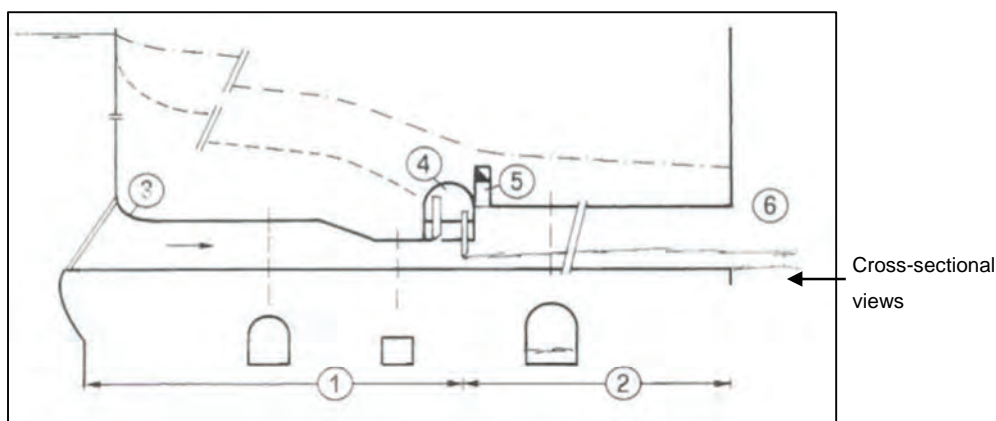


**Figure 3-1: Hydraulic configuration of bottom outlet**

- (---) pressure head line
- (-.-) energy head line
- (1): pressurised flow portion (submerged flow)
- (2): free surface flow portion
- (3): tunnel inlet
- (4): gate chamber
- (5): air supply
- (6): tunnel outlet

The bottom part of illustrates the cross-section of the outlet tunnel at specific sections.

It can be observed from that pressurised flow occurs upstream from the gate (1), and free surface flow occurs downstream from the gate (2). The water is accelerated to the tunnel velocity at the tunnel inlet (3). The cross-section contracts to a rectangular section just upstream of the gate chamber (4), with the aim to create the necessary backpressure and to accommodate the gates. An air vent (5) discharging air behind the gate chamber is required to supply air to achieve free surface flow under atmospheric pressure and to inhibit sub-atmospheric pressures in the conduit. To avoid the submergence of the gate chamber, the transition from pressurised to free surface flow must occur exactly behind the gate (Vischer & Hager, 1998).

Particular hydraulic problems with bottom outlets are cavitation, abrasion and aerated flow due to the high velocity ( $V$ ) at the outlet. The velocity at the bottom outlet is almost as high as the velocity obtained from the Torricelli formula,  $V = (2gH_0)^{1/2}$  [Equation 3.3.12], where  $H_0$  is the head on the outlet (m) and  $g$  the gravitational acceleration ( $m/s^2$ ). A bottom outlet must not be used permanently due to the hydraulic problems associated with cavitation, abrasion, vibrations, air entrainment, hydrodynamic forces, energy dissipation, vortex formation at intakes and erosion (Vischer & Hager, 1998).

### 3.3.2 The Need for Air Vents

High flow velocities occur downstream of a partially opened gate of a high-head outlet conduit, resulting in *sub-atmospheric* pressures along the bottom surface of the gate. These pressures can theoretically be as low as the vapour pressure of water, which causes structural damage due to destructive cavitation and vibration, and are therefore undesirable from an operating and structural point of view (Sharma, 1976). Cavitation occurs when flow velocities reach or exceed 13 to 15 m/s (Lewin, 2001). If the pressure behind the gate reduces to vapour pressure, water column separation and re-joining may occur, which leads to water hammer problems (Aydin, 2002). Therefore an air vent discharging air behind an emergency gate chamber (with relative high upstream head) is needed to inhibit sub-atmospheric pressures in the conduit. (Sharma, 1976).

No provision was made for air vents in the earlier high-head gate designs, which resulted in severe damage to the gates and conduits. The Pathfinder Dam in the USA was constructed in 1909 with four slide gates, each 1.1 m by 1.96 m. Hammering and echoing sounds were

heard when the dam was in operation. As the flow through the gates increased, the intensity of the sounds increased. At maximum discharge, the dam started to shake. After the conduit was closed, large masses of concrete and rock were found below the damaged gate and the 19 mm steel lining was torn. An air vent was cut through the roof immediately downstream of the gates and the conduit was repaired. This solution proved to be successful once the dam was put into service again. High-head gate designs have been provided with air vents since this incident in order to allow large volumes of air into the water passage downstream of the gate to keep pressures near atmospheric pressure (Erbisti, 2004).

### 3.3.3 Flow Under Gates

The primary cause of air demand just downstream of the emergency gate is the flow conditions at the gate. The types of flow that occur at gates in high-headed conduits may be either free surface flow or pressurised flow (submerged flow). For *pressurised flow* the space upstream of the gate is submerged and pressurised. For *free surface flow* the space downstream of the gate is filled with air. A *hydraulic jump* is the result of the transition from the one flow type to the other (pressurised flow to free surface flow) (Naudacher, 1991). However, the hydraulic jump is unstable, because the flow downstream of the gate is not subcritical. Pressurised flow increases the risk for cavitation and vibration damage and should be avoided, as discussed in **Section 3.3.1**. Thus, a bottom outlet should always be designed for free surface flow, as it reduces the potential structural damage (Vischer & Hager, 1998).

**Figure 3-2** below depicts the three different sources of air entrainment in the outflow in gated bottom outlet tunnels (Vischer & Hager, 1998).

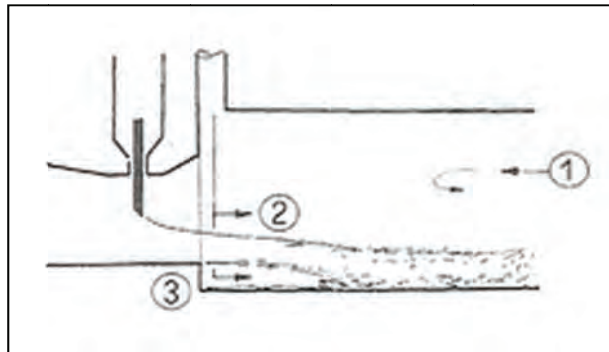


**Figure 3-2: Origin of aeration**

The aeration of flow may originate from three different sources, namely (1) the counter-current air from the tunnel, (2) the air vent for surface aeration and (3) the bottom aerator (Vischer & Hager, 1998).

The air discharge through the air vent depends on the rate of the air entrained by the high-velocity water discharge, and on the rate that air above the air-water mixture is being discharged at the exit of the conduit. Both these factors vary as they are influenced by structural and hydraulic features of the conduit and the method used to operate the conduit. Studies conducted by Sharma classified two-phase flow regimes downstream of a gate in bottom outlets without bottom aerators. Six types of flow that cause air demand were identified and are illustrated in **Figure 3-3** below (Sharma, 1976):

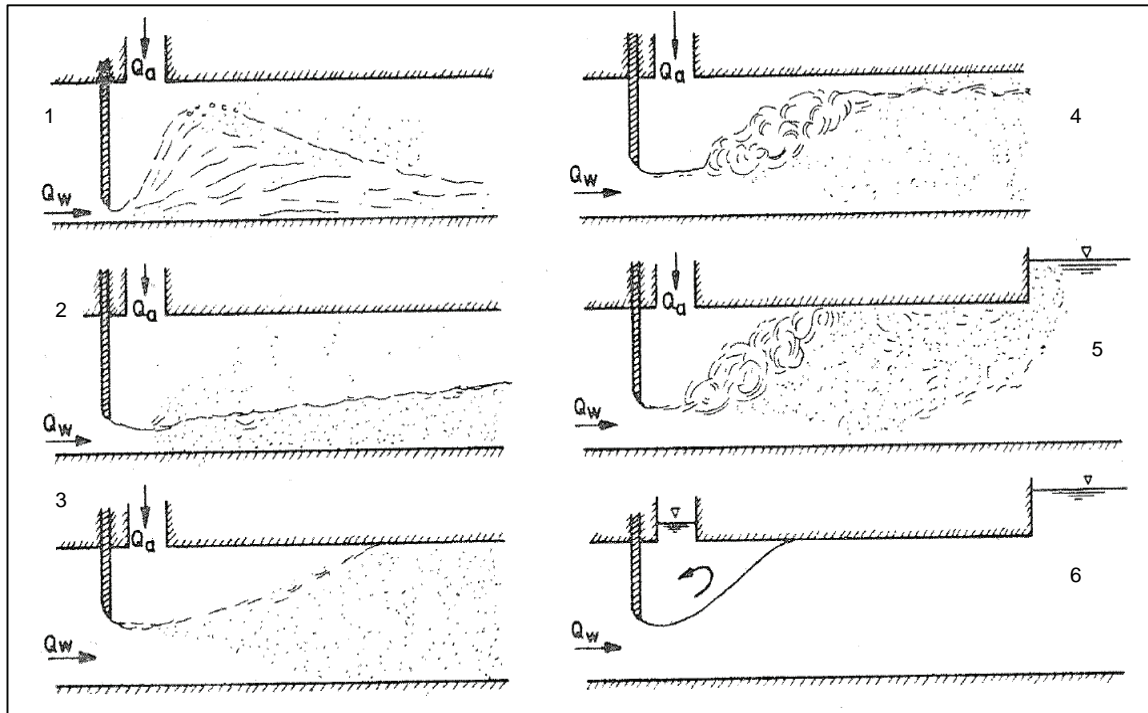


**Figure 3-3: Classification of flow types in bottom outlets without bottom aerators**

The classification of the flow types, as illustrated in **Figure 3-3** above, is as follows (Sharma, 1976):

1. *Spray flow* for relatively small gate opening below 10%, with an extremely high air entrainment.
2. *Free flow* as typical for bottom outlets, and accompanied by features of supercritical flow, such as shockwaves and two-phase flow.
3. *Foamy flow* for a tunnel almost full with an air-water flow, but still not flowing under pressure.
4. *Hydraulic jump* followed by free surface tailwater flow due to tailwater submergence (transition from pressurised flow to free surface flow).
5. *Hydraulic jump with transition to pressurised tailwater flow* (pipe flow).
6. *Fully pressurised flow caused by deep tailwater submergence, no air demand.*

From the above mentioned it is clear that, when the discharge in the conduit is not influenced by tailwater conditions and a hydraulic jump does not form in the conduit, the jet



from small gate openings forms spray flow, which fills the conduit and is dragged downstream of the conduit by the underlying flow velocity (USACE, 1980).

A hydraulic jump forms in the conduit at large gate openings, the jet will entrain air as mentioned previously, but the turbulence of the jump will entrain air that is discharged at the top of the conduit and will be pumped downstream into the conduit by the jump action. Both these air flow conditions in the conduit are responsible for pressure reduction behind the gate and at the air vent exit, which results in air being discharged through the air vent into the conduit to stabilise the hydraulic pressures behind the emergency gate (USACE, 1980).

Under free surface flow conditions, the pressure in the tunnel just downstream of the gate,  $\Delta p/\gamma \leq 0$ , is dependent on the air entrainment intensity in the emerging water jet and the ventilation efficiency through the air vent. If it is assumed that the velocity distribution in the emerging jet is uniform, then the discharge under a high-headed gate may be expressed by the following formula (Naudacher, 1991):

$$Q = C_c ab [2g(H - H_e - C_c a - h_a)]^{1/2}$$

**Equation 3.13**

where

Q:	discharge (m <sup>3</sup> /s)
C <sub>c</sub> :	contraction coefficient
a:	gate opening (m)
b:	gate width (m)
H:	head in reservoir (m)
H <sub>e</sub> :	energy loss from the entrance to the gate section (m)
h:	head on contracted jet (m)

The symbols in **Equation 3.13** are explained in **Figure 3-4** below (Vischer & Hager, 1998).

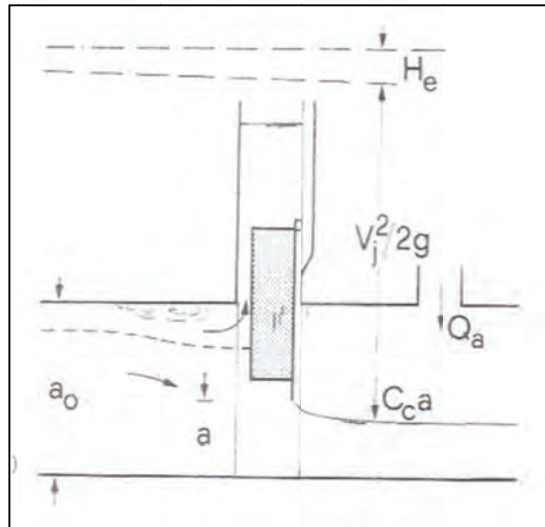


**Figure 3-4: Definition sketch for free flow**

It is clear from **Figure 3-4** that air should be sucked into the conduit through the air vent, which is in contrast to the measured air vent velocities during the commissioning test in 2008. Therefore, it is deemed necessary to investigate the reasons for the release of air through the air vent.

The discharge coefficient  $C_d$  of the flow underneath the gate can be obtained by the following formula:

$$C_d = \frac{Q}{\sqrt{2g\Delta H}}$$

**Equation 3.14**

where  $\Delta H$  is the difference in head according to the underflow discharge formula. The parameter  $C_d$  is dependent on various parameters, namely the relative gate opening,  $\eta = C_c ab/A_0$  [**Equation 3.15**], with  $A_0 = a_0 b_0$  as the approach section, the loss factor, the aspect ratio and the distribution of the approaching velocity. The literature recommended the use of the contraction coefficient  $C_c$  in the equations, rather than the lump parameter  $C_d$ . The contraction coefficient  $C_c$  is dependent on the Froude number ( $F_j = V_j/(gC_c a)^{1/2}$ ) [**Equation 3.16**] of the flow downstream of the gate, provided that the Froude number is less than four. Large Froude numbers are normally present in the high-headed gate

prototype, thus neither the free surface nor the viscosity effect on the flow need to be taken into account. The geometry of the gate has a significant effect on  $C_c$  (Vischer & Hager, 1998).

Another formula for discharge under a vertical sluice gate under free flow conditions was developed by Franke and Valentin by means of measuring the pressure at the floor directly below the gate lip and comparing this value to the geometry of the jet. This formula has been extended by Yong and Fellerman for submerged flow conditions. The general formula for discharge under a gate is as follows (Lewin, 2001):

$$Q = C_d \times G_o \times W \sqrt{2gH}$$

**Equation 3.17**

where

- Q: discharge ( $\text{m}^3/\text{s}$ )
- $C_d$ : coefficient of discharge (dimensionless)
- $G_o$ : gate opening (m) (represented by  $b$  in **Figure 3-5**)
- W: gate width (m)
- g: gravitational constant ( $\text{m}/\text{s}^2$ )
- H: upstream water head (m)

The flow line characteristics of the approaching flow and the flow leaving the orifice are the primary parameters that influence the coefficient of discharge. In turn, these flow lines depend on the gate opening ( $G_o$ ), and the upstream water head (H). **Figure 3-5** below shows these variables, which affect the discharge characteristics (Lewin, 2001).  $Y_1$  (m) is the upstream water depth and  $Y_3$  (m) is the water depth downstream of the gate, with  $b$  the gate opening (m).

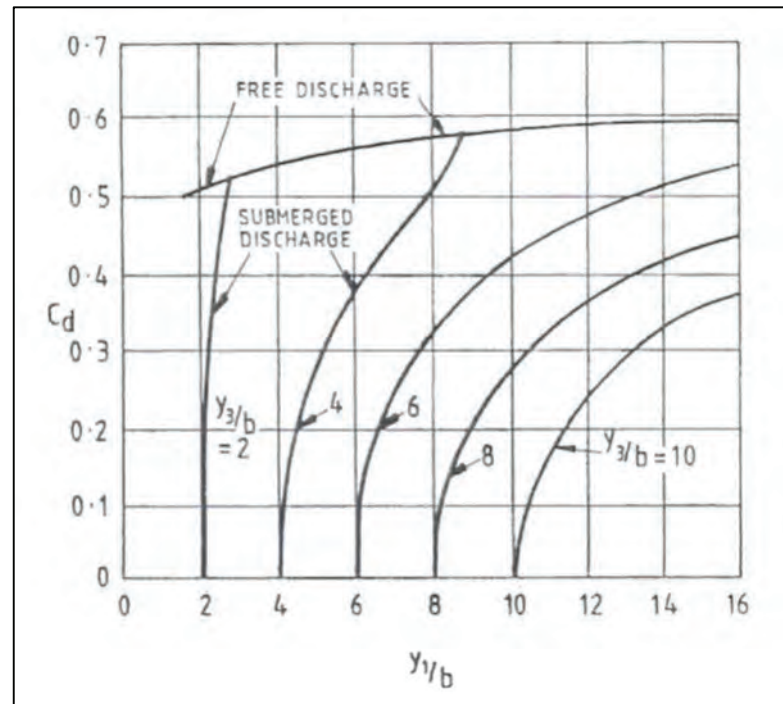


**Figure 3-5: Coefficient of discharge for free and submerged flow under a vertical gate**

The hydraulics of air-water flow in high-headed bottom outlets has been studied by numerous researchers. The problem of determining the air demand is not yet fully understood and is not amenable to rigorous mathematical formulas, due to the inherent limitations. As a result, only empirical equations have been collaborated to determine the air demand, and these are based on laboratory and field measurements. These equations compare the ratio of the volumetric airflow ( $Q_a$ ) rate to that of the water ( $Q_w$ )(henceforth called *air demand ratio*, indicated by  $\beta = Q_a/Q_w$ ) to the Froude number of the flow at the vena contracta if free flow conditions are experienced, or at the location of the jump in case a hydraulic jump occurs. The  $\beta$ -values obtained from these equations differ substantially from one another, so that it is impossible to select a  $\beta$ -value that will meet all the requirements. Consequently, hydraulic modelling is recommended for important case studies. According to Sharma (1976), the problem to determine the required quantity of air for the different flow types remains unsolved, as field measurements have indicated that the air demand ratio ( $\beta$ ) in prototypes is larger than what was predicted by his model studies.

### 3.3.4 Air Entrainment

#### 3.3.4.1 Air Entrainment Upstream of Gate (Vortex Formation)

Air can be entrained upstream of a gated outlet through the formation of vortices (see photos in **Figure 3-6** below).



**Figure 3-6: Photos of Vortices ( (Rindles & Gulliver, 1983)**

In the US Army Corps of Engineers' design guidelines for reservoir outlets Gordon's Curve (**Figure 3-7**) for unsymmetrical pipe flow is recommended for determining the minimum submergence of the outlet to avoid vortex formation (USACE, 1980). This curve was, however, based on the data of only four vortex-forming installations and was not derived using dimensionless parameters so cannot be considered universal for all designs (Rindles & Gulliver, 1983). Despite these limitations the curve is widely used (the data points from three subsequent vortex events have also been included in the graph given in Figure 3-7).

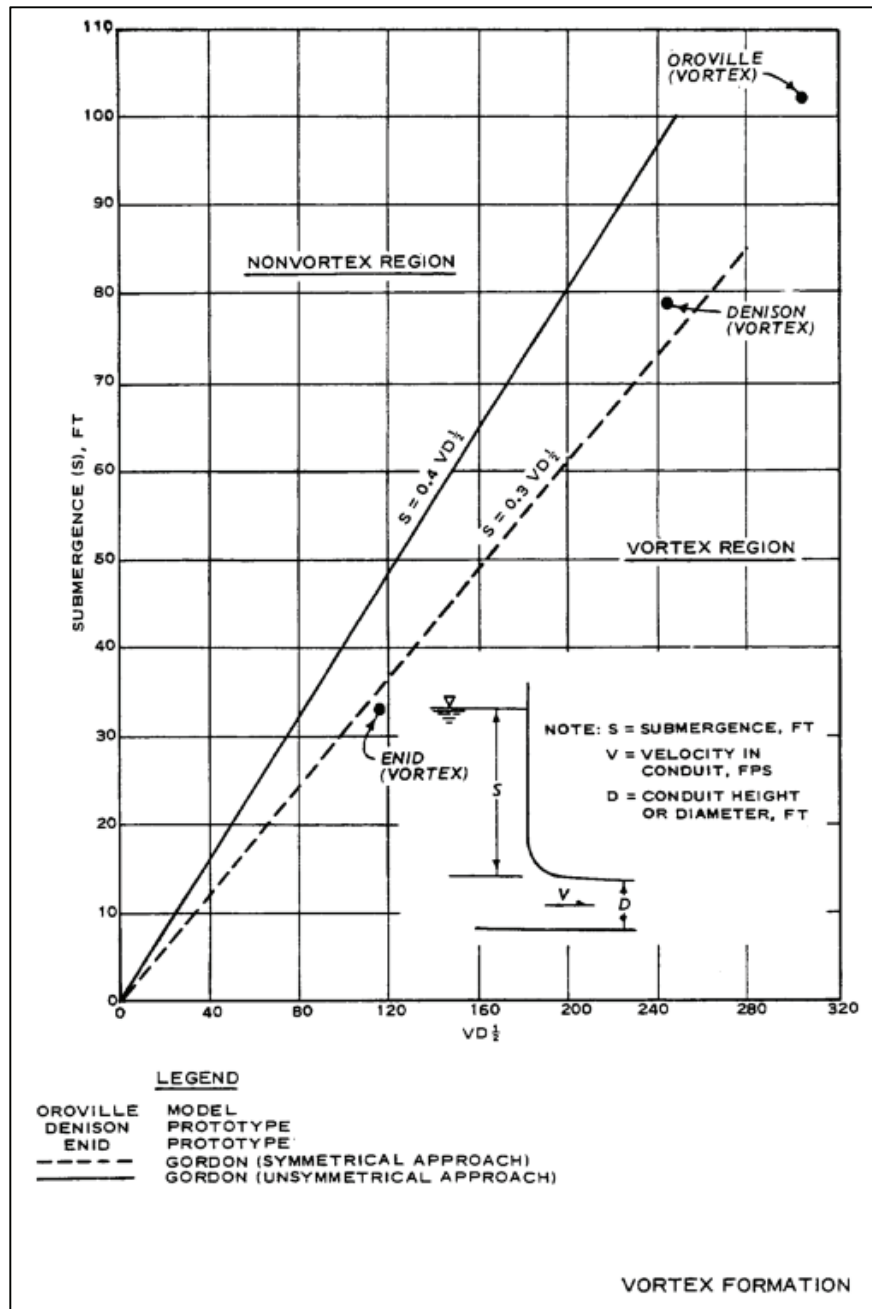
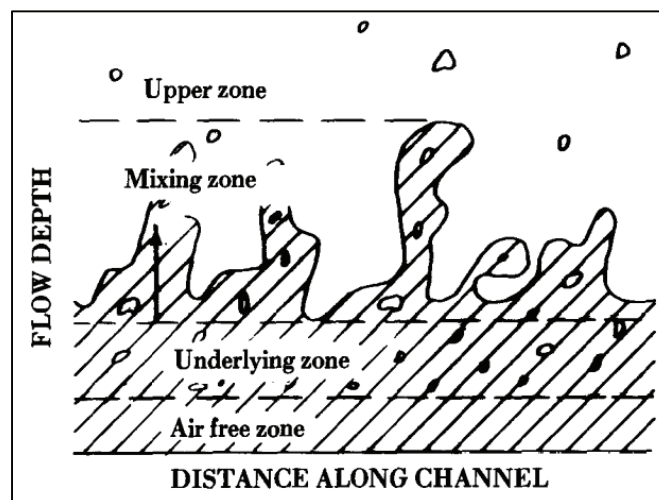


Figure 3-7: Gordon's curve of minimum submergence (USACE, 1980)

### 3.3.4.2 Air-Water Flow in Partially Filled Conduits

Flow in a partially filled conduit can be thought of as open-channel flow in a closed conduit. The vertical structure of highly turbulent flows in open-channels can be divided into four zones, as shown in Figure 3-8 below (Falvey, 1980)

1. Upper zone of flying drops of water
2. Mixing zone where water surface is continuous
3. Underlying zone where bubbles are diffused within the water body
4. Lower, air free zone



**Figure 3-8: Vertical structure of highly turbulent flows (Falvey, 1980)**

In a conduit with an air supply shaft, the total volume of air supplied by the shaft is the sum of the volumes entrained into the flow and that dragged above the flow as a result of air-water shear forces.

$$Q_{a \text{ total}} = Q_{a \text{ insufflated}} + Q_{a \text{ dragged}}$$

**Figure 3-9** below shows a picture of the volume fraction contours of air at a hydraulic jump in a conduit generated with a numerical model by Hirt (2003); and **Figure 3-10** shows sketches of air flow above a surface in a conduit.

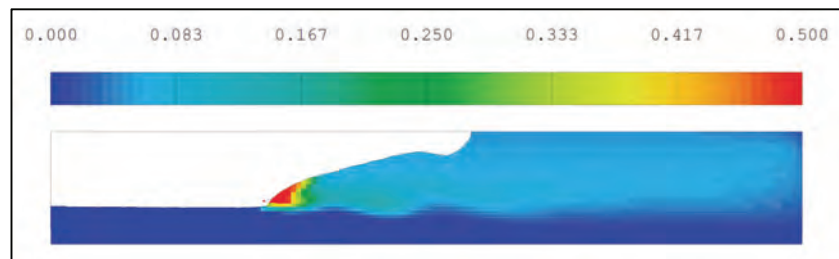


**Figure 3-9: Numerical model output showing air entrainment at a hydraulic jump (the colours indicate volume fraction of air) (Hirt, 2003)**

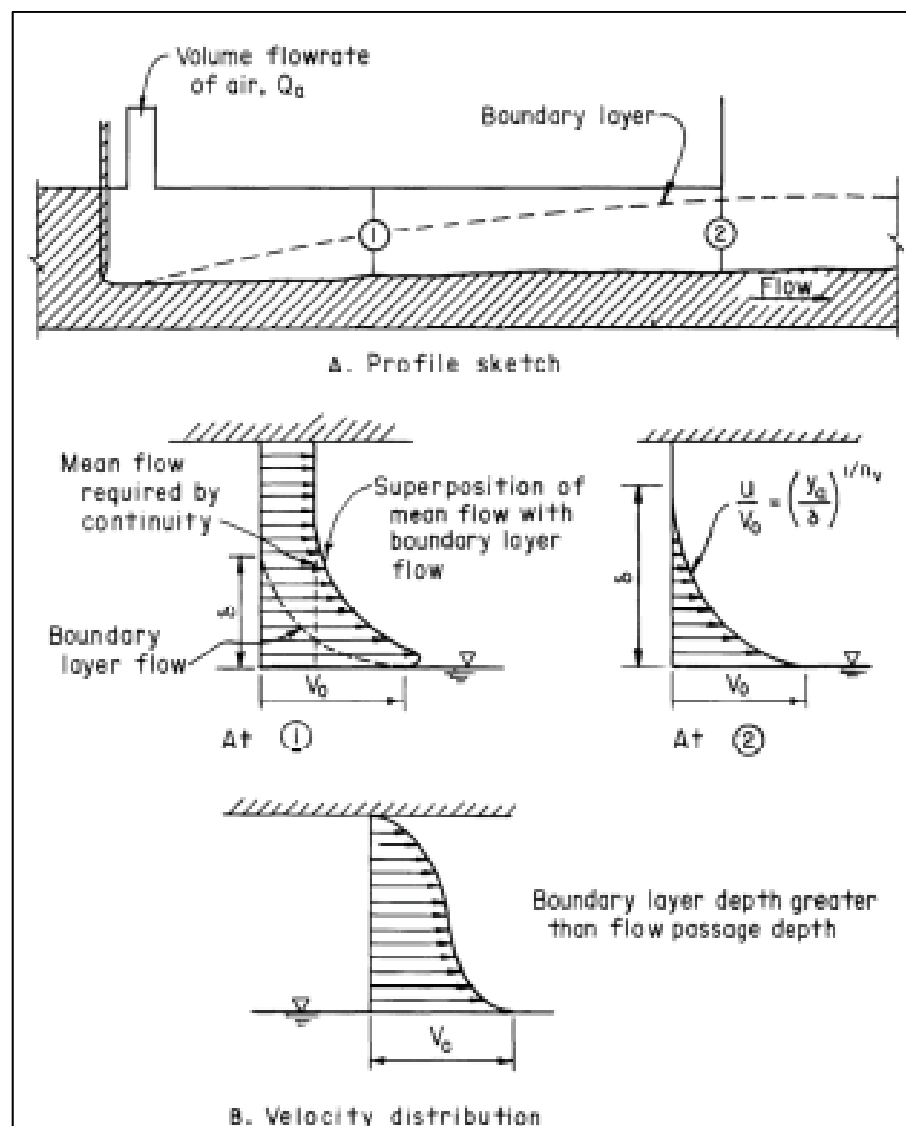


**Figure 3-10: Airflow above a water surface**



### 3.3.4.3 Upstream Moving Air (Blowback)

A number of prototype cases have occurred in which pockets of air have been blown violently upstream back into the intake works of reservoir outlets (Webby, 2003). This phenomenon is referred to as air blowback and can cause operational problems as well as structural damage to reservoir outlets (FEMA, 2004).

**Figure 3-11** shows the direction of slug motion as a function of conduit slope, flow rate and diameter. In the figure the five + symbols indicate structures which have experienced blow-back damage for their design discharge. Two of these experience upstream air movement at their design discharge while the other three must have experienced the blowback at less than design discharge (when gate was only partially open). (Falvey, 1980) In all these cases the air blowback has been attributed to the slope of the conduit.

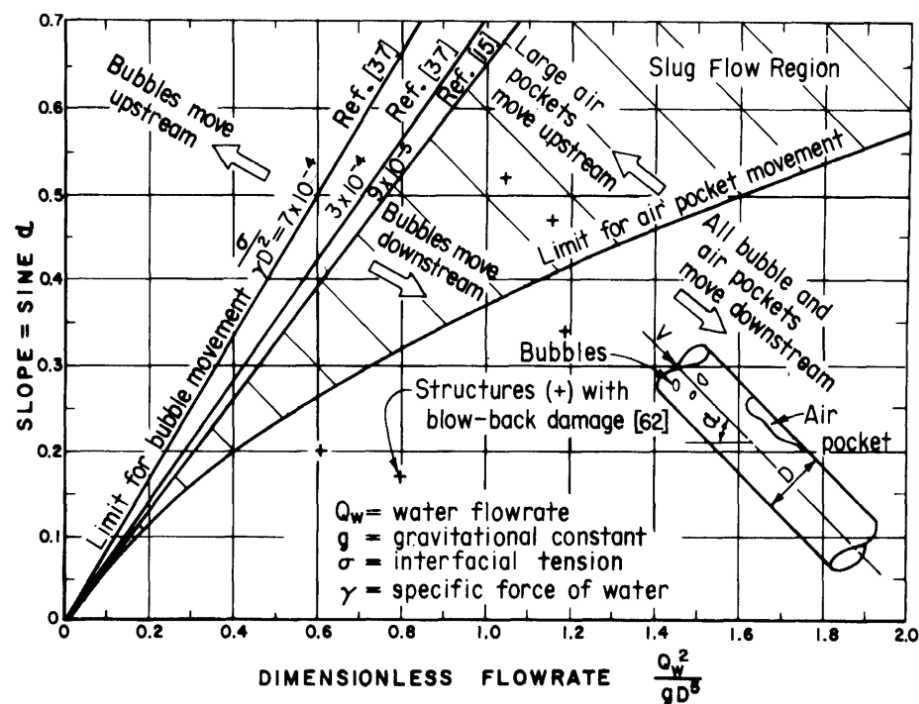


**Figure 3-11: Bubble motion in closed conduits flowing full (Falvey, 1980)**

According to Falvey (1980) blowback problems are not normally experienced for slopes of less than 0.1.

A model study on the glory-hole spillway of the Owyhee Dam (Oregon, USA) after a blowback incident in 1936 cited constriction of the flow at the outlet (submerged) as a result

of wave action as the cause of the air flow reversal (Lowe, 1944). **Figure 3-12** below shows a sketch of the Owyhee outlet works.

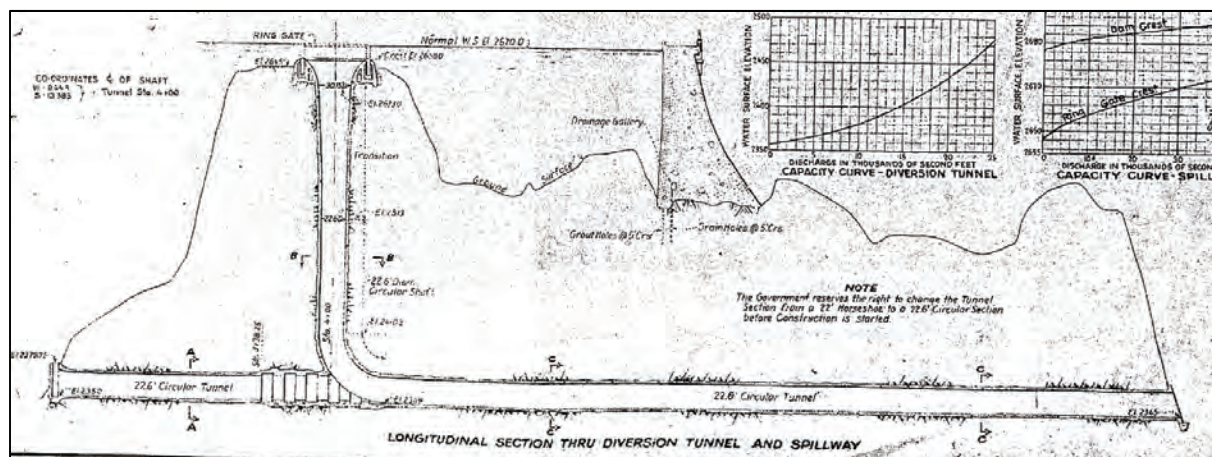


**Figure 3-12: Long section of Owyhee Dam outlet (Lowe, 1944)**

Another study was concerned with the Rangipo (Hydro) Power Station in New Zealand which experienced damaging blowbacks in 1987 and twice in 1995. It concluded that the blowbacks occur only at low flow rates, and can be explained by **Figure 3-11** above. It recommended the drilling of a 300 mm air vent to the conduit as a preventative measure against future blowbacks (see **Figure 3-13** below). (Webby, 2003)

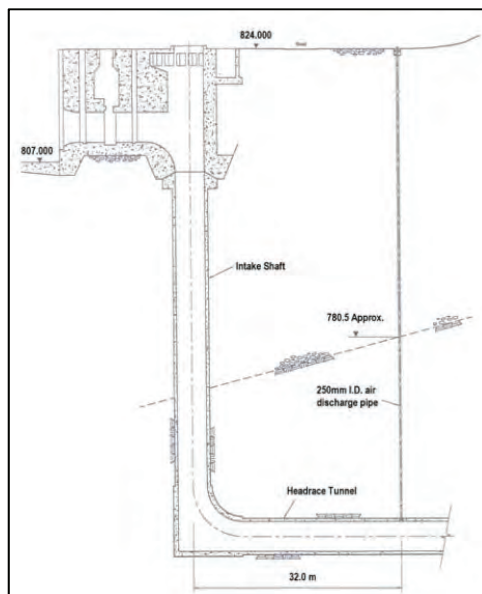


**Figure 3-13: Outlet at Rangipo Hydropower Station, 300 mm extra vent proposed as preventative measure for future blowback (Webby, 2003)**

### 3.3.5 Functions and Features of Air Vents

Air vents are essential in high-head gates. The primary functions of air vents are as follows (Erbisti, 2004):

- Sub-atmospheric pressure is reduced or eliminated in the conduit during emergency or partial gate operations.
- They make it possible to drain the conduit.
- They allow air to escape when the conduit is being filled.

It is vital that the inlet of an air vent be constructed above the maximum reservoir water level on the downstream face of the dam to avoid interference with the air flow. Generally, air vents are circular in shape, but sometimes square or rectangular cross-sections are used to simplify the moulding process. The vent must be as straight as possible, with the minimum number of bends and sharp corners, and there may not be an abrupt change in the cross-section (Erbisti, 2004).

Usually, air vents are constructed in the conduit ceiling immediately downstream of the gate, as the air requirements in this region are the most critical and reach a maximum value when the gate is operated at some partial opening under the highest reservoir head.

For optimal effectiveness the outlet of the vent should not be located further than **2 m** from the emergency gate (Erbisti, 2004).

The velocity of the air being drawn into the conduit may not exceed 40 to 50 m/s in order to avoid discomfort for the maintenance staff and to prevent the vacuum behind the gate from increasing (Borodina, 1969). Air may not be drawn in from either structural cavities or from nearby areas where staff work (Erbisti, 2004).

### 3.3.6 Air Demand ( $\beta$ )

Various studies have been conducted by numerous researchers to develop formulas for calculating the ratio of air flow to water flow ( $\beta$ ), but in most cases air demand is not subject to a rigid analysis. Therefore, for design purposes the quantitative empirical estimations of the air required have been based on suitable experimental and prototype data (USACE, 1980).

A study by Kalinske and Robertson concluded that the entrainment of air is a function of the Froude number at the vena contracta, and expressed the air demand ratio ( $\beta$ ) in terms of the air discharge and water discharge. It is defined as follows (Kalinske & Robertson, 1943):

$$\beta = \frac{Q_a}{Q_w}$$

**Equation 3.18**

where

$\beta$ : air demand ratio (dimensionless)

$Q_a$ : flow rate of air ( $\text{m}^3/\text{s}$ )

$Q_w$ : water discharge ( $\text{m}^3/\text{s}$ )

The air demand ratio ( $\beta$ ) is dependent on various parameters, for instance the geometry of the conduit and gate, the water flow velocity and the depth at the vena contracta and the water head. The majority of published papers recommend the following formula for calculating the air demand ratio (Erbisti, 2004):

$$\beta = K(F_c - 1)^n$$

Equation 3.19

where

K and n: empirical coefficients

$F_c$ : Froude number at vena contracta

$$= F_c = \frac{V_c}{\sqrt{gh_c}} = \frac{\sqrt{2gH}}{\sqrt{gh_c}} = \sqrt{\frac{2H}{h_c}}$$

Equation 3.20

g: gravitational acceleration ( $\text{m/s}^2$ )

$V_c$ : velocity of water at vena contracta ( $\text{m/s}$ )

$h_c$ : depth of water at vena contracta (m) (refer to **Figure 3-14**)

H: effective head at vena contracta (m) (refer to **Figure 3-15**)

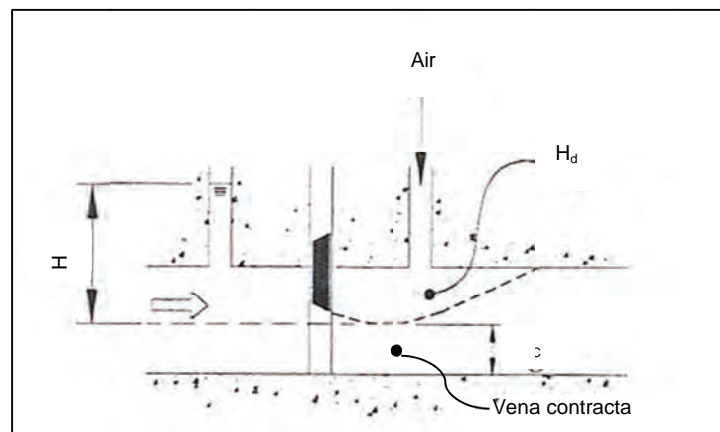


**Figure 3-14: Schematic layout of parameters influencing air entrainment**

The recommended formula for design purposes for air entrainment in conduits *without* a hydraulic jump<sup>1</sup> is as follows (USACE, 1980)

<sup>1</sup> It is recommended to design outlets for free-surface supercritical flow

$$\beta = 0.03(F_c - 1)^{1.06}$$

Equation 3.21

The air demand ratio for a hydraulic jump which fills the conduit was determined by Kalinske and Robertson (1943) to be:

$$\beta = 0.0066(F_c - 1)^{1.4}$$

Equation 3.22

The results regarding air demand obtained from other studies are described below.

**a) Rabben and Rouvè (1985)**

Air demand was defined by introducing a fictitious conduit cross-section of  $A_a^* = A_a(1 + \sum \xi_i)^{-1/2}$  [Equation 3.3.23], where  $\sum \xi_i$  represents the sum of all head losses from the atmosphere to the gate chamber. For spray flow (refer to **Figure 3-14 (1)**) when the gate opening is less than 6% and  $F_c \geq 20$  (Froude number at vena contracta), the air ratio obtained is as follows (Rabben & Rouvè, 1985):

$$\beta = \left( A_a^* / A_d \right) F_c$$

Equation 3.24

where

$A_d$ : tailwater area section ( $m^2$ )

$F_c$ : Froude number at the vena contracta

$$= F_c = q / [g(C_c a)^3]^{1/2} \quad \text{[Equation 3.25]}$$

Where the water discharge is defined as  $Q_w = qb_g$ , with  $b_g$  being the gate width (m)  $q$  is the specific discharge,  $g$  is the gravitational acceleration ( $m/s^2$ ) and  $a$  is the gate opening (m).

Under free surface flow conditions (Figure 2.3 (2) and (3)) with a gate opening greater than 12% and  $F_c \geq 40$ , an expression for the air ratio, according to Rabben and Rouvè, is as follows (1985):

$$\beta = 0.94 \left( A_a^* / A_d \right)^{0.90} F_c^{0.62}$$

**Equation 3.26**

Under tunnel flow conditions where a hydraulic jump occurs (Figure 3.3 (4) and (5)), the tailwater depth or the corresponding pressure head for pipe flow must be determined by means of a backwater curve for similar conditions to free flow. The air demand can be determined by the following formula (Rabben & Rouvè, 1985):

$$\beta = 0.019 \left( A_a^* / A_d \right) F_c$$

**Equation 3.27**

The above three approaches were established for short tunnels. Less air will be entrained in longer conduits due to de-aeration processes (Vischer & Hager, 1998).

**b) Campbell and Guyton** (Erbisti, 2004)

For gated conduits, the air demand ratio according to the study conducted by Campbell and Guyton is defined as follows (Erbisti, 2004):

$$\beta = 0.04(F_c - 1)^{0.85}$$

**Equation 3.28**

The Froude number in the above formula refers to the flow immediately downstream of the gate at the vena contracta. This formula assumes that the maximum air demand occurs when the conduit is flowing half full.

**c) Levin** (Erbisti, 2004)

According to Levin (Erbisti, 2004), the air demand ratio is defined as follows:

$$\beta = K(F_c - 1)$$

**Equation 3.29**

The coefficient K is taken according to **Table 3-2** below (Erbisti, 2004).

**Table 3-2: K-coefficients**

Conditions	K
Vertical lift on gate in circular tunnel	0.025 to 0.04
Same as above, with progressive transition from circular to rectangular section, followed by a very progressive transition (invert angle with horizontal lower than 10°) to circular section	0.04 to 0.06
Same as above, with fast transition from circular to rectangular section, and from rectangular to circular section	0.08 to 0.12

**d) Sharma** (1976)

The first four flow types as classified in **Figure 3-8** correspond to free surface flow. Under these scenarios, prototype observations have shown that air demand is dependent on the Froude number at the vena contracta, the ratio of the conduit length downstream of the gate ( $L_g$ ) and the diameter or height of the conduit ( $D_g$ ). **Figure 3-15** shows a series of curves that is based on experimental data of free-flowing conduits in the form of  $(1+\beta)$  versus  $\frac{A_c}{A_T}$  for different Froude numbers.  $A_c$  is the area of flow at the vena contracta ( $m^2$ ) and  $A_T$  is the cross-sectional area of the conduit ( $m^2$ ). The values obtained from this graph are only approximations and are not accurate, as the curves were based on specific values of  $L_g/D_g$  (Sharma, 1976).

The following formula represents the upper curve on the graph (Erbisti, 2004):



$$1 + \beta = \frac{1}{A_c/A_g}$$

Equation 3.30

This formula relates to the maximum possible air flow through the tunnel where the Froude number at the vena contracta is large enough to create foamy flow and the flow depth at the vena contracta is comparable to the vertical dimension of the conduit. These two conditions are hardly ever satisfied in practice.

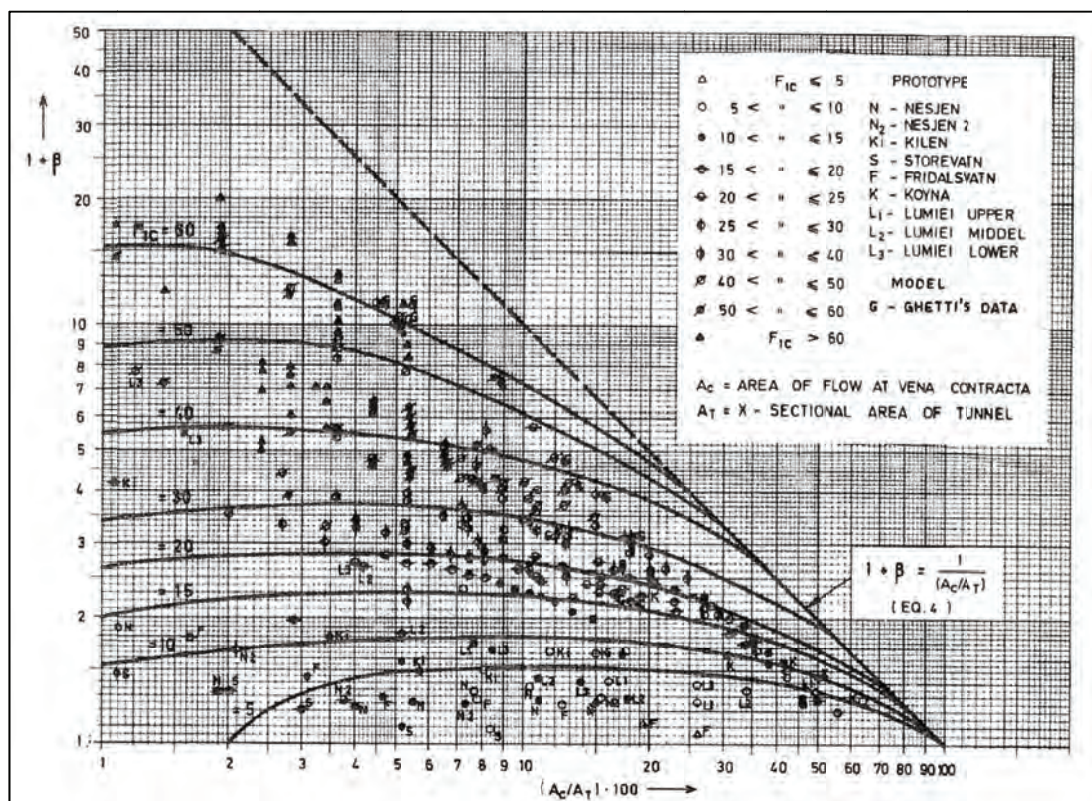


Figure 3-15:  $(1+\beta)$  versus  $(A_c/A_T)$  for different Froude numbers

Figure 3-15 (5) shows the scenario in which a hydraulic jump occurs in a bottom outlet and is followed by pipe flow with the conduit exit submerged and a low  $L_g/D_g$  ratio, or during the emergency closure of the gates. For these scenarios, Sharma suggested a slight modification in the formula of Kalinske and Robertson, with replacement of the Froude number at the jump location by the

Froude number at the vena contracta. The results obtained from the formula were found to give comparable results for model and prototype observations. The modified formula is as follows (Sharma, 1976). (This is Equation 3.21, the relation recommended in the USACE (1980) design guidelines)

$$\beta = 0.0066(F_c - 1)^{1.4}$$

**Equation 3.31**

The comparison between the various calculation formulas for determining the air demand ratio for bottom outlets with the lower end drowned (type 5 flow) is illustrated in **Figure 3-16**. The coefficient K in Levin's curve was assumed to be equal to 0.04.

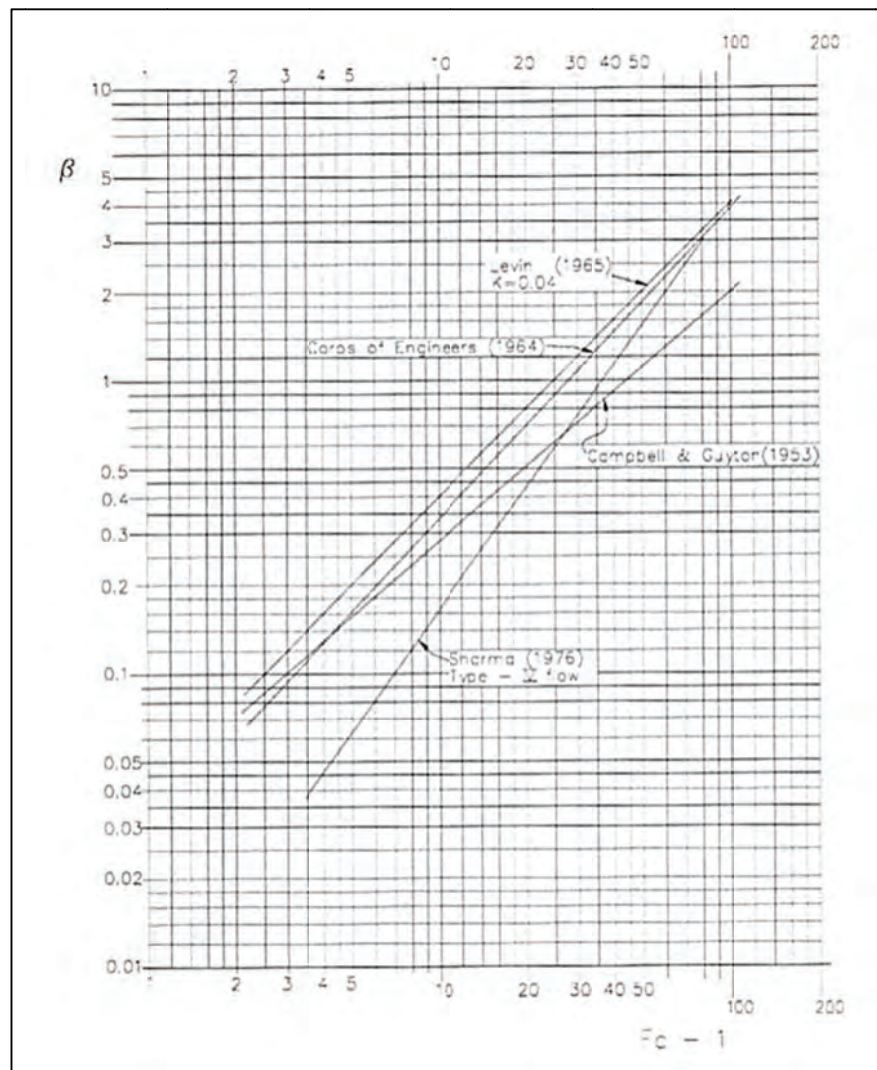


**Figure 3-16: Comparison between the various calculation formulas**

The maximum air demand under free surface flow conditions is generally not when the gates are fully open. Normally, two maximum air demand ratios exist, one for very small gate openings (4% to 8%), which result in spray flow, and the second when the gate opening is between 40% and 70% (Lewin, 2001), as depicted in **Figure 3-17** below.

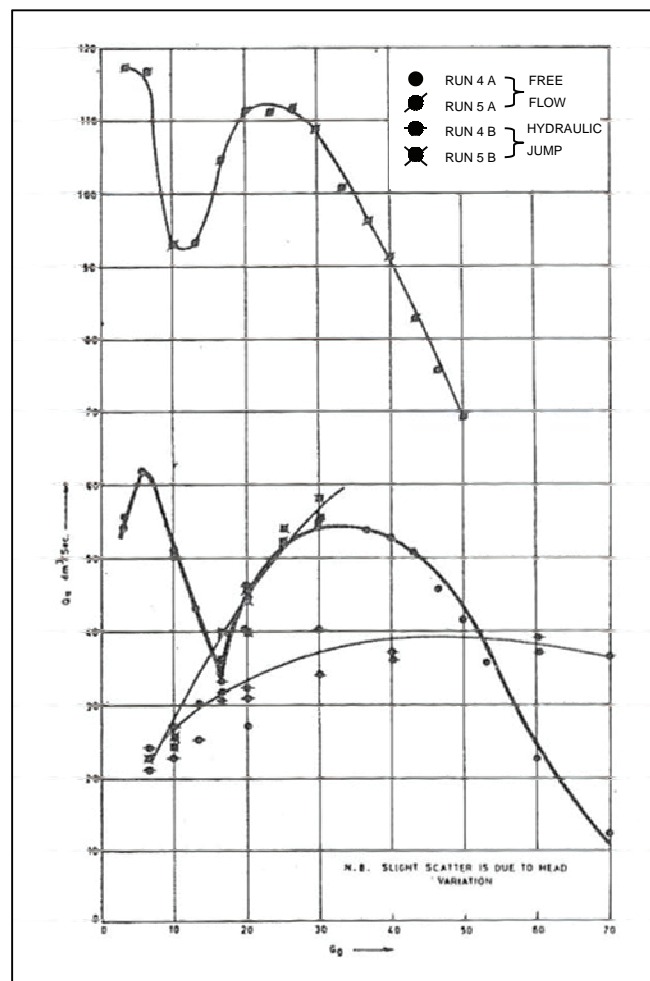


**Figure 3-17: Air demand versus gate opening ( $G_o$ ) (Sharma, 1976)**

According to Sharma (1976), the maximum air demand can be assumed to occur at a gate opening of 80%. The gate contraction coefficient can be expected to be 0.8 for a  $45^\circ$  gate lip and 0.6 for a sharp-edged gate lip. The maximum air velocity must be limited to 45 m/s to prevent excessive pressure loss due to flow resistance in the conduit (USACE, 1980).

The empirical formulas for calculating the air demand are not very accurate, as discussed above. Therefore, physical modelling of gated tunnels is required for the purpose of

determining the aeration ratio ( $\beta$ ), the gate rating curve, the pressures and the cavitation index along the conduit, and the flow conditions downstream of the gate.

### 3.3.7 Recent Studies

Najafi and Zarrati (2010) used a 3D numerical model to simulate flow conditions in a tunnel of a high headed outlet with ten gate openings from 10% to 100%. The aeration ratio ( $\beta$ ) obtained from the 3D numerical model was compared with empirical equations and a physical model as shown in **Figure 3-18**. It can be seen that the results of the numerical model had a better agreement with the physical measurement when compared with the results obtained from the empirical equations.

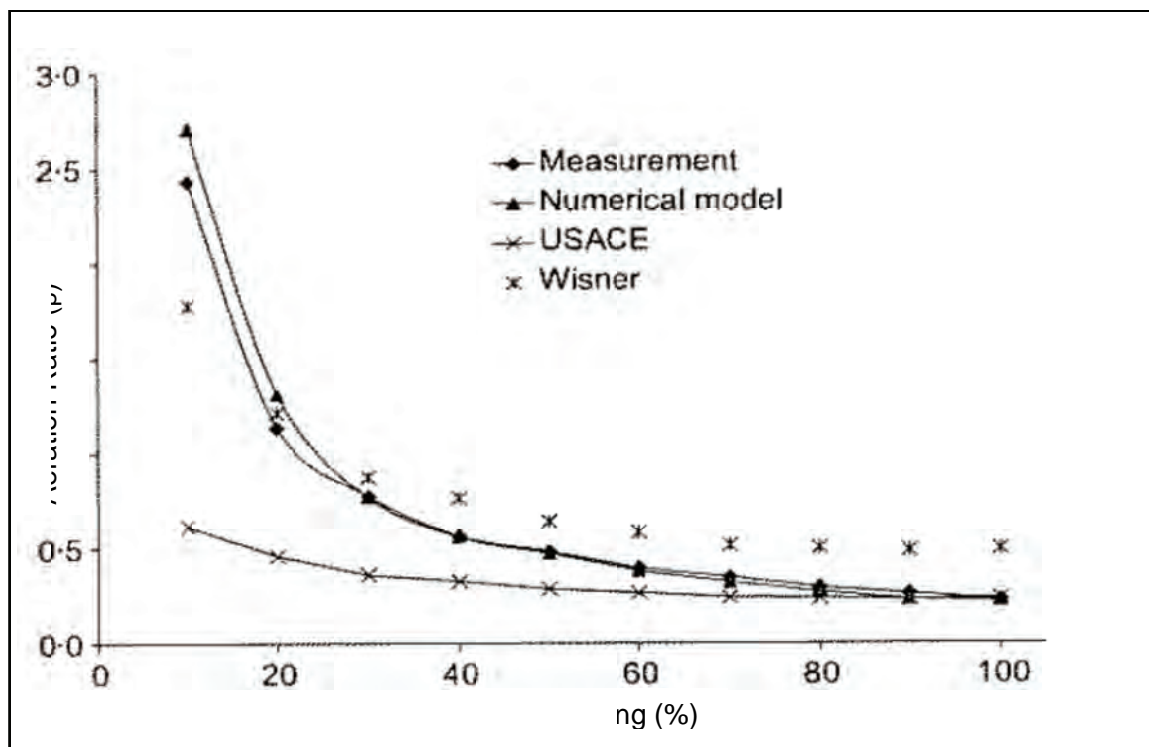


**Figure 3-18: Comparison of measured aeration versus gate opening with 3D numerical model and two empirical equations**

(Najafi & Zarrati, 2010)

A similar study involving physical and 3D numerical modelling (using computational fluid dynamics or CFD) of a long straight bottom outlet with a constant cross-section, was

performed at the Sharif University of Technology in Iran in 2006 (Shamsai & Soleymanzadeh, 2006). The air demand ratios found from the physical and numerical models were found to be similar to those predicted by most of the empirical correlations.

A recent CFD study was done as part of the design for a new dam in South Africa (Logan et al., 2011), after the unexpected behaviour during the 2008 Berg River Dam emergency gate commissioning test was observed. This bottom outlet incorporates a long straight conduit which splits into 2 just before the downstream outlet. This study concluded that the maximum air demand was significantly higher than predicted by any of the empirical methods, and that the maximum occurred at a gate opening of between 20% and 40% (in between the 2 maxima predicted by previous studies).

It appears that the empirical formulations for air demand in bottom outlets are suitable for very simple geometries, but deeper understanding of air-entrainment behaviour is still needed for situations where more involved geometries lead to flow patterns of greater complexity.

### 3.3.8 Air Vent Dimensioning

The maximum airflow rate must first be estimated in order to design an air vent. The permissible velocity, in addition to the air demand, determines the required size of the air vent. Undesirable noises and excessive reduction in pressure in the conduit can be caused by extremely high airflow velocities. Field studies of prototypes have concluded that the airflow velocity should not exceed 45 m/s, which will result in a nominal head loss in the vent or pressure drop in the conduit. To minimise cavitation tendencies, the total pressure drop across the air vent should be limited to 1.5 m water head. Dimensioning the air vent and calculating the pressure drop along the air vent makes it possible to estimate the reduced pressure that is acting downstream of the gate, which is an important parameter to analyse the imposed loads on the structural components (USACE, 1980).

The airflow in the air vent can be calculated by the following formula (Erbisti, 2004):

$$Q_a = 28m_a A \sqrt{2gH_d}$$

**Equation 3.32**



where

- $Q_a$ : airflow in air vent ( $\text{m}^3/\text{s}$ )  
 $m_a$ : flow coefficient of air vent (dimensionless) (refer to **Equation 3.36** below for calculation method)  
 $A$ : cross-sectional area of air vent ( $\text{m}^2$ )  
 $g$ : gravitational acceleration ( $\text{m}/\text{s}^2$ )  
 $H_d$ : Air pressure below atmosphere downstream of the gate (m water)

The water discharge is determined by the following formula (Erbisti, 2004):

$$Q_w = B_c h_c \sqrt{2gH}$$

**Equation 3.33**

where

- $Q_w$ : Water discharge ( $\text{m}^3/\text{s}$ )  
 $B_c$ : width of water at vena contracta (m)  
 $h_c$ : depth of water at vena contracta (m)  
 $g$ : gravitational acceleration ( $\text{m}/\text{s}^2$ )  
 $H$ : effective head at vena contracta (m)

The volumetric airflow is related to the water flow as follows, as discussed in **Section 3.3.6**:

$$Q_a = \beta Q_w$$

**Equation 3.34**

Thus, the cross-sectional area of the air vent can be determined as follows:

$$28m_a A \sqrt{2gH_d} = \beta B_c h_c \sqrt{2gH}$$

$$\therefore A = \frac{\beta B_c h_c}{28m_a} \sqrt{\frac{H}{H_d}}$$

**Equation 3.35**

The flow coefficient of the air vent is calculated with the following formula (Erbisti, 2004):

$$m_a = \frac{1}{\sqrt{\sum C_0 + \lambda \frac{L}{d}}}$$

**Equation 3.36**

where

$m_a$ : flow coefficient of air vent (dimensionless)

$\sum C_0$ : sum of loss coefficients of obstacles such as entrances, exits, elbows, curves and screens

$\lambda$ : friction loss coefficient (dimensionless)

$L$ : length of air vent (m)

$d$ : diameter of air vent (m)

The Moody chart can be used to determine the friction loss coefficient ( $\lambda$ ) in the air vent as a function of the Reynolds number and relative roughness ( $\epsilon/d$ ).

The flow coefficient ( $m_a$ ) of the air in the vent is determined by trial and error, by starting with the air vent geometry and estimating a value for the diameter, after which head losses and the cross-section area can be determined. The diameter also must be verified; if it differs from the initially assumed value attributed to it, another value for the diameter must be assumed and the above calculation must be repeated (Erbisti, 2004).

The air velocity in the air vent is dependent on the depression downstream of the gate. If the flow coefficient ( $m_a$ ) is less than 0.5, the airflow velocity can be determined by the following formula (Erbisti, 2004):



$$V_a = 28m_a\sqrt{2gH_d}$$

**Equation 3.37**

where

- $V_a$ : airflow velocity (m/s)  
 $m_a$ : flow coefficient (dimensionless)  
 $g$ : gravitational acceleration (m/s<sup>2</sup>)  
 $H_d$ : depression downstream of gate (m)

The depression ( $H_d$ ) downstream of the gate should not exceed certain limits, as described above ( $H_d < 1.5$  m), to reduce the probability of cavitation.

The cross-section of rectangular air vents is calculated as if the section was circular. The following ASHREA formula gives the equivalent sections for circular and rectangular vents that have the same length, flow and head losses (Erbisti, 2004):

$$D_e = 1.3 \sqrt[8]{\frac{(ab)^5}{(a+b)^2}} = 1.3 \frac{(ab)^{0.625}}{(a+b)^{0.25}}$$

**Equation 3.38**

where

- $D_e$ : diameter of the equivalent circular section (m)  
 $a$ : rectangular dimensions (m)  
 $b$ : rectangular dimensions (m)

For the particular case of a square cross-section, the equivalence is given by:

$$D_e = 1.093 a$$

**Equation 3.39**

where  $a$  is the length of the square side (m).

An empirical equation was developed by Sarkaria and Hom to calculate the diameter of an air vent for closed conduits without surge tanks. The formula is as follows (Sarkaria & Hom, 1959):

$$d = 0.291 \left( \frac{P^2 L}{H_n^2} \right)^{0.273}$$

**Equation 3.40**

where

- d: diameter of the air vent (m)
- P: rated output of the turbine (MW)
- L: length of the air vent (m)
- H<sub>n</sub>: rated head of the turbine (m)

Erbisti (2004) recommended that the diameter of the air vent as calculated by the above formula be considered a minimum recommendation.

## 4. PHYSICAL MODEL OF THE BERG RIVER DAM OUTLET

### 4.1 General Description

A 1:14.066 scale physical model of the Berg River Dam outlet works was constructed in the Stellenbosch University hydraulics laboratory to simulate the closure of the emergency gate under similar water levels and intake gate configuration as at the time of the commissioning test in 2008, and with the radial gate at the end of the conduit fully open to determine the reasons for the release of very large volumes of air from the air vent (report on 2008 commissioning test is attached in Appendix B). The laboratory provided a sufficient water supply from the sump pumps and a constant head tank to imitate the release of the high flows.

The model was constructed according to the as-built drawings (attached in Appendix A) and incorporated a tank to simulate the reservoir, the wet well, the bottom outlet conduit, the emergency gate chamber, the air vent, the radial gate chamber and the ski-jump. The model was made of transparent Perspex to allow clear observation of the flow behaviour, as well as satisfy the requirements for a smooth surface. **Figure 4-1** below shows a photograph of the model and **Figure 4-2** on the following page shows a line sketch of the model layout.

**It should be noted that the parameters recorded in the model study and presented in this report has been transformed to reflect the values as would have been observed in the prototype, unless stated otherwise.** Elevations are reduced to meters above sea level (masl).

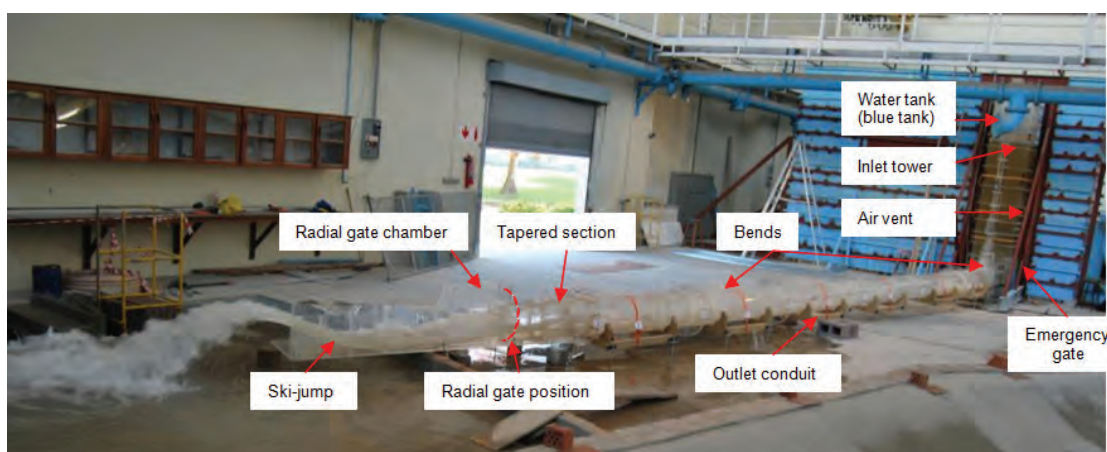


**Figure 4-1: Photograph of Physical Model**

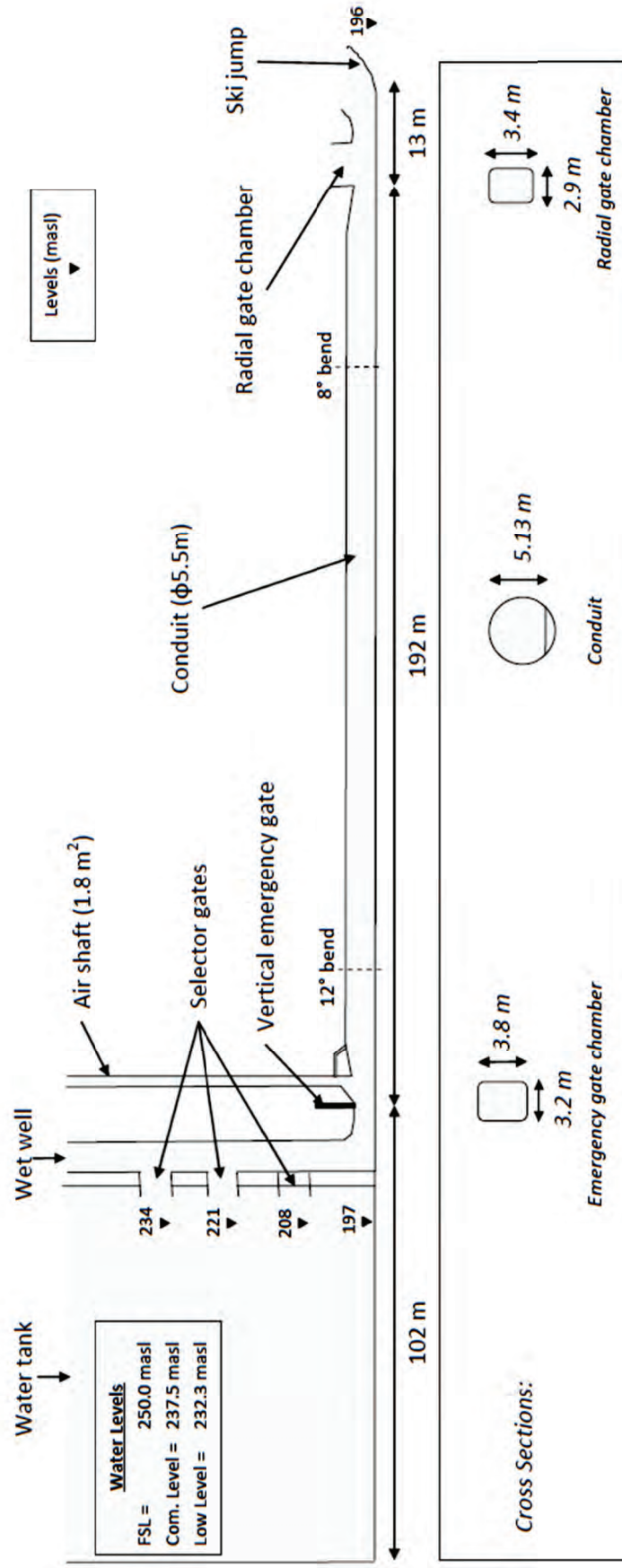


Figure 4-2: Line sketch of physical model layout (prototype dimensions given)

## 4.2 Model Scale

The model of the Berg River Dam was designed at a 1:14.066 natural scale. The odd scale of the model was determined by the inside diameter of the available Perspex pipe that was used to model the outlet conduit. The large scale of the model ensures that forces other than gravity forces (Froude values) remain insignificant and makes it possible to readily observe the detailed behaviour of the flow.

The model size was determined in accordance with Froude's law of similitude, as a free surface gradient was present in the outlet conduit and the forces acting on the flow were largely inertial and gravitational forces. There is geometric similarity between the model and the prototype, and the flows initiated by the model act in accordance with Froude's Law, therefore the ratio of gravitational and inertial forces acting on the fluid particles are the same in the model and in the prototype. Thus, the Froude numbers ( $F_r$ ) of the model and the prototype are equal:

$$F_{r_{Prototype}} = F_{r_{Model}}$$

**Equation 4.1**

The Froude number ( $F_r$ ) is defined as

$$F_r = \frac{V}{\sqrt{gL}}$$

**Equation 4.2**

where

- V: flow velocity (m/s)
- g: gravitational constant (9.81 m/s<sup>2</sup>)
- L: characteristic dimension (depth/length)

Using suffix 'm' to denote model and 'p' to denote prototype dimensions, the following scale relationships are true for the model of the Berg Rive Dam for a scale of 1: $x$ , assuming equality of the Froude number and geometric similarity between the model and the prototype:

Linear ratio:  $\frac{L_p}{L_m} = x = 14.066$

Area ratio:  $\frac{L_p^2}{L_m^2} = x^2 = 197.852$

Volume ratio:  $\frac{L_p^3}{L_m^3} = x^3 = 2782.991$

Velocity ratio:  $\frac{V_p}{V_m} = x^{1/2} = 3.750$

Discharge ratio: (Velocity ratio) x (Area ratio)

$$\frac{V_p}{V_m} \times \frac{L_p}{L_m} = x^{5/2} = 742.0387$$

Time ratio:  $\frac{(\text{Length ratio})}{(\text{Velocity ratio})} = x^{1/2} = 3.750$

Froude number ratio:  $x_p^{0.5} / x_m^{0.5} = 1$

#### 4.3 Parameters Recorded and Instruments Used

During the physical model tests the static pressures were recorded at 8 different points in the model, and the air velocity (with its direction) was measured at the top of the airshaft. **Figure 4-3** below shows the location of the measurement instruments.

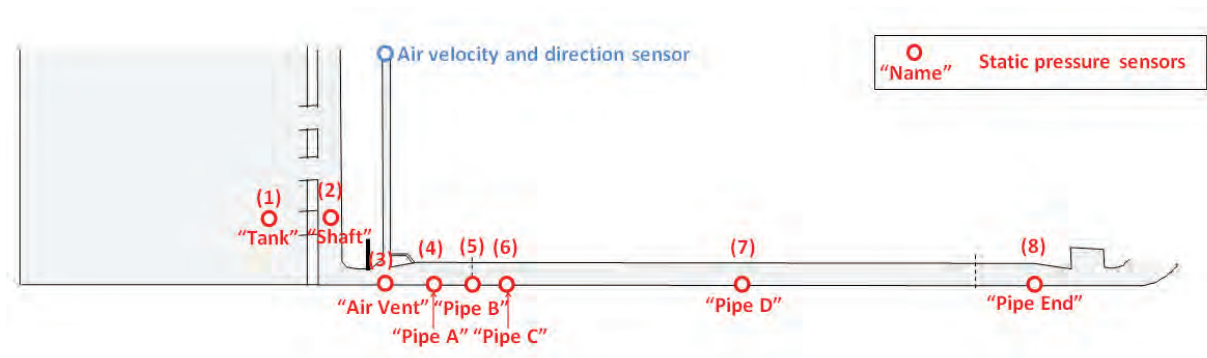


**Figure 4-3: Location of Measuring Instruments in the Model**

### 4.3.1 Pressure Measurements

Eight S-10 type pressure transducers were used to measure the static pressures and pressure fluctuations in the water tank, water shaft and outlet conduit.

The locations of the pressure transducers are shown in red in **Figure 4-3** above. One pressure transmitter was placed in the water tank and one in the wet well. Six pressure transmitters were placed along the floor of the outlet conduit.

Two sets of S-10 pressure transmitters were used, namely a 20 mA and 4 mA (accuracy under different pressures). **Table 4-1** summarises the pressure range of each pressure transmitter set and at which location it had been installed in the model with reference to Figure 4-3.

**Table 4-1: Pressure Transducers**

Pressure transmitters	Maximum measure range	Minimum measure range	Location
20 mA	+ 5 m	- 1 m	1, 2, 3, 4, 5 and 6
4 mA	+ 1 m	- 1 m	7 and 8

The pressure transmitters measured the pressure in milli-Ampere (mA). This was converted to Volt (V) by a 120  $\Omega$  resistor (R), since  $V = I \times R$ . In turn, the pressure measured in Volt was converted to metres (m water), according to **Table4-1** for the 20 mA and 4 mA pressure transmitters respectively:

$$Y_{[m]} = \frac{(+5_{[m]}) - (-1_{[m]})}{(20_{[mA]}) - (4_{[mA]})} \times \left( \frac{x_{[Volt]}}{120_{\Omega}} \times 1000 \right)^{-2.5}$$

**Equation 4.3**

$$Y_{[m]} = \frac{(+1_{[m]}) - (-1_{[m]})}{(20_{[mA]}) - (4_{[mA]})} \times \left( \frac{x_{[Volt]}}{120_{\Omega}} \times 1000 \right)^{-1.5}$$

**Equation 4.4**

The frequency of both sets of pressure transmitters was 20 Hz, with an accuracy of 0.5% of the total pressure range, thus 30 mm for the 20 mA pressure transmitter and 10 mm for the 4 mA pressure transmitter (model values).

#### **4.3.2 Air Velocity Measurements and Direction Indicator**

The air velocity in the air vent was measured by means of a Lutron hot-wire anemometer. The probe of the anemometer has a wire, which is heated. The anemometer measures the cooling rate of the wire when air is blowing over it, and this is converted to air velocity (m/s). Refer to **Appendix C1** for a photo of the anemometer used in the study.

The combination of the hot wire and the standard thermistor of the anemometer deliver rapid and precise measurements, even at low air velocities. The measurement range of the anemometer is between 0.2 m/s and 20 m/s, which are measured at a resolution of 0.1 m/s. It has a  $\pm 5\%$  accuracy over the total measurement range (0.2 m/s to 20 m/s), thus 0.99 m/s. The apparatus has a frequency of 0.8 Hz.

A wind direction indicator that was constructed by Stellenbosch University was installed in the top section of the air vent in order not to impose on the air velocity within the air vent. This apparatus had a mechanical flap that would be in the zero position (horizontal) if no wind was blowing in the air vent and would be directed in the direction of the wind if air was being sucked into or released from the air vent. Air sucked into the conduit was indicated by a positive sign (+), and air released from the air vent by a negative sign (-).

The wind direction indicator was not accurate for air velocities less than 0.5 m/s (in the physical model translating to 1.87 m/s in the prototype).

#### **4.3.3 Water Discharge Measurements**

The water flow discharge for fixed gate openings was measured with an electromagnetic flow meter (SAFMAG).



## 4.4 Experimental Controls

### 4.4.1 Water Supply

The required water flow was supplied through a pipe that was linked to a constant pressure tank and a pump. The supply system fed the water into the model by pouring the water into the stabilisation tank. The flow approaching the inlet shaft was smoothed by installing a perforate plate and net (acting as baffles) in the stabilisation tank, as shown in **Figure 4-4** below.

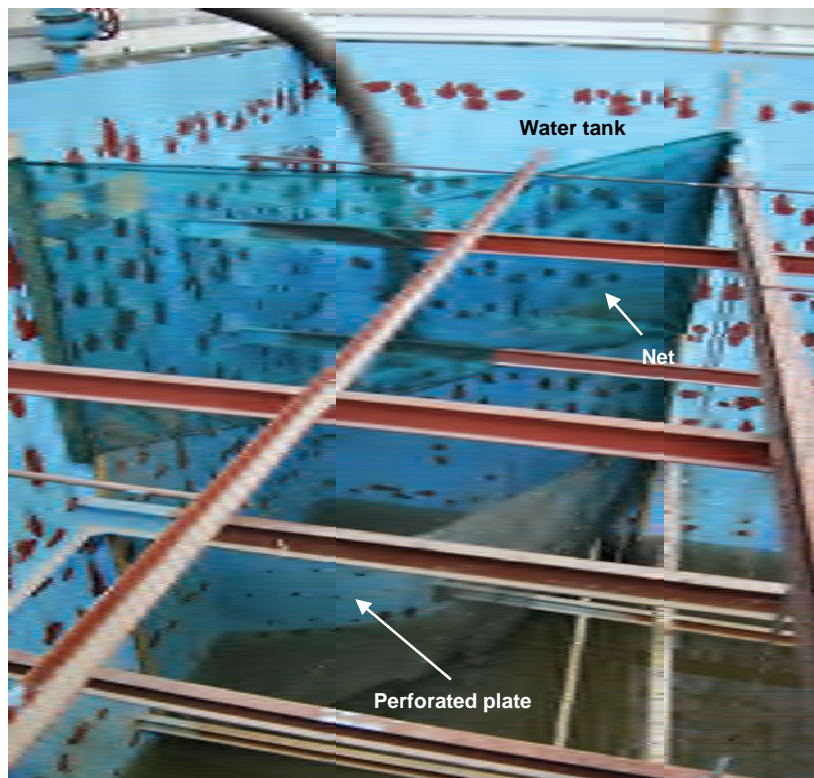


**Figure 4-4: Top view of water tank**

### 4.4.2 Water Levels

The required water flow was obtained by keeping the water level in the tank constant at the water level under evaluation. A tolerance of 50 mm upwards and 50 mm downwards (0.7 m in prototype) of the water level in the water tank was deemed acceptable as the level in the water tank of the model was controlled by hand (the inlet valves were slightly closed when a rise in water level was observed and vice versa when the water level went down). **Figure 4-5** shows the inlet pipe and manually operated valve for the model.



**Figure 4-5: Model inlet pipe and valves**

#### **4.4.3 Selector Gates**

Only the upper two pairs of selector gates (refer to **Appendix A**) of the wet well were fully open for the duration of all the tests performed on the model, as was the case in the field during the commissioning test in 2008.

#### **4.4.4 Emergency Gate**

An electric motor was used to close the emergency gate in order to obtain the required gate closure rate. The emergency gate of the model was never fully closed (smallest gate opening: 20% open), as it was feared that the gate made of Perspex may be damaged under the full pressure load of the water in the tank.

#### 4.4.5 Radial Gate

The tests were performed with the radial gate fully open, as the emergency gate was designed to be used when the radial gate fails to close.

It is unclear whether this was the case during the commissioning test in 2008. The stage discharge rating curve (attached in Appendix F) indicates that the maximum discharge through the Berg River Dam on the day of the tests was  $204 \text{ m}^3/\text{s}$  which would require the radial gate to be slightly closed (The maximum discharge through the model was equivalent to  $256 \text{ m}^3/\text{s}$  in the prototype). However, the accuracy of the measuring station directly below the dam is not known for such high discharges and some of those present at the tests report that the radial gate was indeed completely open during the tests (Basson, 2012).<sup>2</sup>

### 4.5 Experimental Procedure

The aim of this research was to find the cause of the air reverse flow in the air shaft of the Berg River Dam's bottom outlet. Accordingly a number of tests were initially performed on the as-built configuration of the bottom outlet to investigate possible vortex formation upstream of the gate as well as other possible reasons for the air reversal in the air shaft. Thereafter tests were performed on a number of modifications to the as-built outlet to determine possible ways of solving or mitigating the air reversal problem. The procedures for each of the tests on the as-built outlet are discussed below. The configurations of the modifications are presented in Section 5.3 after the results of the as-built tests.

#### 4.5.1 Stationary Emergency Gate Opening Simulations

Tests were conducted on the model (according to as-built drawings), initially with stationary emergency gate openings in order to examine the water and air flow requirement for each gate opening under steady flow conditions. The stationary gate openings used were as follows:

---

<sup>2</sup> Subsequent tests were performed with a radial gate slightly closed to ensure a flow of  $204 \text{ m}^3/\text{s}$ . This only required the gate to be closed by 200 mm, and lead to almost identical results. This test is presented in Appendix G.

- 80% open
- 70% open
- 60% open
- 50% open
- 40% open
- 30% open
- 20% open

The water level in the tank was kept constant at a level that corresponded with the water level measured during the commissioning test in 2008 (237.5 masl).

The gate was lowered slowly between each gate opening interval, after which there was a pause of approximately two minutes in order for the flow conditions to stabilise (no ripples or waves on the water surface in the water tank)

#### 4.5.2 Transient Gate Closing Simulations

A total of 29 tests were conducted on the model with its configuration according to the as-built drawings. The air flow in the air vent, water discharge and pressures in the conduit were measured.

Four different gate closure times were used in the tests, namely:

- Four minutes and 16 seconds (for 100% gate opening to 20% gate opening). This gate closure rate is equivalent to full closure in **20 minutes for the prototype**, which corresponds to the gate closure rate used at the commissioning test of 2008. (Refer to Section 4.2 for the equation of the time scale relationship between the model and the prototype.)
- Two minutes and 30 seconds (for 100% gate opening to 20% gate opening), which is equivalent to full closure in **12 minutes for the prototype**, which corresponds to the designed emergency gate closure rate according to the design report for the Berg River Dam (Van Vuuren, 2003).
- One minute and 17 seconds (for 100% gate opening to 20% gate opening), equivalent to full closure in **6 minutes for the prototype**.
- Six minutes and 24 seconds, (100% gate opening to 20% gate opening), equivalent to full closure in **30 minutes for the prototype**.

The initial gate closure rates for 12 minute and 20 minute closures were selected on the basis of the design manual for operating the emergency closing gate and the emergency gate closure rate used in the Commissioning Test of 2008 respectively, as listed above. Further rates were selected as the experimental work progressed, namely six minutes and 30 minutes. However, it was found that the movement of air (air velocity released or sucked into air vent) through the air vent was not sensitive to the closure rate, but was directly related to the water head (higher head = higher velocity). Given this, the initial tests were not redone to include the six minute and 30 minute closure rates.

These tests were also conducted at three different water levels for each of the four abovementioned gate closure rates. The water levels are summarised in **Table 4-2** below.

**Table 4-2: Water Levels**

WATER LEVEL NAME	PROTOTYPE (masl) [Datum = sea level]	MODEL (m) [Datum = bottom of outlet conduit]
Full supply water level	250.0	3.8
Commissioning water level	237.5	2.9
Lower water level	232.3	2.5

The *full supply level* is the level of the dam spillway.

The *commissioning water level* corresponds to the water level that was measured in the field during the commissioning test of the Berg River Dam in June 2008.

The level where vortices started to form in the water tank (vortex water level) was determined to be 227.12 masl. This is 0.12 m (prototype) above the soffit of the vertical selector gates. The *lower water level* mentioned in **Table 4-2** was taken halfway between the commission test water level and the vortex water level.

### **4.5.3 Vortex Formation Test with 100% Open Gate**

A test was performed on the as-built configuration with the gate 100% open to specifically investigate possible vortex formation upstream of the gate.

During this test the water level was initially set at the commissioning level, and the wet well was stirred in an attempt to induce vortices<sup>3</sup>. Thereafter the water level was gradually lowered to the point where vortices formed to determine the vortex formation level.

---

<sup>3</sup> Here a vortex is referred to as a rotational flow of water which sucks air right down into the outlet conduit, and not merely as any rotational flow.

## 5. RESULTS

In order to verify the model of the as-built Berg River Dam outlet would be to calibrate it with prototype recordings. The only data available for this purpose at the time of writing were the observations of air flow during the commissioning tests. The record of the commissioning tests will first be presented and its suitability for calibration discussed. Thereafter the results of tests on the as-built outlet are given, before the tests on modified model configurations are discussed.

### 5.1 Air Flow Recordings from Commissioning Test on As-built Prototype

The original report on the commissioning test is attached in Appendix B. For this test the water level was 237.5 masl (commissioning level), and the gate was closed in 20 minutes.

**Figure 5-1** below shows the observed air velocity versus percentage gate opening for the test.

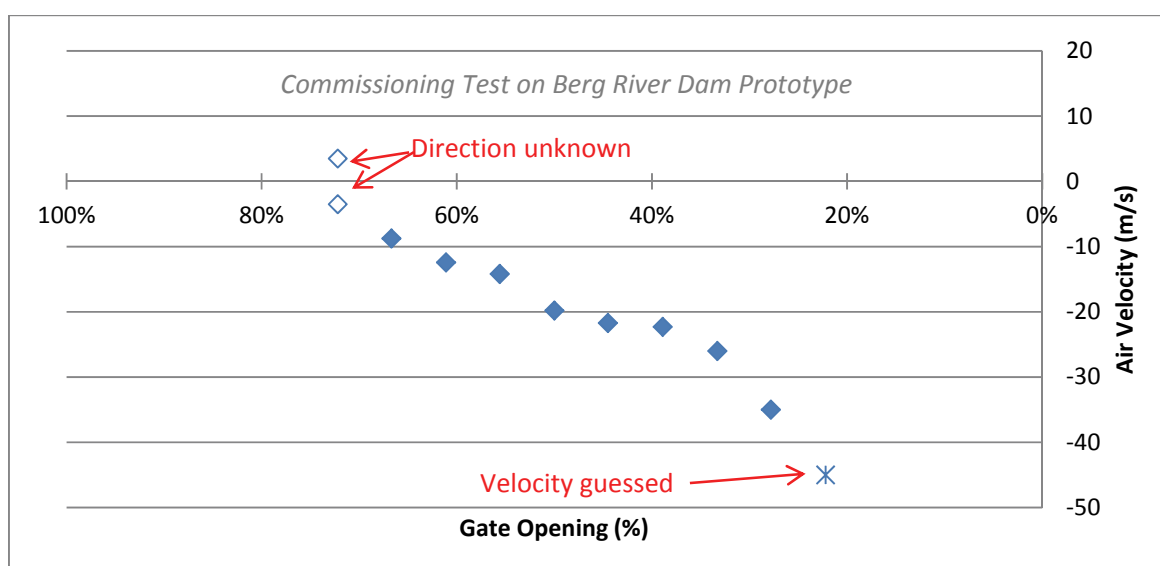


**Figure 5-1: Air Velocity versus Gate Opening for Commissioning Test on Berg River Dam Prototype**

There were a number of deficiencies in the air flow observations. These include

- i. Measurements were taken by a hand held anemometer which can only measure velocity and not direction.
- ii. The velocities were recorded once every minute and not continuously.
- iii. Although outflow surges were observed at approximately 6 second intervals it is not certain whether air inflow occurred between outflow surges. Cyclic in-out behaviour

can only be recorded by continuous measurement with both velocity and direction sensors. The human experience of outflow is more obvious than inflow which is more subtle (see **Figure 5-2**).

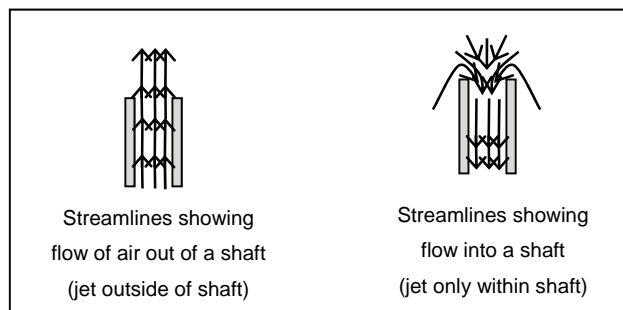


**Figure 5-2: Flow Patterns at the End of an Air Shaft**

- iv. Velocities were only recorded for part of the closure period.

From these deficiencies, the suitability of the commissioning air flow velocities for calibration purposes is doubtful. To date no other tests have been performed on the prototype and it is unlikely that any will be allowed in the near future as such testing could pose an unnecessary risk to the structure.

## 5.2 As-Built Outlet

### 5.2.1 Stationary Emergency Gate Opening Tests

Tests were initially performed on the as-built model at selected fixed gate openings to investigate the flow patterns under steady conditions. The recorded air velocities (with direction), and pressures for these tests are plotted against the percentage emergency gate opening in **Figure 5-3** and **Figure 5-4** below respectively. No vortices were observed upstream of the gate at any of the gate openings.

During these steady-state tests no outflow of air was recorded. It was thus concluded that the air reversal effect only occurs during continuous closure and cannot be studied by stationary gate openings.



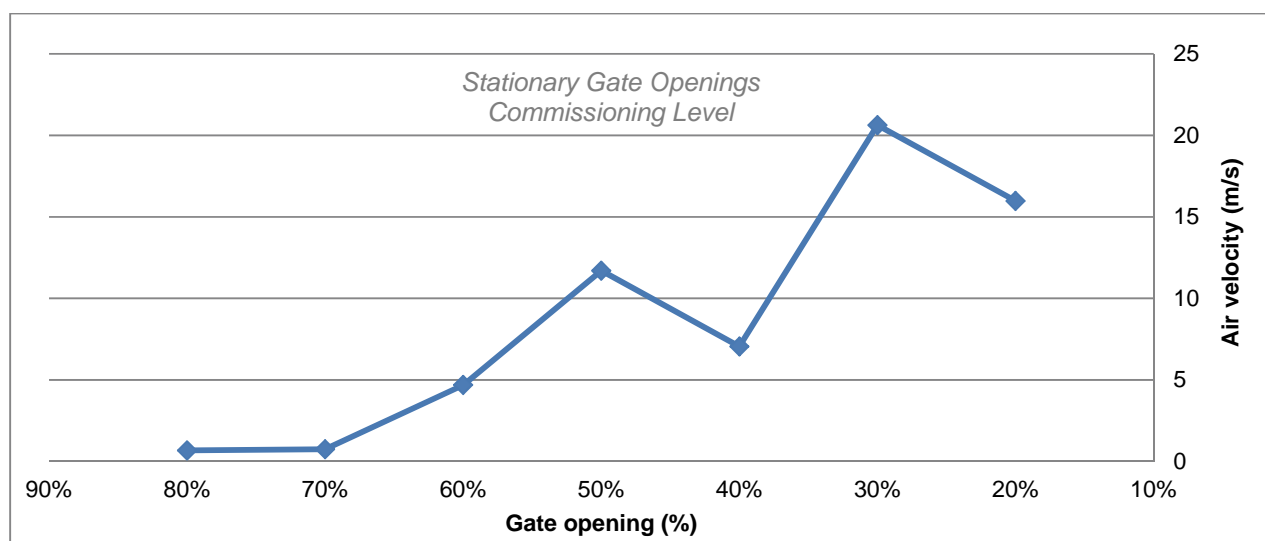


**Figure 5-3: Air velocity versus Gate Opening for Stationary Gate Openings**

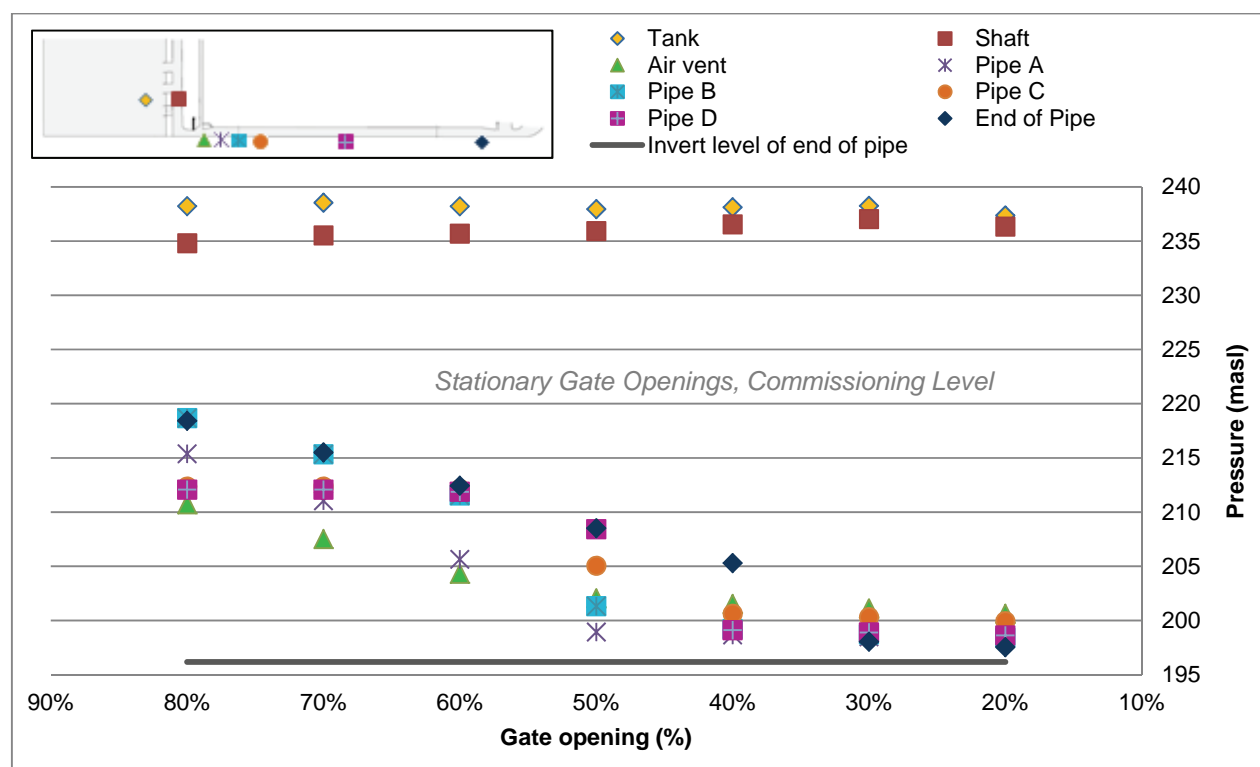


**Figure 5-4: Pressure versus Gate Opening for Stationary Gate Openings**

## 5.2.2 Continuously Closing Emergency Gate Tests

After the stationary gate tests, the gate was fitted with a motor which allowed it to be closed at a constant speed. Tests were performed at various closure rates for three different water levels as described in Section 4.5.2 above.

### 5.2.2.1 Air Velocity and Pressure Results

The air velocity at the air vent and the pressures at various points in the model were recorded continuously for the closing gate tests. The air velocity and pressure values (converted to prototype values) are plotted against percentage gate opening in the graphs which follow. Note that on the air velocity curves air flow into the model (down the air shaft) has been taken as positive.

#### 5.2.2.1.1 Commissioning Water Level

**Figure 5-6** below shows the air velocities recorded for tests of 3 different closure rates on the model for a water level of 237.5 masl (commissioning level), as well as the prototype commissioning test airflow results. For gate openings between 100% and 70%, the air vent acted as a surge tower and the water oscillations in the air shaft caused oscillating air flows of low velocity. Thereafter air flowed into the conduit with an increasing velocity until a gate opening of approximately 35%. Between openings of about 35% and 25% the direction of flow in the airshaft changed rapidly (approximately 0.2 Hz in the prototype). For the 20 minute closure, these fluctuations occurred over a period of about 1.5 minutes (prototype) resulting in approximately 18 blow-back flow reversals.

These results show a very different air flow pattern to the prototype commissioning tests. All recorded velocities are lower than those recorded in the prototype, and the majority of the air flow is in the opposite direction. The lower air velocity magnitude may be due to scale effects, and the distinctions in flow direction may be due to human error during the prototype commissioning tests.

**Figure 5-6** directly below the air velocity graph shows the corresponding pressures recorded for the 20 minute closure test at the commissioning level. (The pressure graphs for the other closure rates are shown in Appendix E). Note that the sensors at “Pipe D” and “Pipe E” were at their maximum range for the first half of the test, and therefore do not give accurate readings.

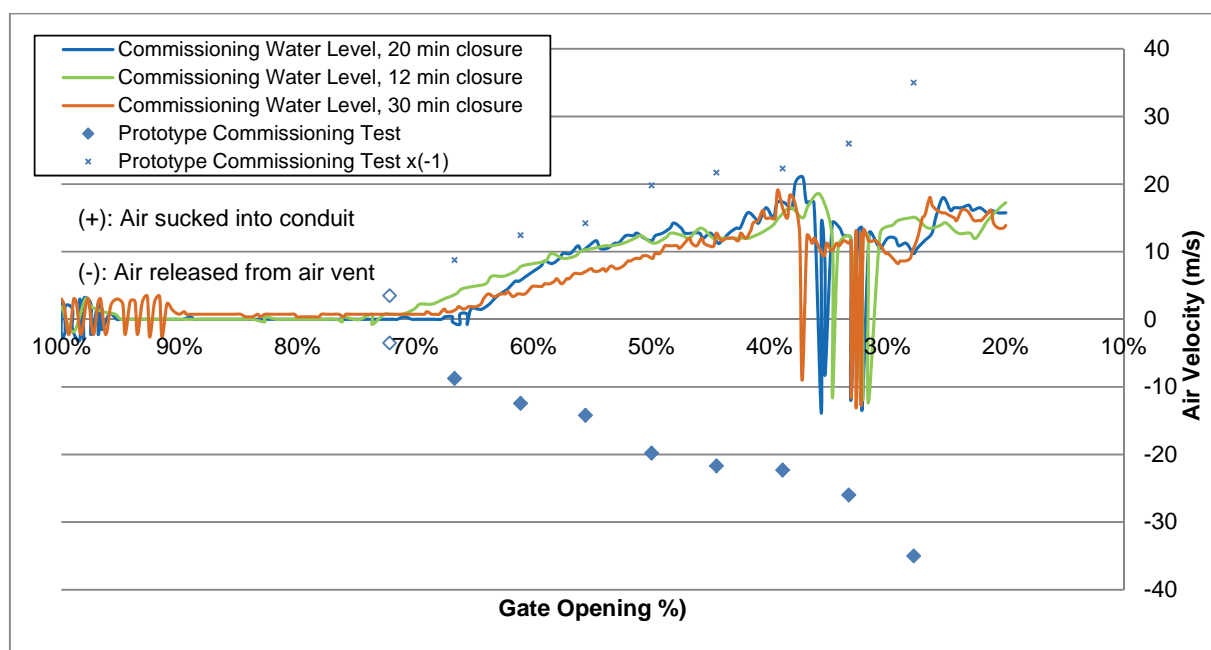


**Figure 5-5: Air Velocity versus Gate Opening for Closing Gate Simulations at the Commissioning Water Level**

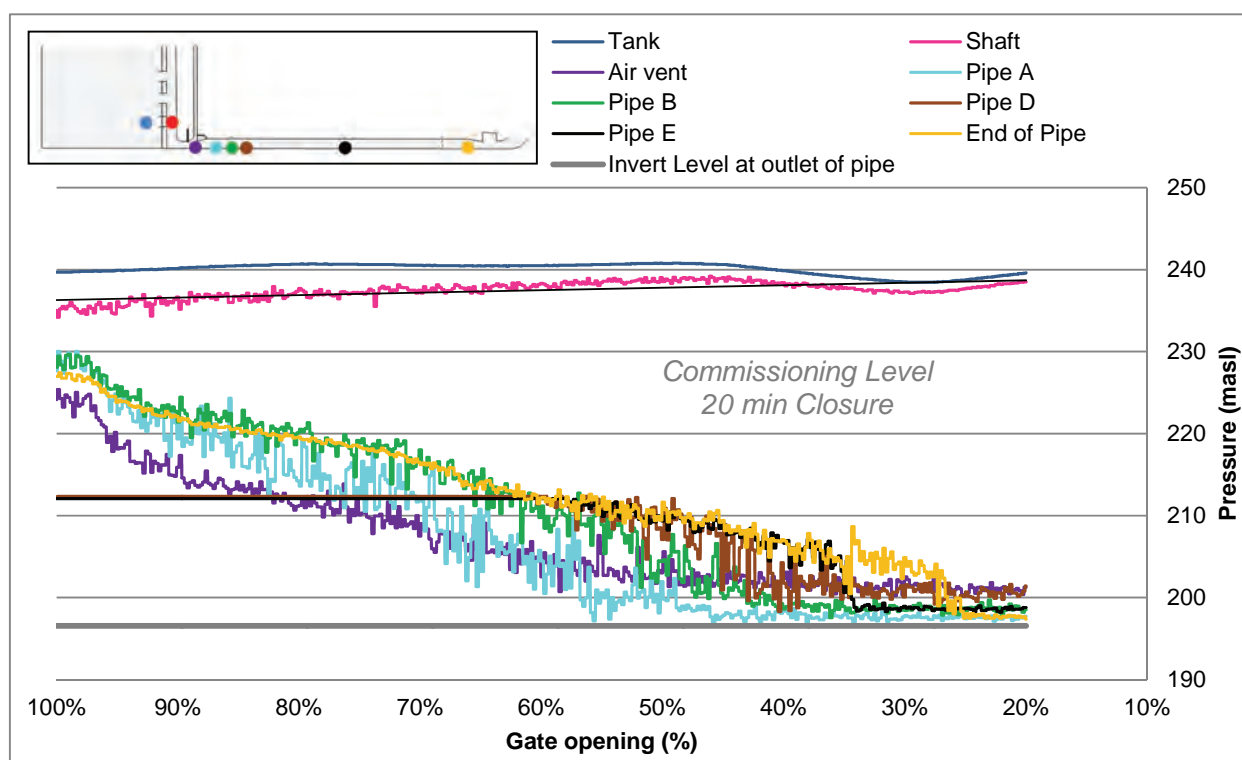


**Figure 5-6: Pressure versus Gate Opening for Simulation of 20 minute Closure at the Commissioning Water Level**

### 5.2.2.1.2 Full Supply Level and Lower Water Level

**Figure 5-7 to Figure 5-10** below show the air velocity and pressure graphs for the full supply level (250 masl) and the lower water level (232.3 masl). Here, again, the pressure graphs are only shown for the 20 minute closure time (pressure graphs for other closure speeds are in Appendix E).

The flow patterns observed were similar to those for the commissioning water level (discussed in the previous section). Further, it can be seen that the air velocities were not sensitive to the gate closure rate, but increased with an increasing water level. The maximum velocity recorded for the full supply level was 36.4 m/s, safely below the maximum recommended velocity of 45 m/s (USACE, 1963).

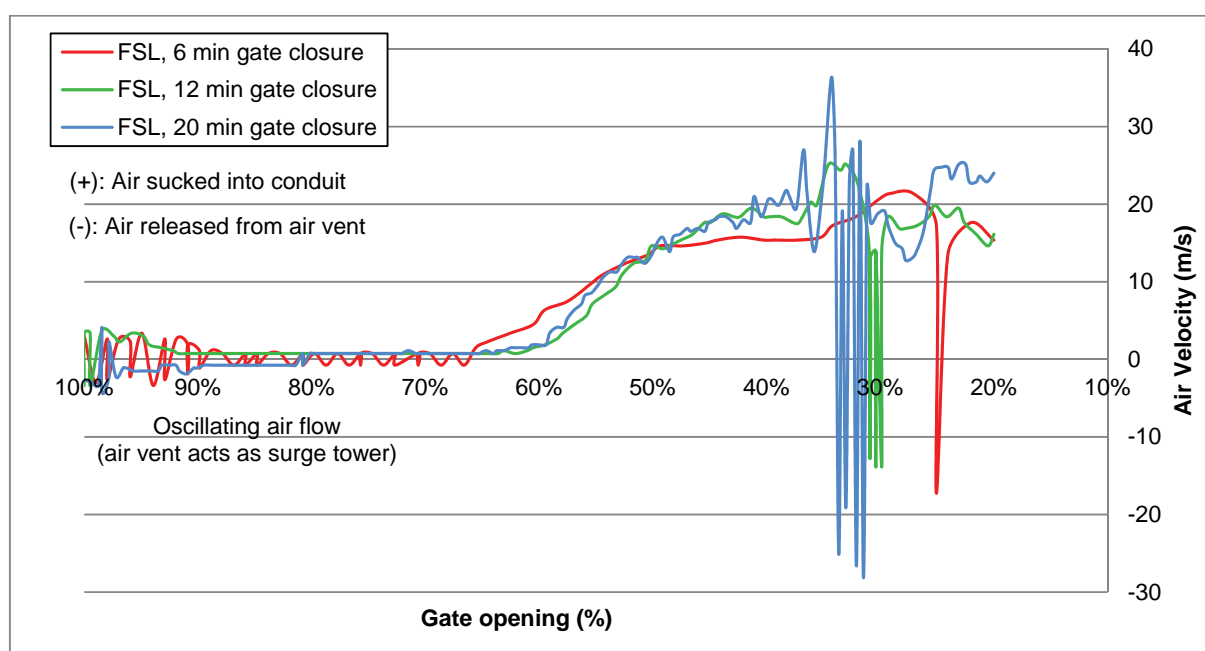


**Figure 5-7: Air Velocity versus Gate Opening for Closing Gate Simulations at the Full Supply Water Level**

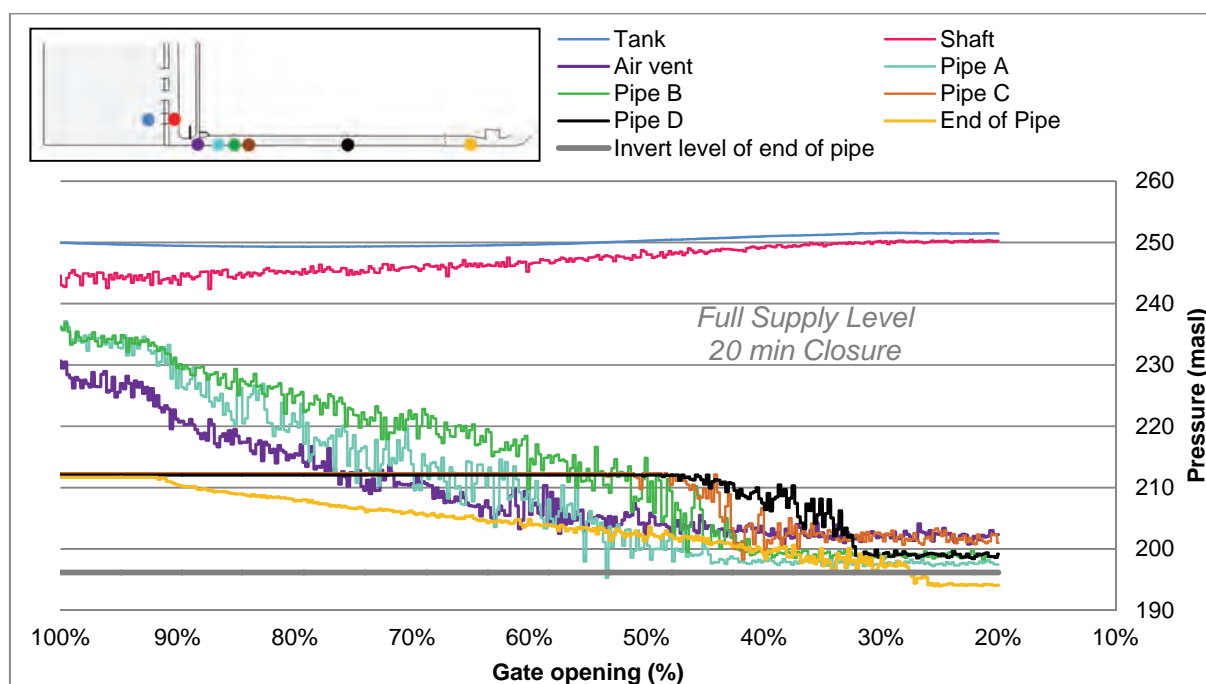


**Figure 5-8: Pressure versus Gate Opening for Simulation of 20 minute Closure at the Full Supply Level**

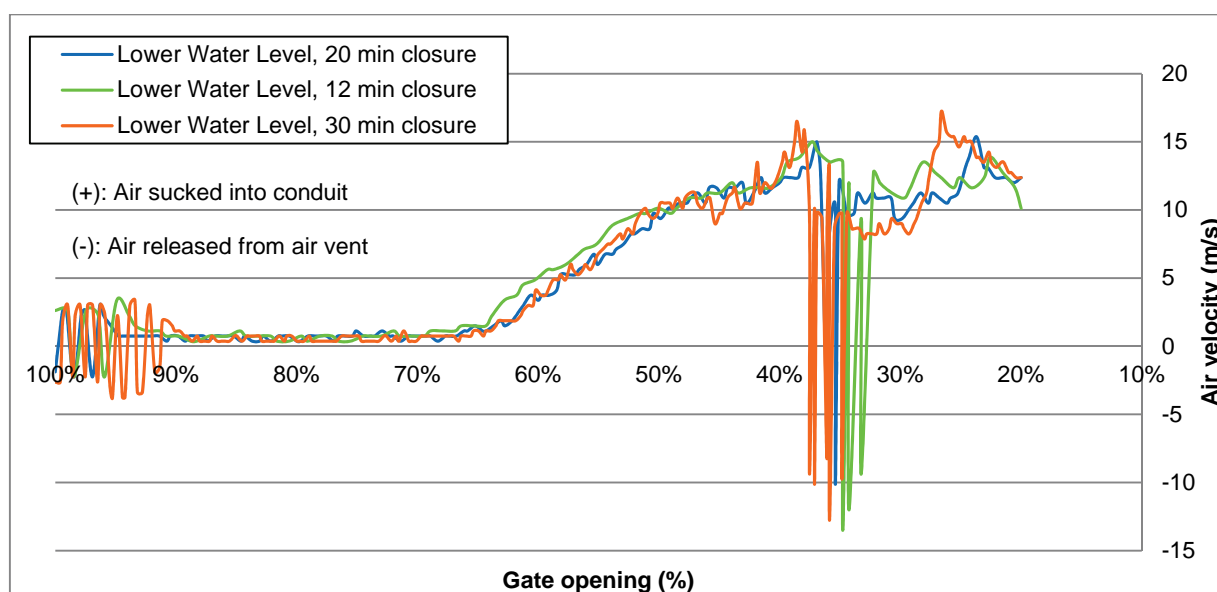


**Figure 5-9: Air Velocity versus Gate Opening for Closing Gate Simulations at the Lower Water Level**

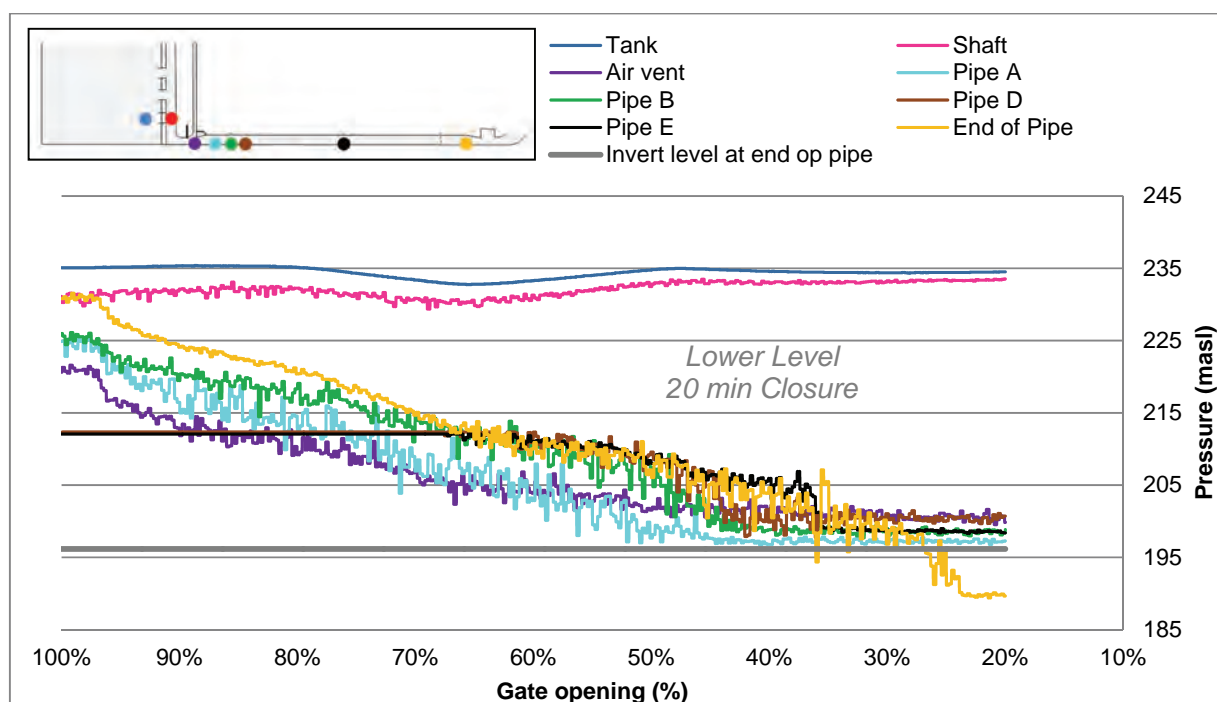


**Figure 5-10: Pressure versus Gate Opening for Simulation of 20 minute Closure at the Lower Water Level**

### 5.2.2.2 Observed Flow Patterns

The flow patterns were similar for all of the tests with a continuously closing gate. A description and explanation of the flow patterns during emergency gate closure is given in **Table 5-1** and **Figure 5-11** below.

From the observations it seems most likely that the cause of the air reversals is the constriction of flow at the radial gate chamber.

**Table 5-1: Description of Flow Patterns for Closing Gate Simulations**

Opening	Description of Flow
100% to 70%	<ul style="list-style-type: none"> <li>Pressurised flow occurs throughout the outlet conduit</li> <li>No air entrainment through the air vent</li> <li>The air vent acts as a surge tower. Initially the water level oscillates in the air vent with a period of 15 seconds (prototype). As the gate closes the water level in the air vent decreases and the oscillations become more irregular.</li> </ul>
70% to 40%	<ul style="list-style-type: none"> <li>Air entrainment through the air vents starts when the gate is 70% open.</li> <li>An unstable hydraulic jump forms just downstream of the emergency gate where flow conditions change from free surface flow to pressurised flow. This hydraulic jump remains “trapped” just upstream of the first bend in the conduit until the gate opening reaches 40%.</li> <li>The roof of the conduit slopes downwards at the end of the conduit to accommodate the radial gate chamber. This tapered section restricts the free release of entrained air at the end of the conduit. Pockets of air thus accumulate under pressure at the downward sloping ceiling and are periodically released giving a pulsating effect. The frequency and intensity of these pulsations increases as the gate closes, and causes vibration in the radial gate chamber.</li> </ul>
40% to 30%	<ul style="list-style-type: none"> <li>At a 40% opening the unstable hydraulic jump is pushed past the first bend in the conduit and begins to move downstream. Free surface flow develops downstream of the hydraulic jump but air still accumulates at the tapered section before the radial gate. The release of air in pulses at the radial gate chamber continues but the rate at which air is released is less than the rate at which it is transported down the conduit by the flow (predominantly as a result of the air-water shear forces discussed in Section 3.3.4.1), so the pressure rises.</li> <li>Between 37% and 32% gate openings the jump intermittently breaks contact with the roof of the conduit (due to reduced discharge and increasing air pressure from behind the jump), and pressurised air from downstream in the conduit is released back upstream and out the airshaft. The hydraulic jump moves downstream with a high velocity as the wetted perimeter is less than when the conduit is flowing full, resulting in less friction.</li> <li>The hydraulic jump becomes trapped again at the radial gate constriction at about 30% opening.</li> <li>The air velocity in the airshaft is highest over this period, and changes direction rapidly as pulses of air are expelled while the unstable hydraulic jump is moving downstream.</li> </ul>
30% to 20%	<ul style="list-style-type: none"> <li>Spray flow occurs just downstream of the emergency gate</li> <li>The unstable hydraulic jump gets pushed out of the conduit between a gate opening of 25% and 20%. Thereafter, free surface flow occurs along the entire outlet conduit.</li> </ul>
All Openings	<ul style="list-style-type: none"> <li>No vortices were observed in the wet well</li> <li>Air movement in air shaft insensitive to gate closure rate but dependent on the tank water level.</li> </ul>

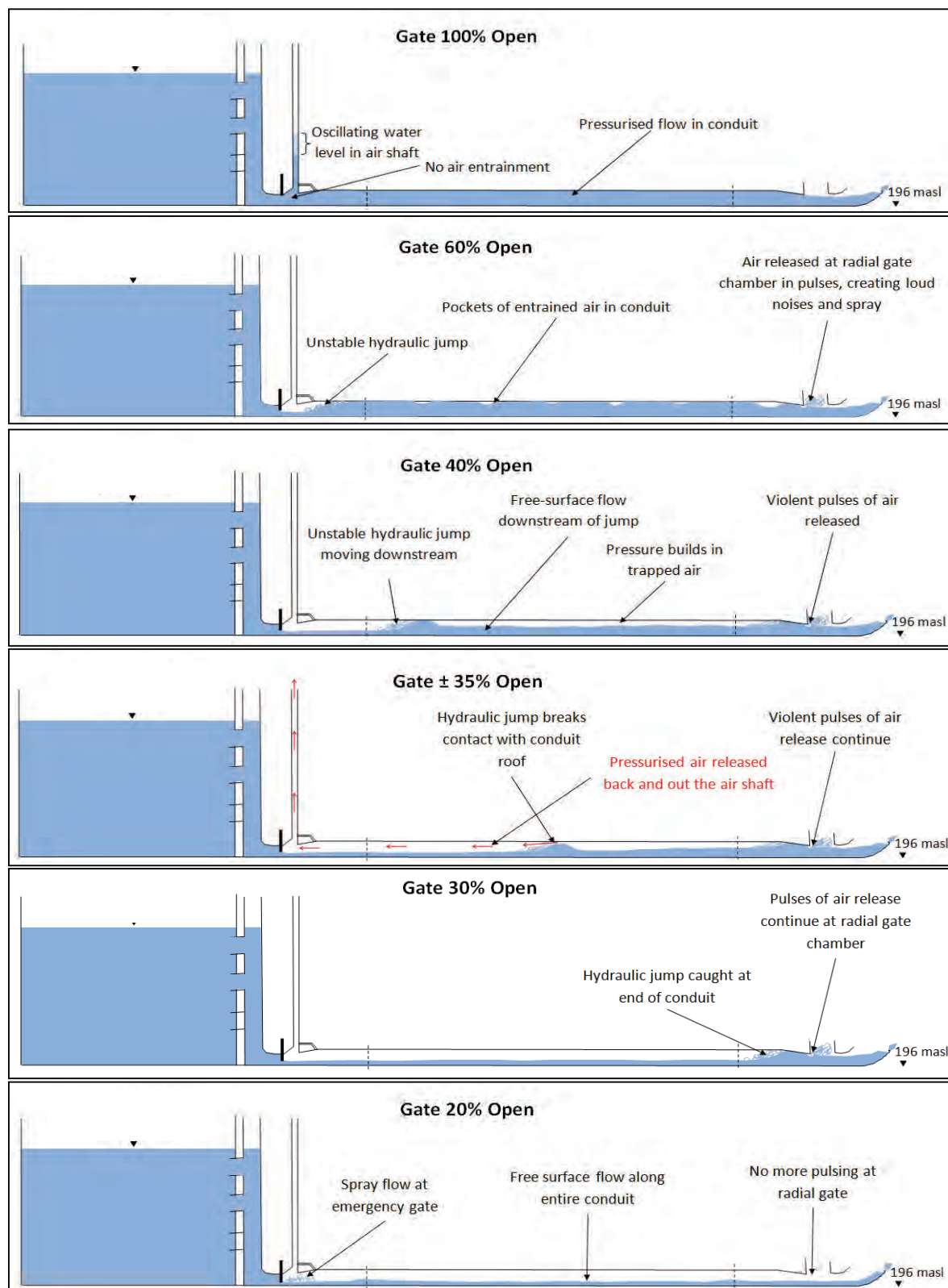


**Figure 5-11: Sketches of Flow Patterns for Closing Gate Simulations**



### 5.2.3 Vortex Formation Test

In the report on the commissioning tests on the Berg River Dam Prototype (Appendix B), vortex formation is cited as the most likely cause of the outflow of air from the air shaft. However, during all of the stationary gate opening tests, and continuously closing gate tests on the model no vortices were observed.

To test further for vortex formation, the water in the wet well was stirred while the emergency gate was 100% open and the water level was at 237.5 masl (commissioning level). Still, no vortices were formed.

The water level was then lowered slowly until vortices were formed. The highest level at which vortices form was found to be 227 masl (10.5 m lower than the commissioning level). At this level all the air sucked into the outlet through the vortices travelled down the conduit and was released downstream.

A test closure of the emergency gate (20 minute closure) was also performed at the vortex formation level (227 masl), the full results of which can be found in Appendix G. During this test there was no outflow of air from the air shaft, and all the air entrained through vortices travelled down the conduit.

### 5.2.4 Conclusions from Tests on As-built Model of Outlet

From the tests on the as-built outlet it can be concluded that the air flow through the airshaft is predominantly inwards, except for gate openings of between about 35% and 25% while the gate is being closed during which period air reverse flows (blow-back) occur approximately every 5 seconds (but irregularly). Instead of a problem of continuous air release through the air shaft (as suggested by the prototype tests), the problem was found to be air flow reversals in the air shaft (or air *blowback*).

The air velocity in the air shaft is not affected by the rate of closure of the emergency gate but increases with increasing water head. The maximum air velocity recorded (for the full supply level) was 36.4 m/s, sufficiently below the maximum recommended velocity of 45 m/s, therefore the size of the air shaft is deemed adequate.

It was found that vortex formation does not occur except at very low water levels, and the most likely cause of the air flow reversal is the constriction at the radial gate chamber.

### 5.3 Modified Model Configurations

In order to confirm the cause of the air flow reversals and to investigate possible solutions, a number of tests were performed on modified model configurations. Although the expected cause of the reversals was the constriction caused by the radial gate chamber, the ski jump and the second bend in the conduit were also identified as components possibly having an effect on the flow. **Figure 5-12** below shows the configurations of the modified model configurations tested. For each of these configurations a series of tests of different closure rates was performed with the commissioning level. The other levels were not tested as the previous tests showed they produced similar trends.

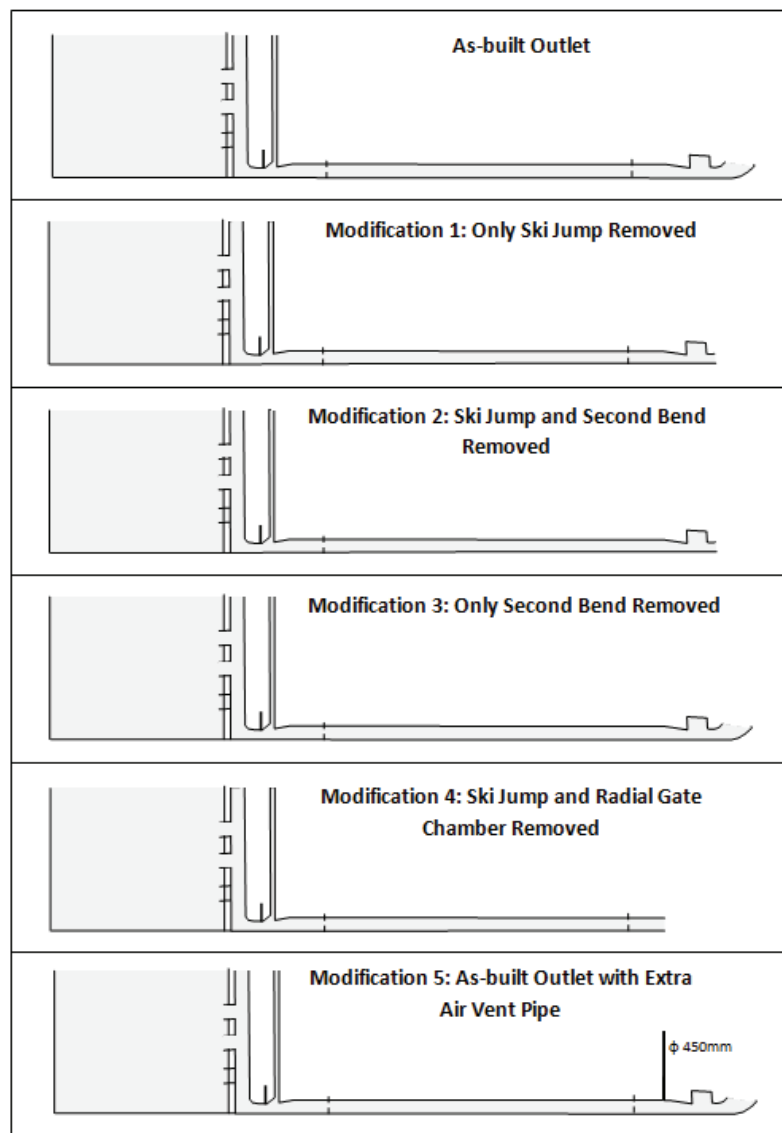


**Figure 5-12: Modified Model Configurations**

### 5.3.1 Removal of Ski Jump and Second Bend

It was found that the removal of the ski jump and the second bed had very little effect on the flow in the conduit. The results of the tests on Modification 1, 2 and 3 from **Figure 5-12** showed very similar trends to those on the as-built outlet and are contained in Appendix D & E.

### 5.3.2 Removal of the Radial Gate Chamber

Removal of the radial gate chamber was found to have a significant effect on the flow patterns in the conduit and to eliminate the air reversals in the air shaft.

The air velocity and pressure versus gate opening graphs are shown in **Figure 5-13** and **Figure 5-14** below respectively. As for the results on the as-built outlet, the air velocity results for various closure times, and the pressures for a 20 minute emergency gate closure are shown. The dashed lines on the graphs show the results from the as-built outlet for comparison purposes.

Without the radial gate constriction, the air velocity is greatest when the gate is 100% open, and gradually reduces as the gate is closed. No air reversals in the air shaft occur. The pressures observed in the conduit are also much lower than those experienced in the as-built tests. This is because free-surface flow occurs throughout the test, instead of partially pressurised flow which occurs when the outlet is constricted. **Figure 5-15** below shows a comparison between the observed flow in the as-built outlet and the modified outlet by the way of sketches at gate openings of 100% and 35%.

Without the constriction at the radial gate chamber the maximum air velocity through the air shaft is significantly higher than for the as-built outlet. The maximum recorded velocity during tests for the commissioning water level of 237.5 masl was 45 m/s (the maximum recommended velocity for air shafts (USACE, 1963)). For higher water levels this velocity is expected to be higher, implying that a larger air shaft would be preferable.

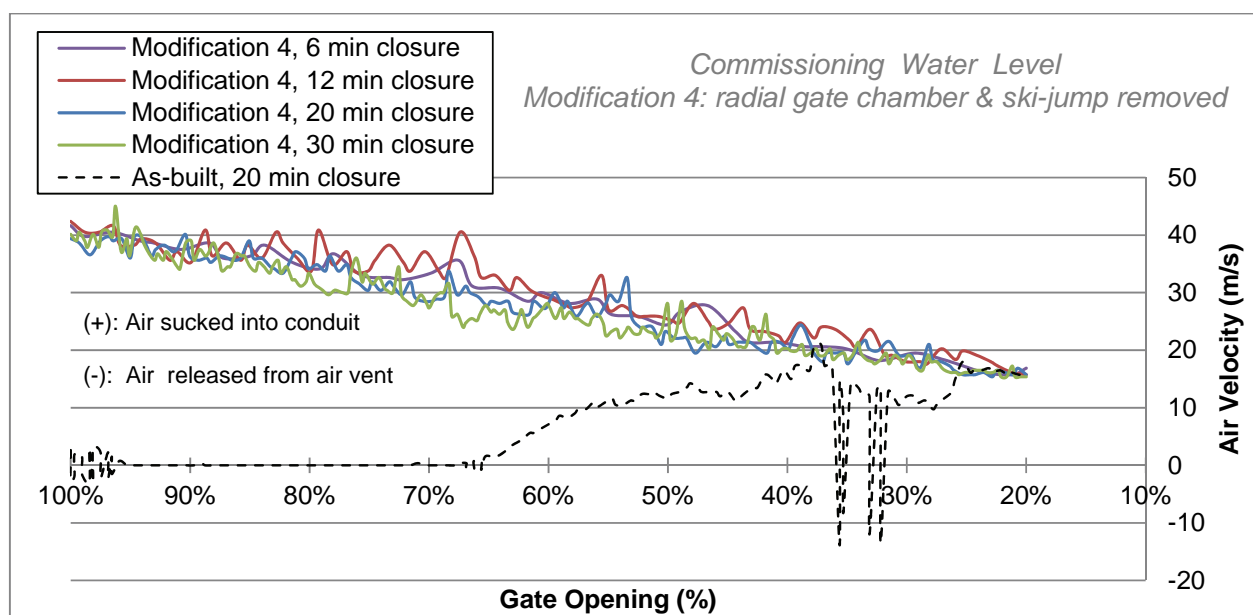


**Figure 5-13: Air Velocity versus Gate Opening for Tests on Conduit with Ski-jump and Radial Gate Chamber Removed (Modification 4)**

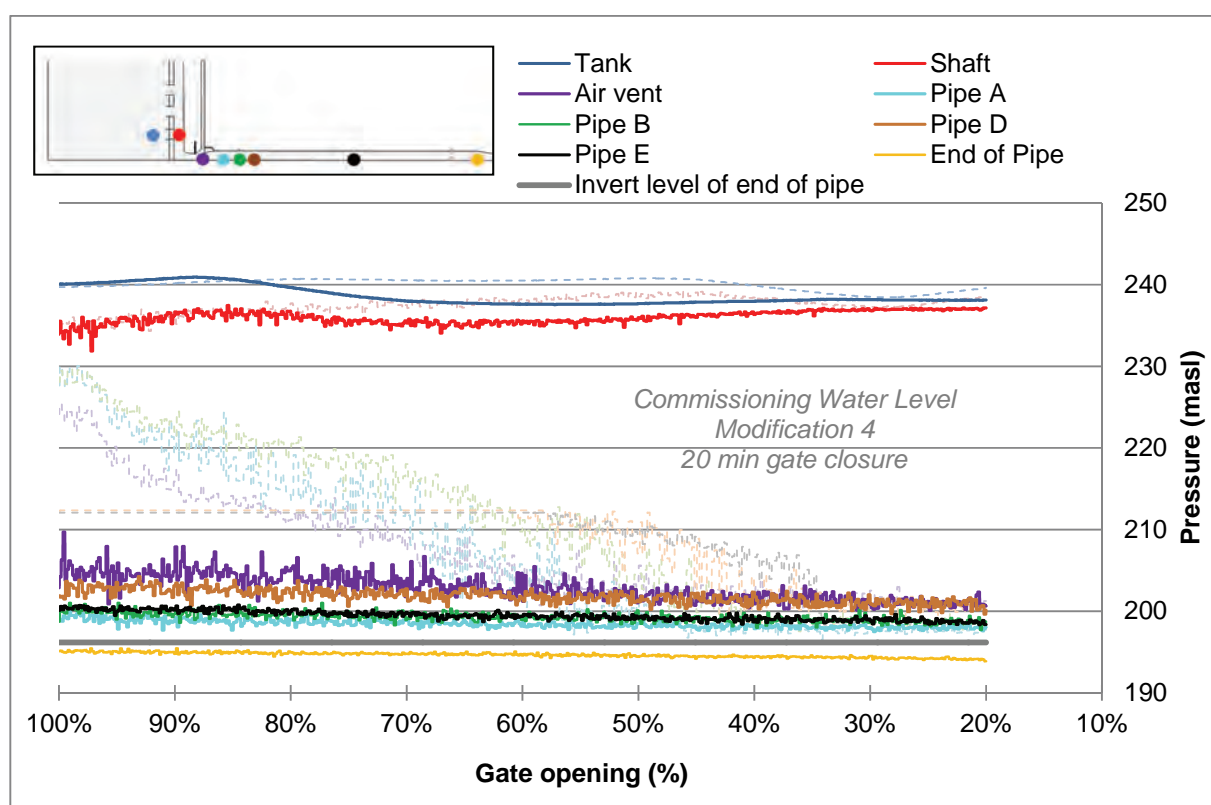


**Figure 5-14: Pressure versus Gate Opening for Tests on Conduit with Ski-jump and Radial Gate Chamber Removed (Modification 4)**

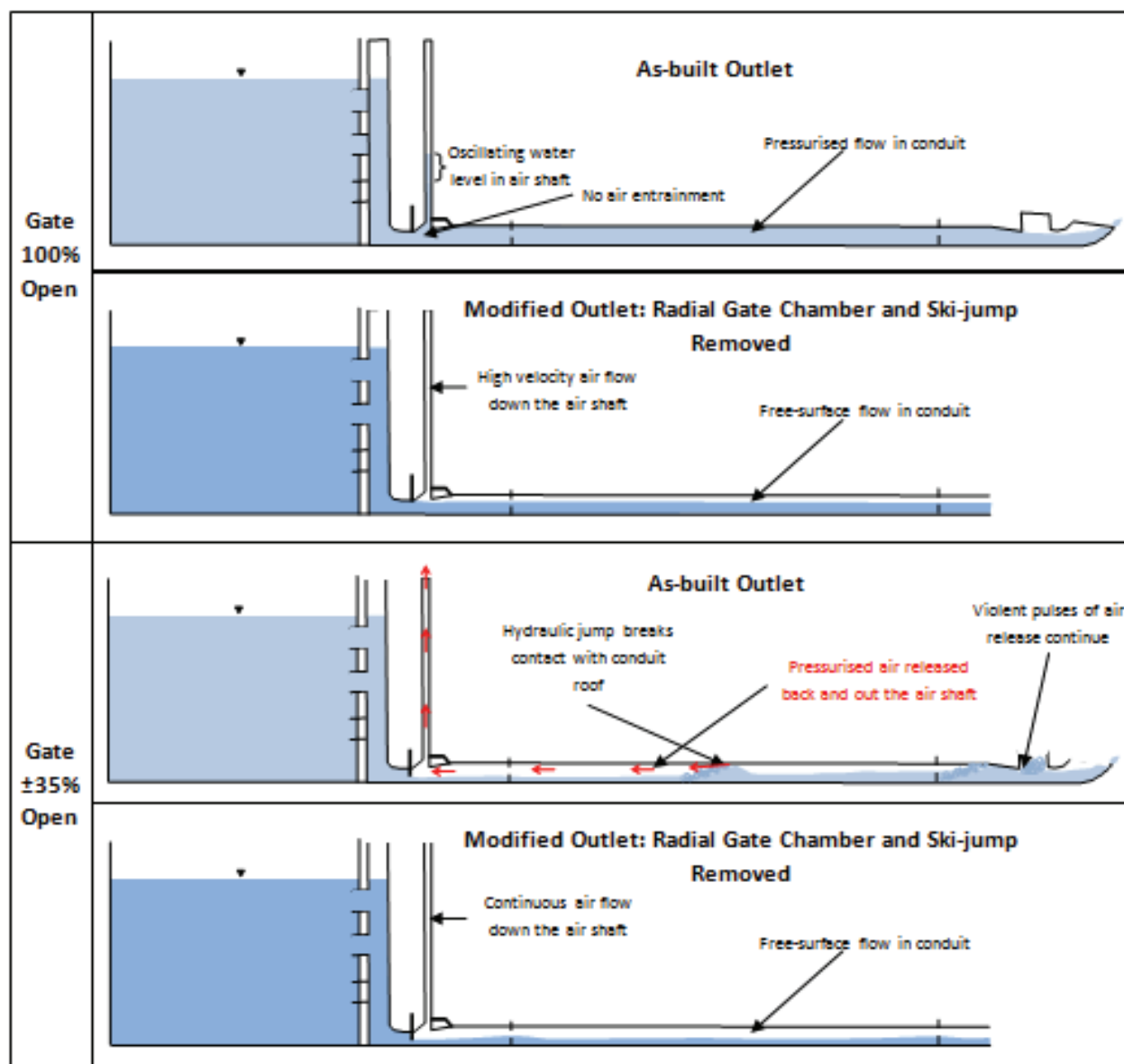


**Figure 5-15: Sketches of Flow Patterns for As-Built Conduit and Modified Conduit with Radial Gate and Ski-jump Removed**

### 5.3.3 Provision of Extra Air Vent at the Radial Gate Constriction

Once it was confirmed that the radial gate constriction was the cause of air flow reversals in the air shaft, it was suggested that an additional air vent placed immediately before the constriction for the radial gate chamber may solve/reduce the air blowback problem. If effective this would possibly be a practical retro-fit solution for the Berg River Dam prototype.

For the tests a 450 mm (prototype) diameter pipe was fitted directly onto the as-built conduit, and tests were performed for a 20 minute closure at the commissioning water level (237.5 masl). **Figure 5-16** below shows a sketch of the downstream end of the outlet with this pipe fitted.



**Figure 5-16: Extra Air Vent Configuration Tested**

In these tests the extra air vent pipe was found to be ineffective in reducing the blow back effect, and the air-flow and pressure results were very similar to those of the as-built tests. During the test water got caught in the extra air vent pipe and blocked the free release of air. For the critical gate openings of 35% to 25% (while the air reversals were experienced in the upstream air shaft), an air-water mixture was intermittently expelled from the extra air vent in an explosive fountain display, shooting water approximately 30 m (prototype) into the air above the top of the vent. The air velocity and pressure results for these tests are contained in Appendix G and photos and videos of the tests are available on request.

It was shown that a 450 mm pipe fitted directly onto the conduit would be ineffective in reducing the air reversal in the air shaft. It is possible however, that a larger pipe or a pipe with an extra chamber would be effective. Examples of other configurations that could be tested are shown in **Figure 5-17** below. Due to time constraints these configurations were not tested as part of this study.

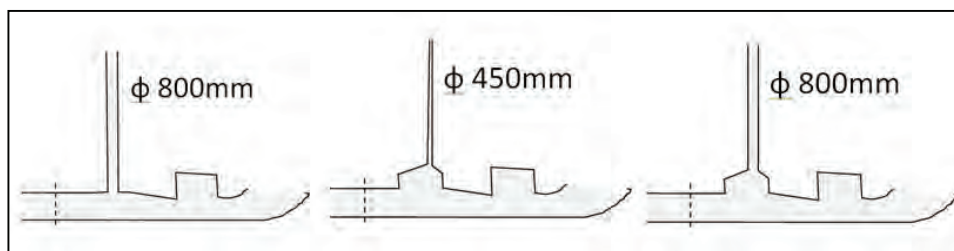


**Figure 5-17: Examples of Other Possible Configurations for an Extra Air Vent**

### **5.3.4 Conclusions from Tests on Modified Model Configurations**

Removal of the second bend in the conduit and/or the ski jump has little effect on the outlet flow conditions.

The cause of the air reversal (blowback) effect in the air shaft is the constriction at the radial gate chamber. When the flow is not constricted here, free-surface flow occurs throughout the conduit for all openings of the emergency gate, and the air reversal problem is solved. However, for this free surface flow the size of the provided air shaft is probably insufficient to limit the air velocities to 45 m/s for the full supply level.

The provision of an extra air vent pipe (450 mm in diameter) directly onto the conduit just upstream of the radial gate constriction is ineffective in reducing the air blowback effect.



## 6. FURTHER DISCUSSION OF RESULTS

### 6.1 Air Blowback

The slope of the Berg River Dam tailrace conduit is approximately 1:200, much lower than 1:10 below which, according to Falvey (1980), blowback problems are usually not experienced. The cause of the blowback in this case is not the slope of the conduit, but rather the constriction at the downstream end. There are similarities between this case and the blowback experienced in the glory-hole spillway of the Owyhee Dam in the 1930's in which the cause of the blowback was cited as constriction of the flow due to wave action at the submerged outlet (Lowe, 1944). Therefore blowback can be caused either by a too steep slope of a conduit or by a constriction of flow.

### 6.2 Comment on Air Transient Pressures Waves in Conduit

The order of magnitude of the shock wave pressure in the air vent due to explosive air blowback in the air vent can be estimated by assuming that air is incompressible (relatively low pressures are expected) and using the Joukowski equation (rigid column theory):

$$\Delta h = \frac{c\Delta v}{g}$$

Where:  $\Delta h$  = air pressure wave amplitude  
 $c$  = speed of shockwave in air (340 m/s)  
 $\Delta v$  = velocity change in air vent  
 $\rho_{\text{air}} = 1,23 \text{ kg/m}^3$

In the air shaft the change in velocity during a blowback event is approximately 20 m/s, therefore:

$$\Delta h = \frac{(340)(20)}{(9.81)} = 639 \text{ m air} = 639 \left( \frac{1.23}{1000} \right) = 0.85 \text{ m water}$$

.

The amplitude of the pressure wave is therefore 0.85 m water, giving a total pressure change (wave height) of 1.7 m water. 1.7 m water = about 17 kPa. Acting on the area of the Mentis grid cover (which covers approximately 15% of the 1.8 m<sup>2</sup> airshaft = 0.27 m<sup>2</sup>) this results in a

force of  $F = PA = 17 \times 0.27 = 4.59 \text{ kN}$  which is enough to lift a mass of about 460 kg! The mass of a Mentis grid cover,  $1.8 \text{ m}^2$ , is approximately 100 kg, so it could be lifted well off the ground by this force.

### 6.3 Air Demand (Aeration Ratio)

The aeration ratio ( $\beta = Q_a/Q_w$ ) discussed in Section 3.3.6 above was calculated for tests on the as-built conduit and on the modified conduit with the radial gate removed (Mod 4). In Figure 6-1 below these are plotted together with the aeration ratios predicted by (the empirical relations) Equation 3.21 (USACE) for air demand in a conduit without a hydraulic jump.

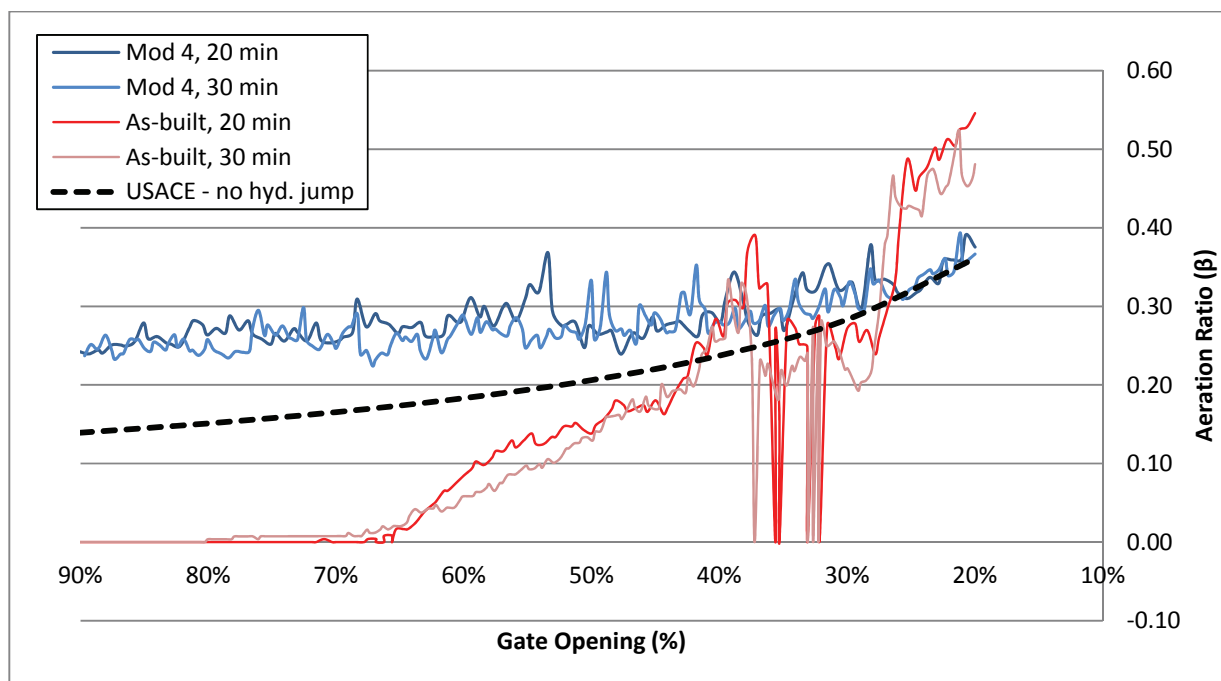


**Figure 6-1: Aeration Ratio ( $\beta$ ) versus Gate Opening**

A significant difference in the air demand can be seen between the as-built conduit and that with the constriction removed (Mod 4).

The USACE empirical relation is recommended for design of conduits without hydraulic jumps; however the figure above shows that it underestimates the air demand for high flows in the Berg River Dam when the free-surface flow occurs.

## 7. CONCLUSIONS

From tests on the as-built model of the Berg River Dam outlet works it was found that the flow through the air shaft was predominantly into the conduit (downwards) during closure of the emergency gate. However, rapid airflow direction reversals occur between gate openings of about 35% and 25%. The problem at the Berg River Dam was therefore determined to be one of air blowback instead of constant air outflow, as previously suggested by the prototype tests.

A description with sketches of the observed flow and probable explanation of the blow back was given in Section 5.2.2.2. Essentially, air enters the conduit through the air shaft and is drawn downstream either insufflated in the flow or above the flow by viscous air-water shear forces. At the downstream end the outflow of air is restricted by the constriction for the radial gate chamber (which has a downwards sloping ceiling), resulting in pressurisation of the air in the conduit. This pressure causes blowback of air in the airshaft when the water surface breaks contact with roof of the conduit.

Tests performed with the radial gate constriction removed confirmed that it had been the cause of the blowback experienced in the latter tests. These tests showed free-surface flow throughout the closure of the emergency gate, and no airflow reversals in the air shaft. Tests on other modified model configurations showed that removal of the ski-jump and second 8° bend in the conduit have little effect. An extra 450 mm air vent pipe fitted directly onto the conduit at the constriction was found to be ineffective in reducing the blowback.

Air entraining vortices did not occur for any tests at the commissioning level, even with stirring. The highest level at which vortices formed was found to be 227 masl, 10.5 m below the water level for the commissioning tests.

The air velocity in the air shaft was found to be independent of the rate of closure of the emergency gate, but to increase with increasing water head.

## 8. RECOMMENDATIONS

### 8.1 Configuration

The cause of the air blowback in the Berg River Dam model was found to be the constriction at the radial gate chamber. The recommendation follows that the conduit should not be restricted. Further, to prevent blowback it is recommended that flow in high headed outlets is never constricted by any structure or mechanism (e.g. wave action as experienced at the Owyhee Dam) for any foreseeable flow conditions.

A potential blowback problem is presented if the radial gate should fail in a partially closed position. In this case a possible solution is a dual radial gate system in which both gates have the capacity for the full design discharge (see **Figure 8-1** below). Under normal operation one gate can be used while the other remains closed. In the case of failure of a gate in a partially closed position, the other gate can be fully opened to allow unconstricted flow before the emergency gate is closed. (Stoplog slots could also be fitted to allow for normal operation should one of the gates need to be repaired).

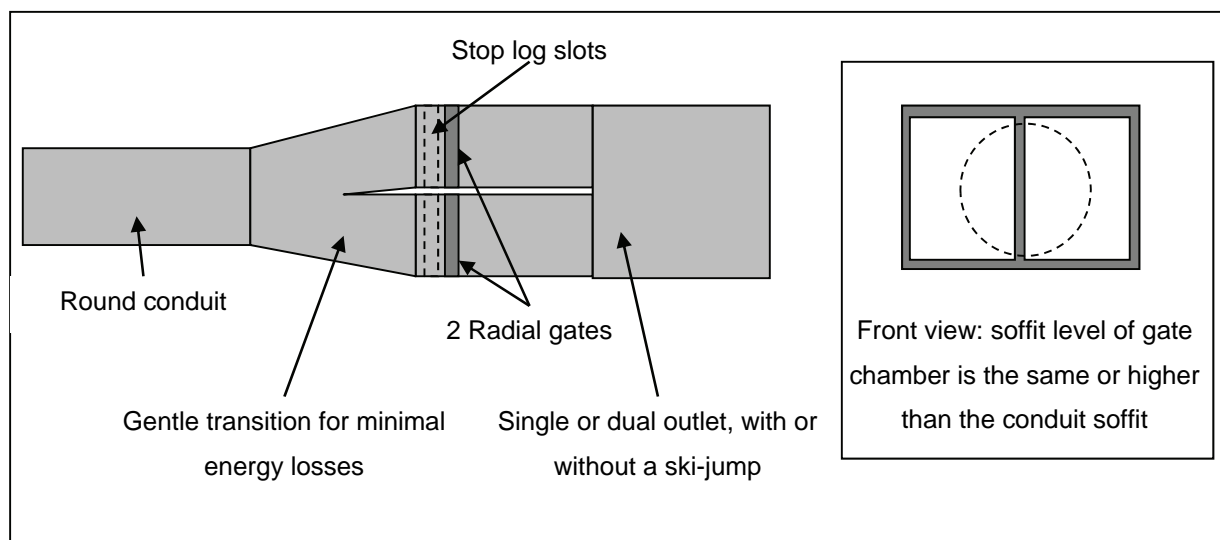


**Figure 8-1: Possible radial gate configuration to prevent blowback**

## 8.2 Berg River Dam Operation

The emergency gate was opened too quickly during the simulations, which increased the pressure on the radial gate chamber. This caused the radial gate chamber to fail, as seen in **Figure 8-2** below.



**Figure 8-2: Failed radial gate chamber**

Given this failure, it is advised that the radial gate and emergency gate should never be operated simultaneously when the outlet conduit of the Berg River Dam has to be filled or drained.

During the commissioning test in 2008, the 1.8 m<sup>2</sup> Mentis grid cover on top of the air vent was blown off and lifted to a height of about 3 to 4 m, tipping the observer, James Metcalf, off the vent top and against the upstream concrete wall. The cover then fell back to the ground, striking the observer's right foot. Dr Mike Shand (2008) recommended that the Mentis grid cover be removed and that the air vent should be extended upwards by at least 1.8 m by constructing a reinforced concrete chimney around the air vent for when the emergency gate is purposefully or unintentionally operated. The top of the air vent should preferably be even higher.

### 8.3 Further Studies

It is recommended that further tests are carried out on the Berg River Dam model used in this study for a partially open radial gate and possibly for the alternative air vent configurations suggested in **Figure 5-17**.

It was recommended that the results of the study of the Berg River Dam model should be compared with a three-dimensional CFD analysis of the closing gate simulations (transient) in order to determine the capability of numerical modelling in simulating complex air-water flow and unstable hydraulic jumps in high-headed gated conduits. This was done and is discussed in Volume II of this report.

For research purposes it would be valuable to perform another prototype emergency gate closure exercise (such as done for the commissioning tests) while recording air velocities with a continuously recording anemometer with a direction sensor. However, it must first be established that such testing would not pose a dangerous risk to the structure.

## **9. GUIDELINES FOR THE DESIGN OF FUTURE BOTTOM OUTLETS**

The following recommendations should be adhered to for the prevention of air flow reversal problems in future designs:

- Large scale (preferably greater than 1:20) hydraulic models should be used in the design process, and tests should include emergency gate closure procedures.
- Bottom outlets should be designed for free-surface flow conditions in the outlet conduit for all foreseeable flow conditions and the formation of hydraulic jumps should be avoided.
- The slope of the tailrace conduit in bottom outlets should be kept as flat as possible, to prevent upstream movement of air and possible blowback problems due to buoyancy forces.
- Air entrapment at all changes in cross section should be avoided by matching tunnel ceiling heights rather than inverts.
- The flow in outlet conduits should not be restricted for all foreseeable flow conditions. The case of a radial gate failing in a partially closed position is a particular scenario which would cause a constriction which may cause a severe restriction of the flow, possibly leading to dangerous air blowback during emergency gate closure. (A possible configuration to prevent blowback in this case is discussed in Section 8 above)
- Where ski-jumps are used the crest height should not be so high that it could cause submergence of the conduit under low flow conditions.

## 10. REFERENCES

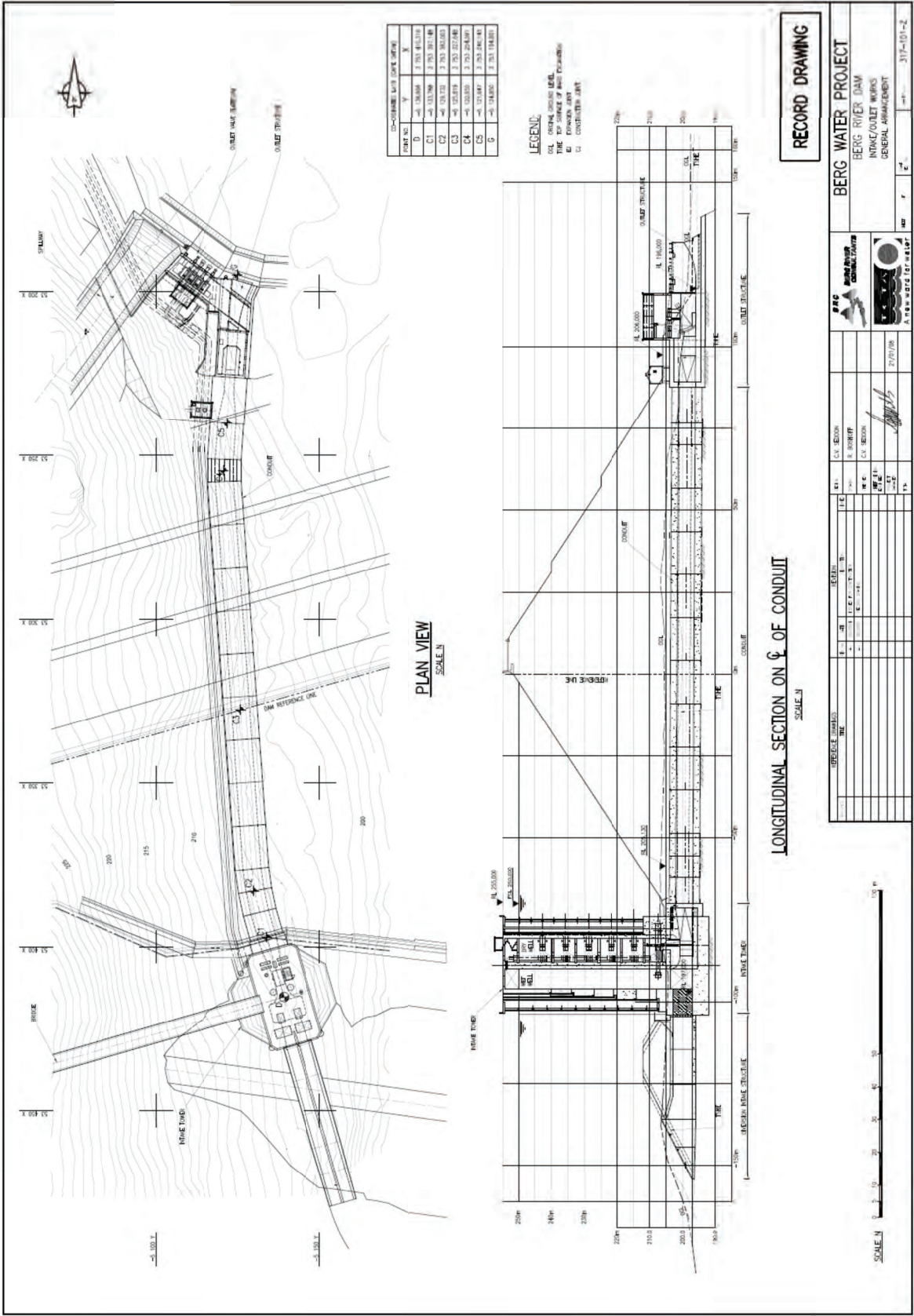
- Spillways, Shockwaves and Air Entrainment*. (1992). Paris: International commission on Large Dams.
- Engineering and Design – Tunnels and Shafts in Rock*. (1997). Engineering Manuals (EM 110-2-2901).
- Abban, B., Shand, M., Kamish, W., Makhabane, M., Van Zyl, B., & Tente, T. (2008). *Decision Support System for the Berg River Dam and Supplement Scheme*. Stellenbosch: University of Stellenbosch.
- Aydin, I. (2002). Air demand behind high head gates during emergency closure. *Journal Hydraulics Division, Vol 40, No. 1*.
- Basson, G. R. (2011, February 17). Commissioning Test of Berg River Dam in 2008. (A. Vos, Interviewer)
- Basson, G. R. (2012, February). Personal Communication.
- Borodina, L. (1969). Aeration behind low level gates. *Gidrotekhnicheskoe Stroitel'stvo, No. 9*, 32-37.
- Chadwick, A., Morfett, J., & Borthwick, M. (2004). *Hydraulics in Civil and Environmental Engineering, Fourth edition*. Abingdon: Spon Press.
- Chaudhry, M. H., & Yevjevich, V. (1981). *Closed-Conduit Flow*. Littleton: Water Resources Publications.
- Erbisti, P. (2004). *Design of Hydraulic Gates*. Netherlands: Swets & Zeitlinger B. V.
- Falvey, H. T. (1980). *Air-Water Flow in Hydrualic Structures (Engineering Monograph No. 41)*. Denver: United States Department of the Interior Water and Power Resources Service.
- FEMA. (2004). *The National Dam Safety Program: Outlet Works*. Denver, Colorado: Federal Emergency Management Agency.
- Hirt, C. W. (2003). *Modelling Turbulent Entrainment of air at a Free Surface*. [www.flow3d.com/](http://www.flow3d.com/) (access only for registered users of software): Technical Note 61, Flow Science, Inc (FSi-03-TN61).
- Kalinske, A. A., & Robertson, J. M. (1943). Entrainment of Air in Flowing Water Closed Conduit Flow. *Transactions, ASCE, Vol. 108*, 1435-1447.
- Levin, L. (1965). *Calcul Hydraulique des Conduits d'Aeration des Vidanges de Fond et Dispositifs Deversants, No. 2*. La Houille Blanche.
- Lewin, J. (2001). *Hydraulic gates and valves in free surface flow and submerged outlets: Second Edition*. London: Jack Lewin and Thomas Telford Limited.



- Logan, C., Louwinger, F., Mongili, E., & Lillie, E. (2011). *Confidential Report*.
- Lowe, F. C. (1944). *Hydraulic Model Studies for the Glory-hole Spillways at Owyhee Dam and Gibson Dam*. Denver, Colorado: United States Department of the Interior Bureau of Reclamation.
- Mortensen, J. D. (2009). *Factors Affecting Air Entrainment of Hydraulic Jumps within Closed Conduits*. Utah State University: All Graduate Theses and Dissertations. Paper 531.
- Murray, R. I., & Simmons, W. P. (1964). *Progress Report No. 1 – Research Studies on Hydraulic Downpull Forces on Large Gates with Special Application to the San Luis Outlet Works Emergency Gates (Report No. Hyd-530)*. Denver, Colorado: United States Department of the Interior Bureau of Reclamation Hydraulics Branch.
- Najafi, M., & Zarrati, A. (2010, July 27). Numerical Simulation of Air-water Flow in Gated Tunnels. *Water Management 163 Issue WM6*, pp. 289-295.
- Naudacher, E. (1991). *Hydrodynamic Forces*. Rotterdam: A.A.Balkema.
- Rabben, S. L., & Rouvè, G. (1985). Belüftung von Grundablässen. *Wasserwirtschaft 75(9)*, 393-399.
- Rindles, A. J., & Gulliver, J. s. (1983). *An Experimental Study of Critical Submergence to Avoid Free-Surface Vortices at Vertical Intakes*. St Paul, Minnesota: Legislative Commission on Minnesota Resources, State of Minnesota.
- Safavi, K., Zarrati, A., & Attari, J. (n.d.). Experimental study of air demand in high head gated tunnels. pp. 105-111.
- Sarkaria, G., & Hom, O. (1959). Quick Design of Air Vents for Power Intakes. *Proceedings of ASCE, Journal of the Power Division*, PO6.
- Shamsai, A., & Soleymanzadeh, R. (2006, March Vol. 4, No. 1). Numerical simulation of Air-Water flow in bottom outlet. *International Journal of civil Engineering*, pp. 14-33.
- Shand, M. (2008). *Berg River Dam Emergency Gatre Commissioning Release of Air*. Cape Town.
- Sharma, H. (1976). Air-Entrainment in High Head Gated Condiuts. *Journal of the Hydraulics Division*, 1629-1645.
- TCTA. (2006). Modellin, Monitoring Nuts and Bolts of Dam Projects. *The Water Wheel*, 29-31.
- TCTA. (2008). Berg River Dam: Designed with Rivers in Mind. *The Water Wheel*, 33-37.
- Tente, T., Malan, S., Mills, L., & Van Wyk, D. (Unknown). *Berg Water Project (BWP): Design, Operation and Cost Implications of Environmental Releases*. South Africa: Unknown.
- USACE. (1963). *Hydraulic Design of Reservoir Outlet structues*. U.S. Army Corps of Engineers (Em 1110-2-1602).

- USACE. (1980). *Hydraulic Design of Reservoir Outlet Structures, Em 1110-2-1602*. Washington DC, USA: US Army Corps of Engineers.
- Van Vuuren, S. (2003). *Berg river Project Hydraulic Model Testing of the Outlet works Model Scale 1:20*. South Africa: Sinotech CC.
- Vischer, D., & Hager, W. (1998). *Dam Hydraulics*. West Sussex: John Wiley & Sons Ltd.
- Webber, N. (1971). *Fluid Mechanics for Civil Engineers, S.I. Edition*. London: Chapman and Hall Ltd.
- Webber, N. (n.d.). *Fluid Mechanics for Civil Engineers*.
- Webby, M. G. (2003). *Investigation of Blowback Incidents at Rangipo Power Station*. Wellington, New Zealand: ANCOLD 2003 Conference on Dams.
- Young, L., & Valentin, F. (1971). *Toome sluices calibration tests, report RR 1105*. B.H.R.A.

## ***APPENDIX A: AS-BUILT DRAWINGS OF BERG RIVER DAM OUTLET WORKS***











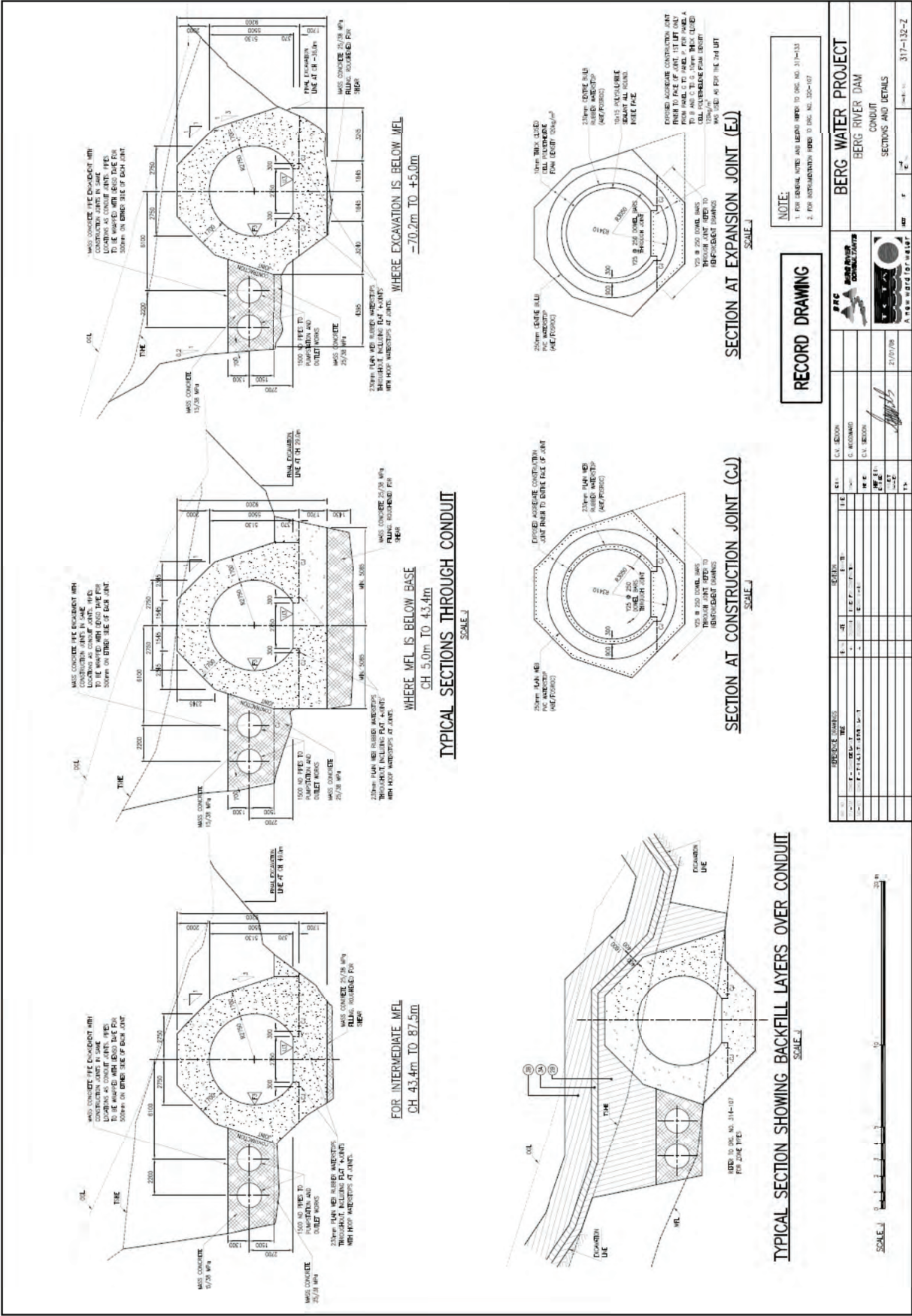






















## ***APPENDIX B: COMMISSIONING TEST ON BERG RIVER DAM – JUNE 2008***

### **BERG RIVER DAM EMERGENCY GATE COMMISSIONING RELEASE OF AIR**

Dr Mike Shand  
30 June 2008

#### **1. Introduction**

Andy Griffiths of Goba and I discussed the possible reasons for the release of very large volumes of air from the air intake shaft during the trial closure of the emergency gate on 12 June 2008. We concluded that the only way that the volume of air released could arise is through the formation of and entrainment of air by a vortex in the intake shaft. Our reasons are set out below.

#### **2. Design of Air Shaft**

The air shaft was designed to allow air to be introduced immediately downstream of the emergency gate on account of the negative pressures that were expected to occur during its partial closure. The final design was based on the 1 in 20 scale hydraulic model tests, which had shown no evidence of vortex formation and had indicated that air would be drawn down the air shaft.

Immediately after the trial release, Prof. Gerrit Basson utilized the 1 in 40 scale hydraulic model that was also used for the original design and is still operational at the University of Stellenbosch, to re-simulate partial closure of the emergency gate but with the water level in the dam at full supply level. This modelling also showed no evidence of vortex formation and indicated that large volumes of air would be drawn down the air shaft.

#### **3. Mechanism for Release of Air from Airshaft**

Contrary to the design, James Metcalf's air shaft velocity measurements shown in Table 1 indicate that, while the emergency gate was closing, very large volumes of air were continuously released from the 1,8 m<sup>2</sup> air shaft commencing when the gate was about 30% closed (i.e. 70% open). The time of commencement of the release of air seems to have coincided with the observations of the following:

- The time that the cavitation noise in the access shaft to the emergency gate ceased, which indicates the presence of air, and
- The time that the release of air from the flow commenced in the radial gate house.

James Metcalf's observations indicate that the velocities of air released through the 1,8 m<sup>2</sup> air shaft increased from 8,75 m/s (32 km/h) at 13h06 to about 45 m/s (160 km/h) at 13h14, corresponding to air releases increasing from 16 m<sup>3</sup>/s to 80 m<sup>3</sup>/s as indicated in Table 2. There are only two potential sources of air:

- The entrainment of air from the downstream end of the conduit at the radial gate: however this would not be possible because of the high velocity of the water flow in the conduit which causes air to be dragged downstream rather than upstream, and because the observations during the trial indicate that for much of the time the conduit was flowing full with considerable volumes of air entrained in the flow. Reports by observers in the housing of the radial gate also indicate that considerable volumes of air were released from the flow as it exited at the radial gate. However the removal of air was also reported and this may have been caused by the suction effect of intermittent fully aerated flow occupying the total area of the opening downstream of the radial gate.
- The only other potential source of air is via a vortex forming in the vertical shaft upstream of the emergency gate, and is the only explanation that is consistent with the velocity observations of the air releases from the air vent and from observations that the flow at the radial gate was highly aerated.

#### **4. Recommendations for Hydraulic Model Tests**

The following recommendations are made to try to gain an improved understanding of the mechanism for the formation of a vortex in the shaft:

- Although the 1 in 50 scale hydraulic model is not sufficiently large to accurately model the formation of vortices, it is nevertheless recommended that this model is utilized to observe the flow patterns as follows:
  - For the dam water level and intake level at the time of the trial and with the radial gate fully open check the flow patterns and air entrainment for small incremental closures of the emergency gate similar to those undertaken for the trial. If possible measure the air releases and the flow of water for the various emergency gate openings.
  - If no vortex forms repeat the above but introduce mild circular perturbations to the water in the intake shaft either by stirring action or by temporarily blocking the flow through one of the intakes into the tower (try clockwise and counter clockwise rotation).
  - Repeat with stronger perturbations until a vortex forms with the gate at about 66% open and then observe the air entrainment and release from the air shaft for incrementally reducing openings. If possible measure the flow of water and of air for the various emergency gate openings.
  - Repeat for other intake gate selections and water levels in the dam.
- Compare the modelled air releases with those measured by James Metcalf on 12 June.
- Obtain from DWAF the actual flow measurements at the Crump weir downstream, and compare these with the hydraulic model results, if necessary adjusted by computer model routing to account for the times of incremental gate lowering and the plunge pool and channel storage effects upstream of the Crump weir.
- Obtain the records for the pressure cells outside the conduit to check whether these also indicate the reducing pressures in the conduit due to the entrainment of air.
- Prepare a report on the above.

## 5. Safety Recommendations

The following recommendations are made:

- Air Shaft: The rectagrids at the top of the air shaft were blown 3 m to 4 m into the air as indicated in Table 1 and fortunately only caused a minor injury to James Metcalf but could easily have killed him and the observer from the Cape Argus. Therefore as human lives would be endangered in the event that the emergency gate is

purposefully or inadvertently operated in the future, it is strongly recommended that the rectagrid is removed and that the air shaft is extended upwards by at least 1.8 m by constructing a reinforced concrete chimney around the air shaft.

- **Radial Gate House:** The accounts of observers that the intermittent release and removal of large volumes of air could perhaps have damaged the radial gate house have already been taken into account and the contractor has been instructed to replace all windows with grids. It is also understood that there was a considerable amount of water spray in the gate house during the emergency gate closure and earlier during the commissioning tests there was also spray from the leaking gate seals.

As the electrical equipment for operating the radial gate will be exposed to the weather to a greater extent by the removal of the windows and possibly to spray, it is suggested that consideration be given to constructing a small weatherproof enclosure around the electrical equipment in the gate house.

**Table 1. Air Shaft Velocity Observations by James Metcalf on 12 June 2008**

Time	Hand-held Schiltnecht Anemometer Air Shaft ( $\pm 1.5 \text{ m} \times 1 \text{ m}$ ) Air Velocity Reading: (32 second average logged by electronic unit)	Gate Degree Closed	Remarks (NB: Anemometer held down on top of Mentis Grid Cover)
12 June 08	m/s		
13h00	Observer not present	0%	Air velocity & direction unknown (suspect <u>ingestion</u> of air – i.e.: “down shaft”)
13h01	Ditto	5.5%	
13h02	Ditto	11.1%	
13h03	Ditto	16.7%	
13h04	Observer setting up instrument	22.2%	
13h05	3.5 m/s	27.8%	Air Vel Direction unknown
13h06	8.75 m/s	33.3%	Notebook in which air velocity readings were being recorded handed to second observer (Cape Argus Reporter) since up-velocity (out of shaft) causing



			notebook to be "blown away"
13h07	12.44 m/s	38.9%	Up-shaft air flow
13h08	14.2 m/s	44.4%	Ditto
<b>Time</b>	<b>Hand-held Schiltnecht Anemometer Air Shaft (±1.5 m x 1 m) Air Velocity Reading: (32 second average logged by electronic unit)</b>	<b>Gate Degree Closed</b>	<b>Remarks</b> (NB: Anemometer held down on top of Mentis Grid Cover)
13h09	19.8 m/s	50%	Ditto
13h10	21.7 m/s	55.5%	Increasing difficulty in holding anemometer down on shaft top grid cover due to high-velocity outflow (anemometer wooden case became air-borne at about this stage)
13h11	22.3 m/s	61.1%	Air flows "surging" constantly at (say) 10 cycles per minute and getting stronger all the time
13h12	26.0 m/s	66.7%	Observer finds it increasing difficult to hold down anemometer and to hold his arm horizontal whilst lying down on the shaft top cover, due to progressively rising air up-flow velocity
13h13	35 m/s	72.2%	Last reading before.....
13h14	Probably of the order of 45 m/s (160 km/hr)	77.8%	Mentis grid cover blown off top of shaft, lifted to a height of about 3 or 4 metres, tipping observer off the shaft top and against the upstream concrete wall, and then falling back to the ground, striking/injuring <sup>4</sup> the observers right foot (which was aligned along the toe of the wall)
13h15	?	83.3%	Anemometer retrieved from the top of the shaft (loss prevented by being attached to the output cable to the electronic unit)
13h16	?	88.9%	No further readings
13h17	?	94.4%	
13h18	?	100%	

<sup>4</sup> "Ring toe" found to be crushed; writer is taken to a Franschhoek surgery wef ±2pm. Wound inspected by Dr Alex Heywood at about 3 pm, stitched up & dressed & appropriate medication given

**Table 2. Air Velocities and Flows Released from 1.8 m<sup>2</sup> Air Shaft**

Time	Air Velocity		Air Flow cu m/s
	m/s	km/hr	
13h06	8.75	32	16
13h07	12.44	45	22
13h08	14.2	51	26
13h09	19.8	71	36
13h10	21.7	78	39
13h11	22.3	80	40
13h12	26	94	47
13h13	35	126	63
13h14	45	162	81

## ***APPENDIX C1: PHOTOS OF THE 1:14.066 BERG RIVER DAM MODEL***



**Photo 1: Layout of Berg River Dam Model**



**Photo 2: Emergency gate, base of air vent and outlet conduit**



**Photo 3: Radial gate chamber and ski-jump at end of outlet conduit**



**Photo 4: Outlet conduit**



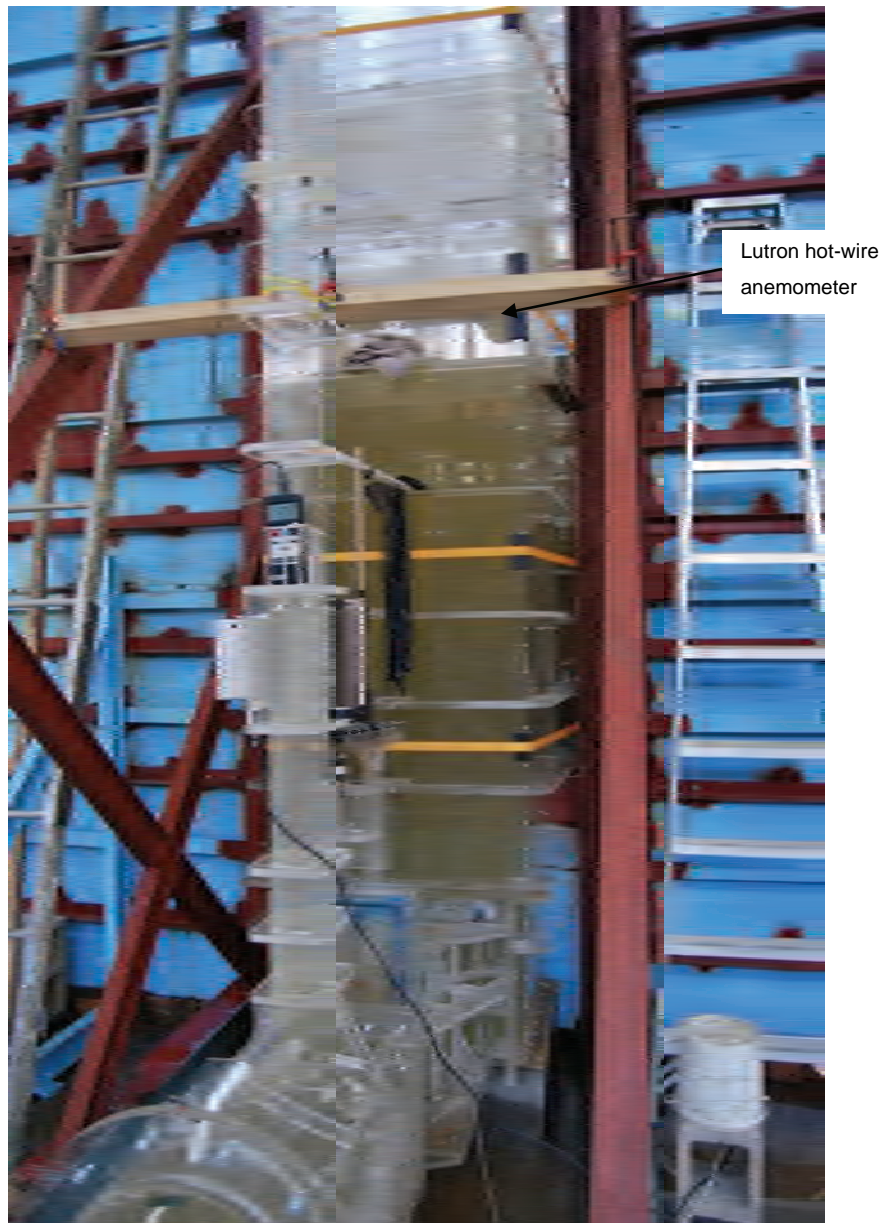


**Photo 5: Lutron hot-wire anemometer (wind velocity meter)**



**Photo 6: Second bend**

## ***APPENDIX C2: PHOTOS OF THE BERG RIVER DAM (PROTOTYPE)***

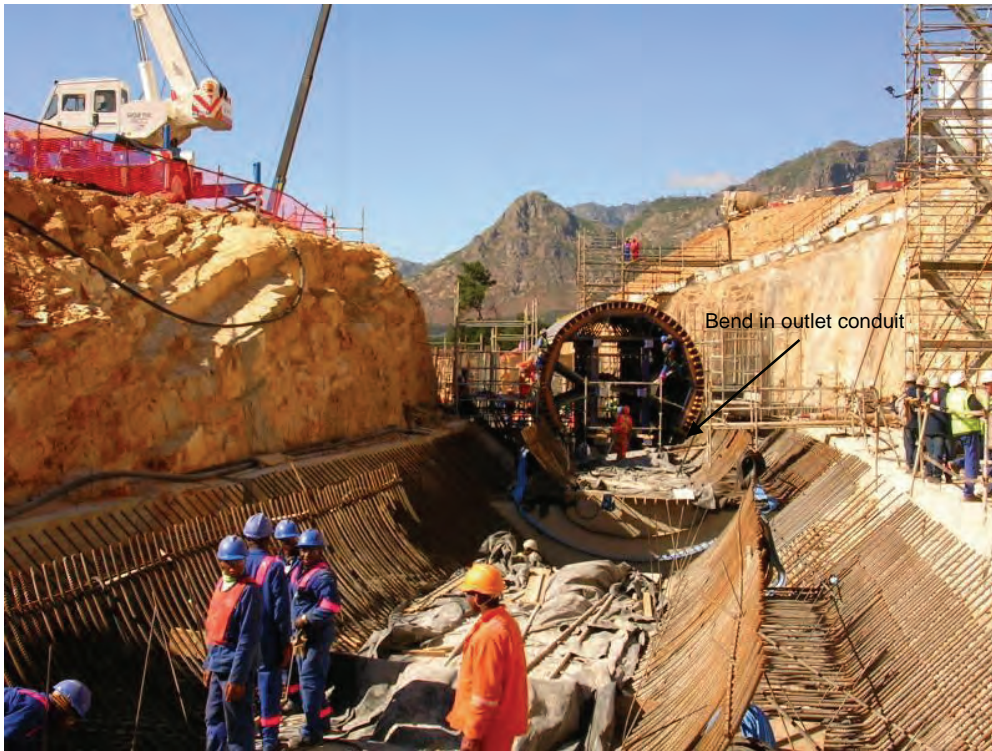


**Photo 7: Outlet conduit being built**





**Photo 8: Commissioning test**



**Photo 9: Release of SEF during commissioning test (2008)**



**Photo 10: Release of SEF during commissioning test (close-up)**



**Photo 11: Inside radial gate chamber**





**Photo 12: Top view of release of SEF during commissioning test (2008)**



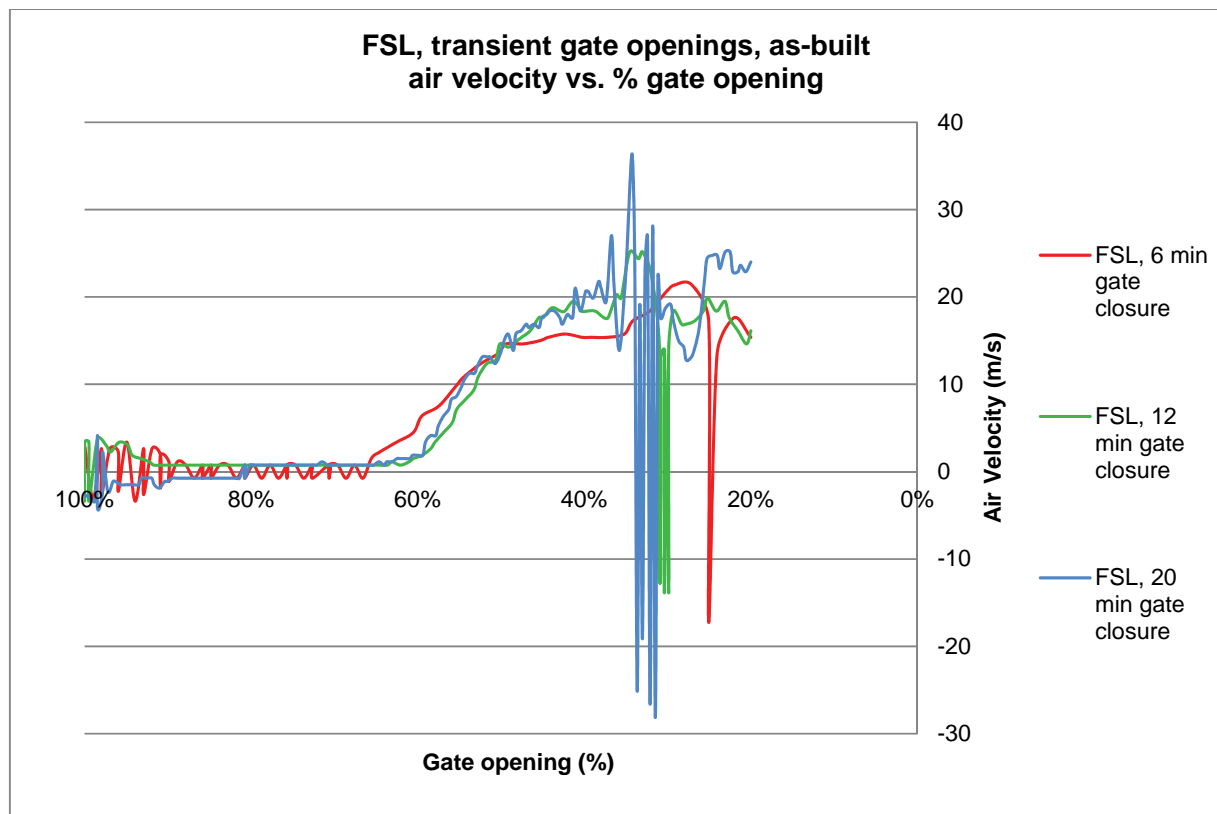
**Photo13: Berg River Dam outlet structures during construction phase**



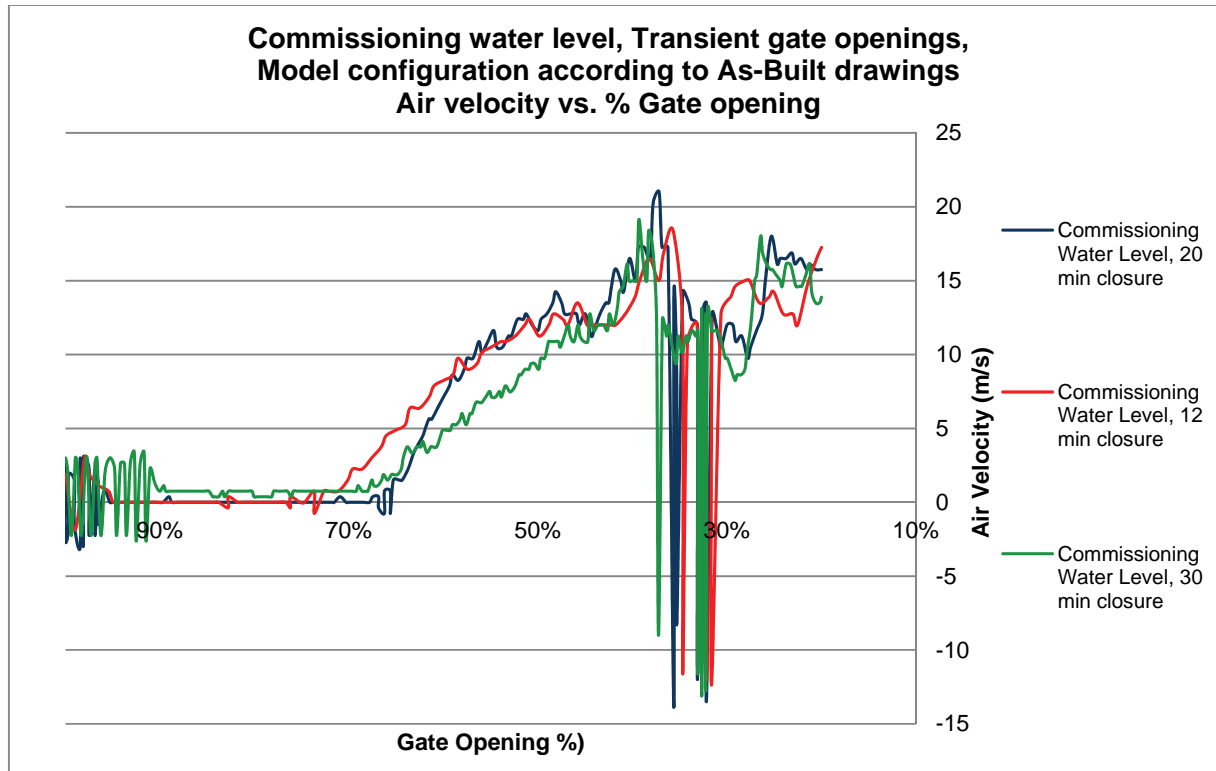
**Photo 14: Inlet tower (wet and dry well) and bridge to inlet tower under construction**

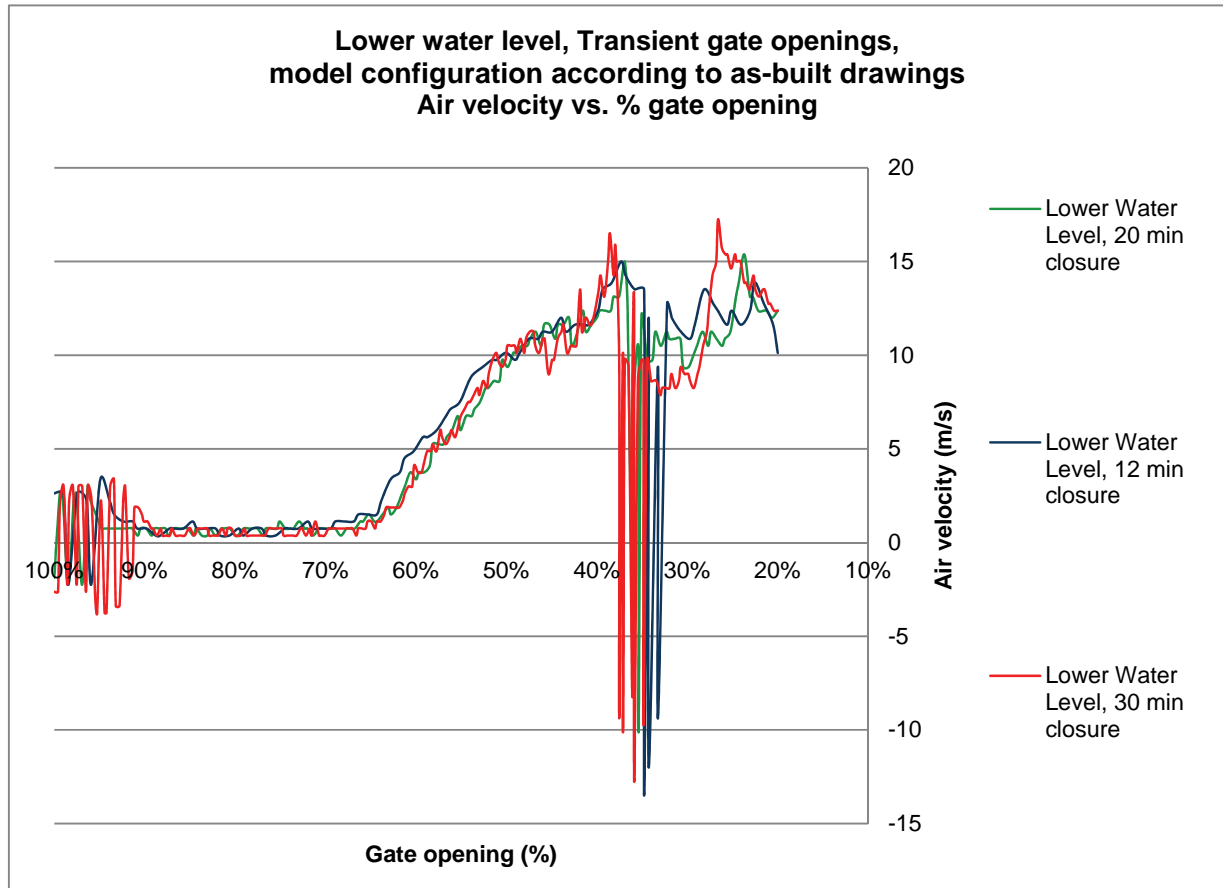
## APPENDIX D: AIR VELOCITY GRAPHS

### APPENDIX D1: Air Velocity – Closing Gate Simulations; FSL Water Level; As-Built



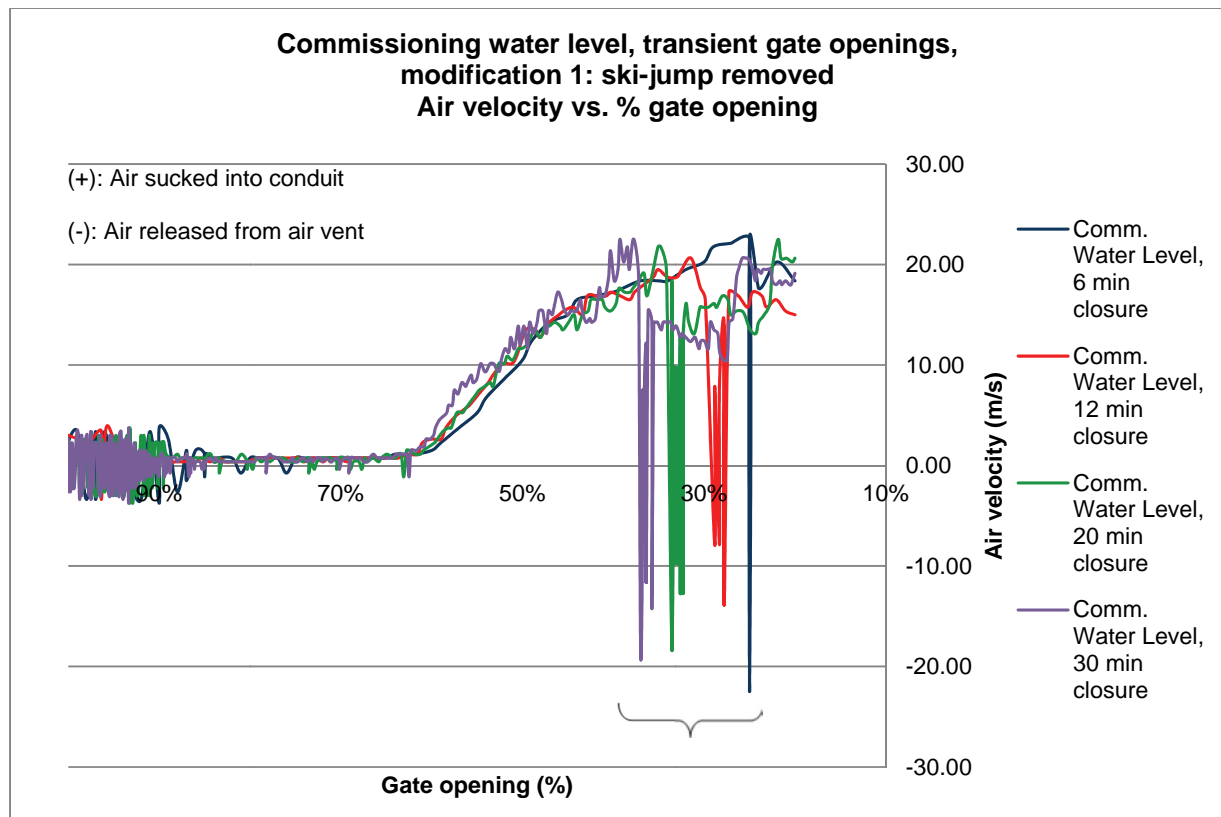
## APPENDIX D2: Air Velocity– Closing Gate Simulations; Commissioning Water Level; As-Built



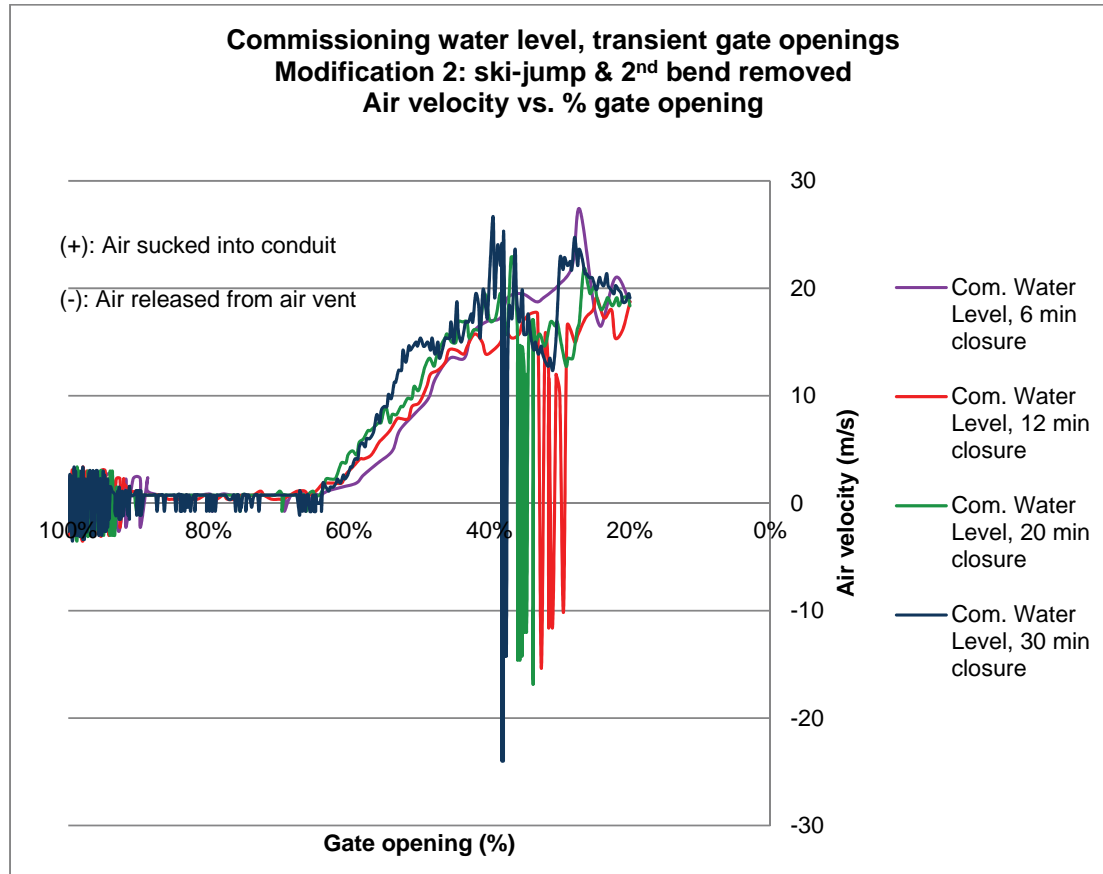
**APPENDIX D3: Air Velocity – Closing Gate Simulations; Lower Water Level; As-Built**



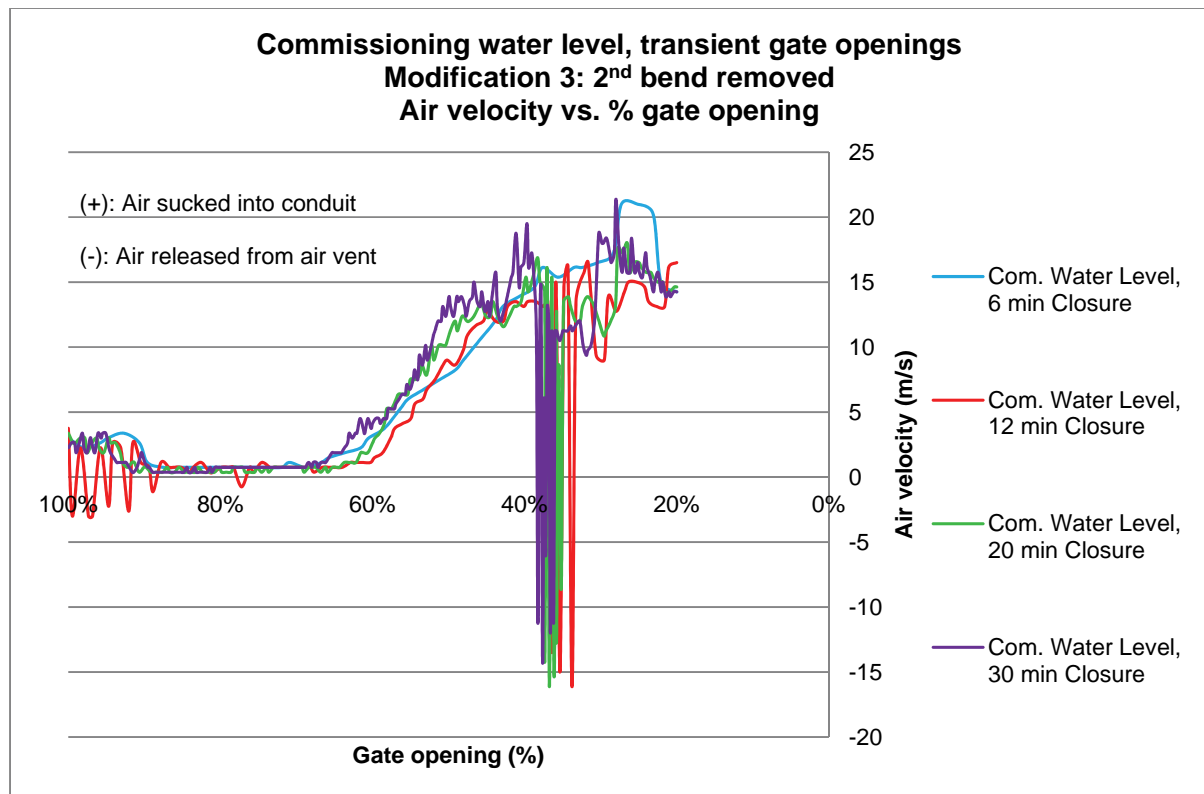
#### APPENDIX D4: Air Velocity – Closing Gate Simulations; Commissioning Water Level; Modification 1



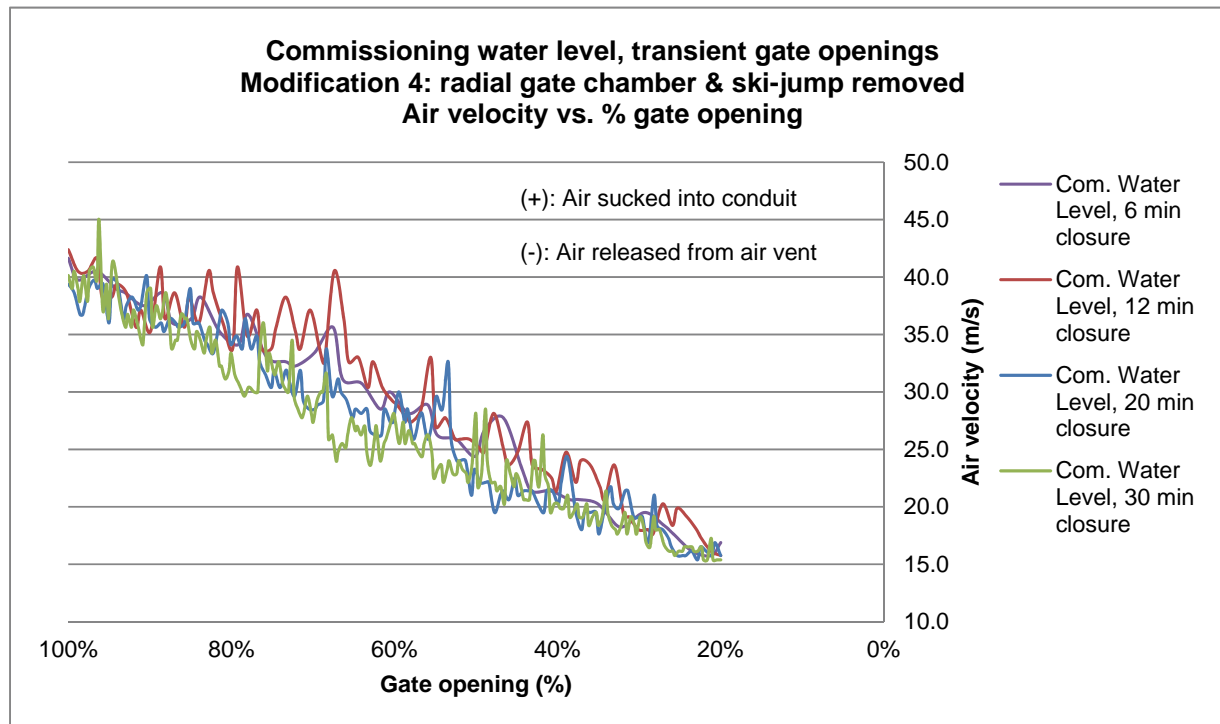
## APPENDIX D5: Air Velocity – Closing Gate Simulations; Commissioning Water Level; Modification 2



## APPENDIX D6: Air Velocity – Closing Gate Simulations; Commissioning Water Level; Modification 3

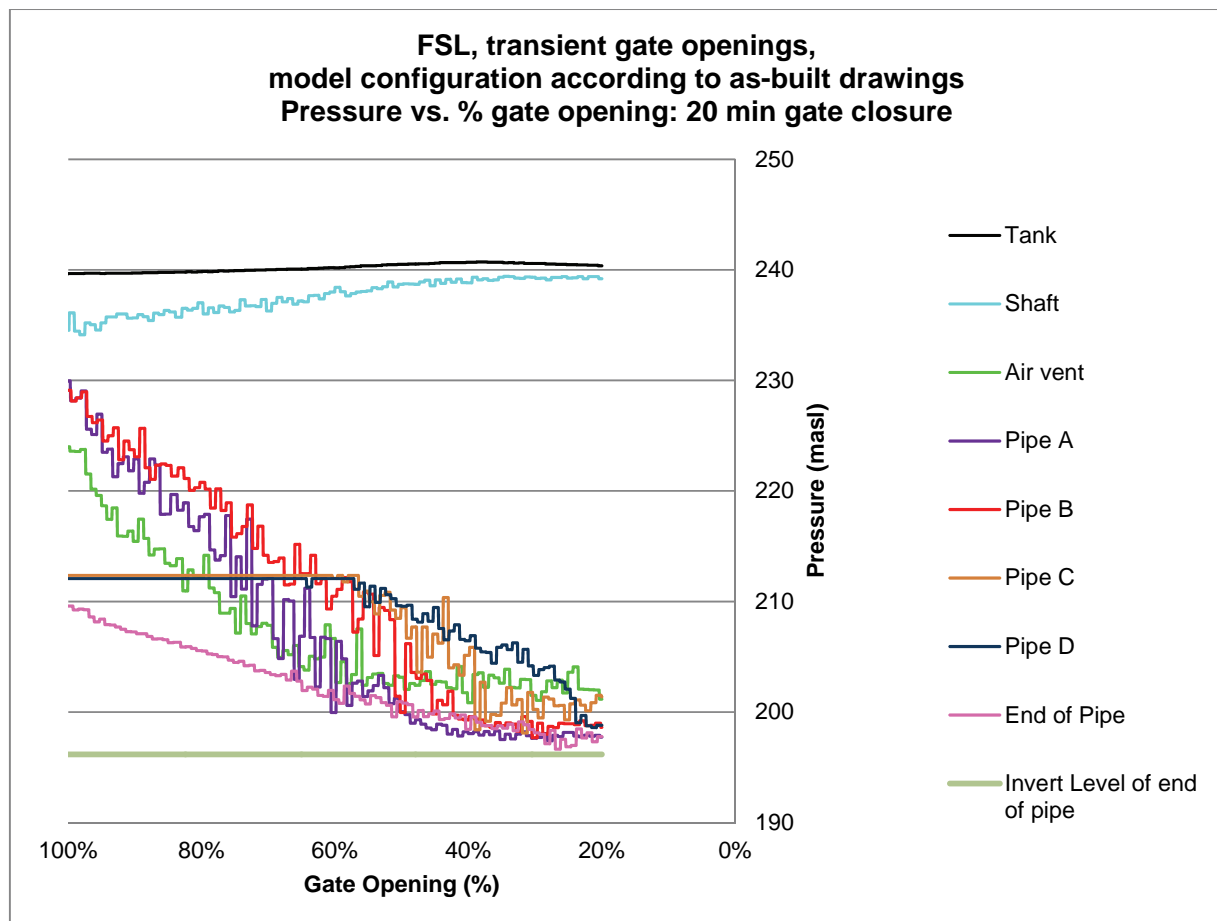


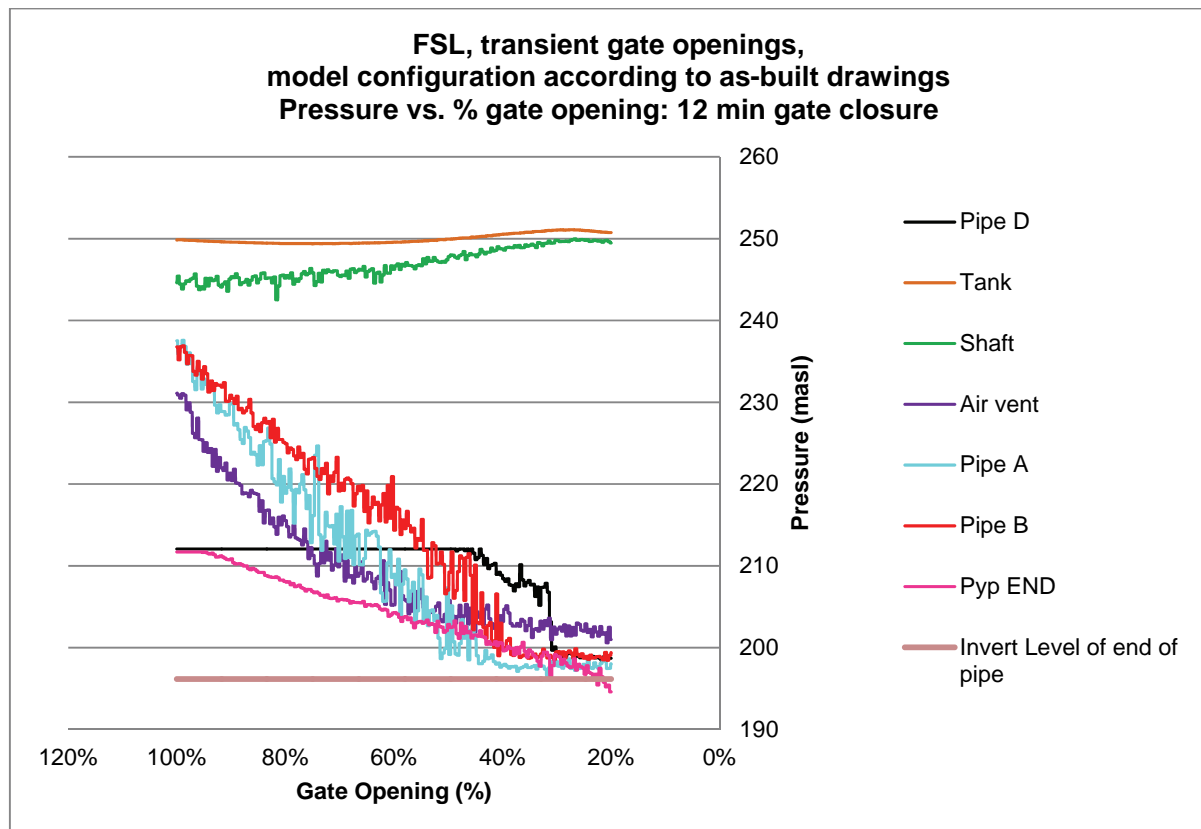
## APPENDIX D7: Air Velocity – Closing Gate Simulations; Commissioning Water Level; Modification 4

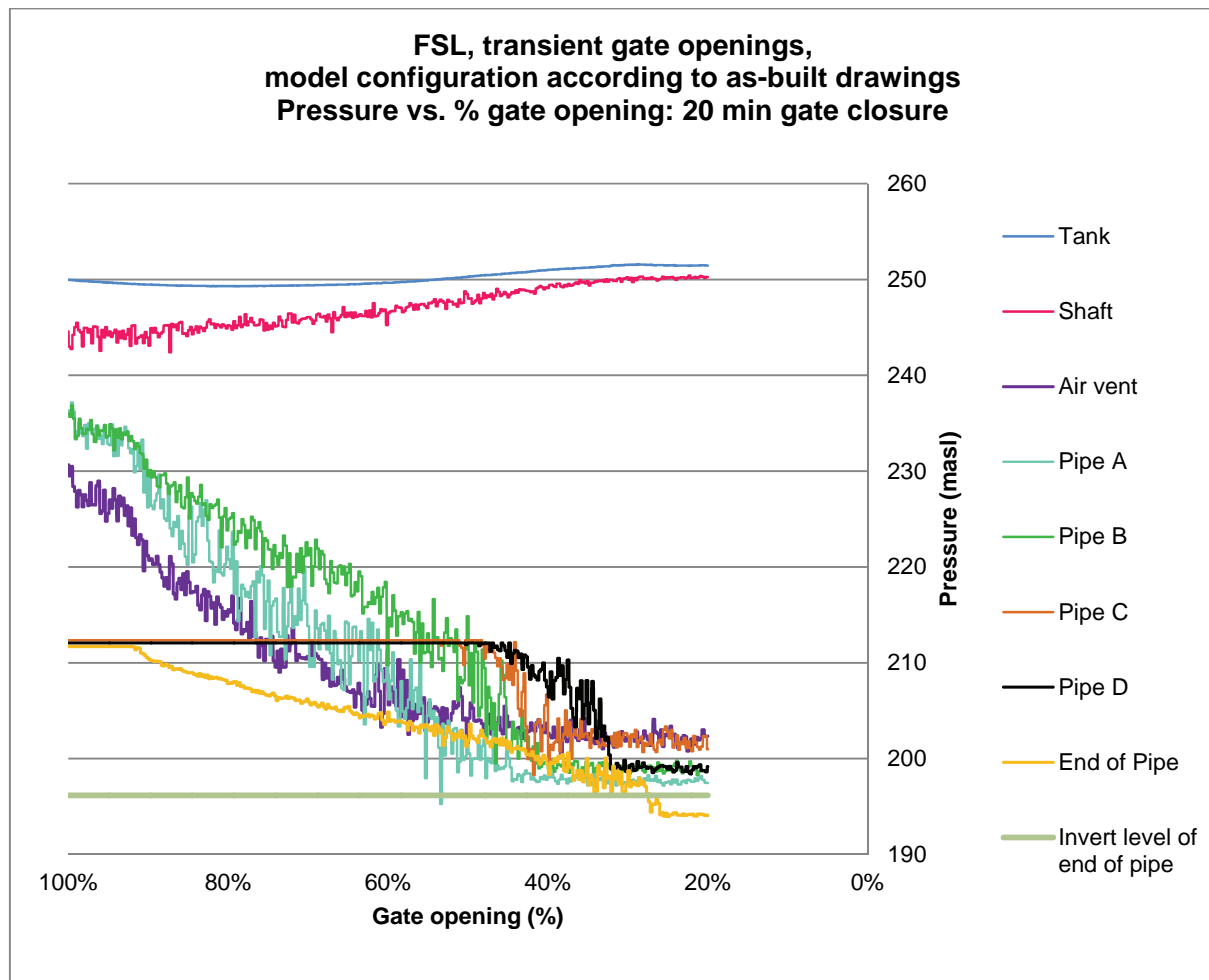


## APPENDIX E: PRESSURE GRAPHS

### APPENDIX E1: Pressures – Closing Gate Simulations; FSL; As-Built

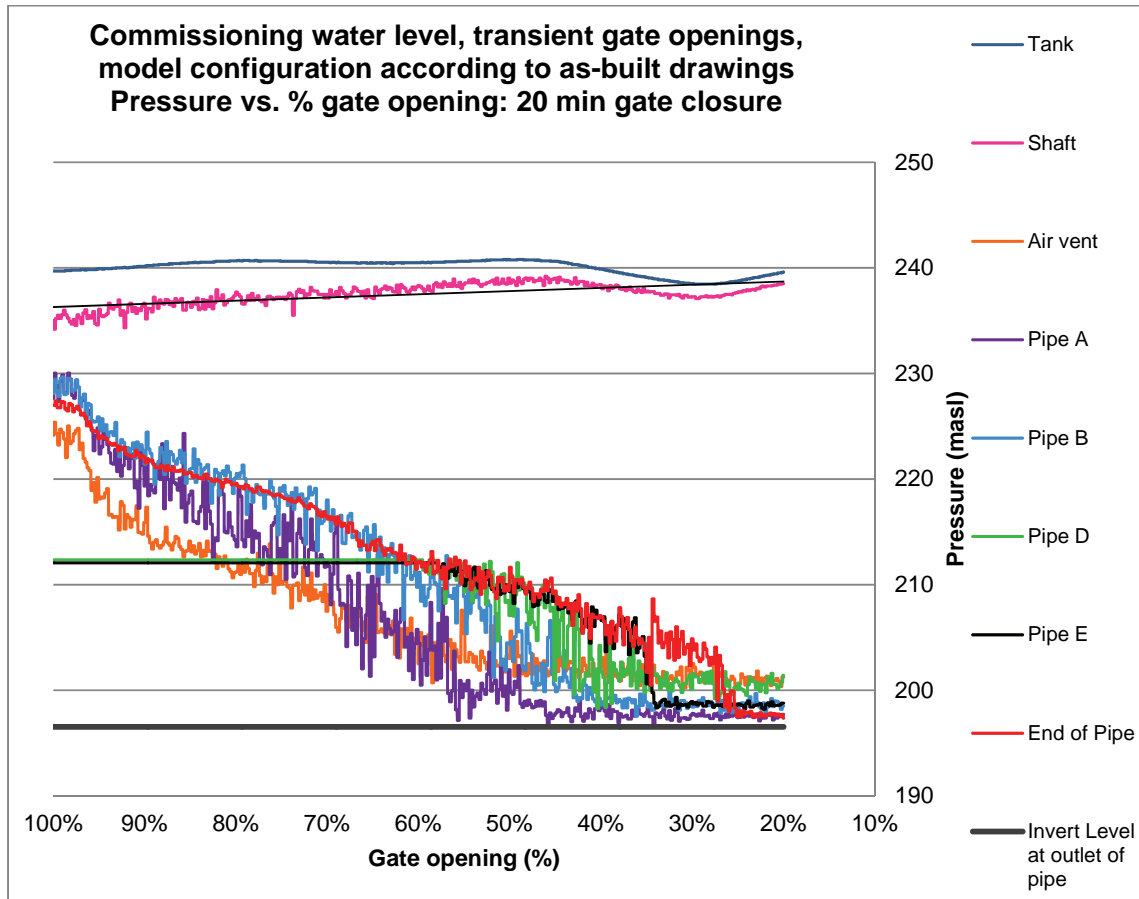


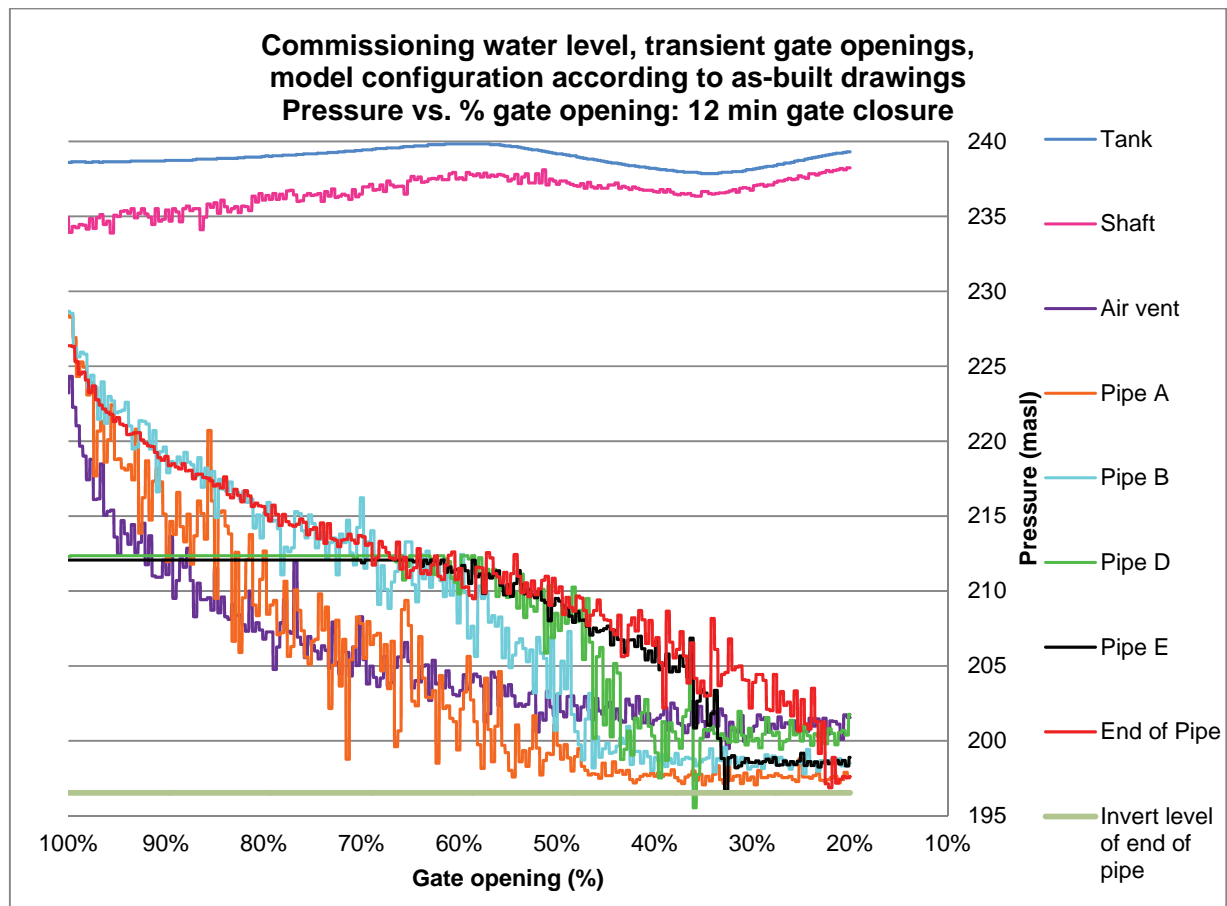


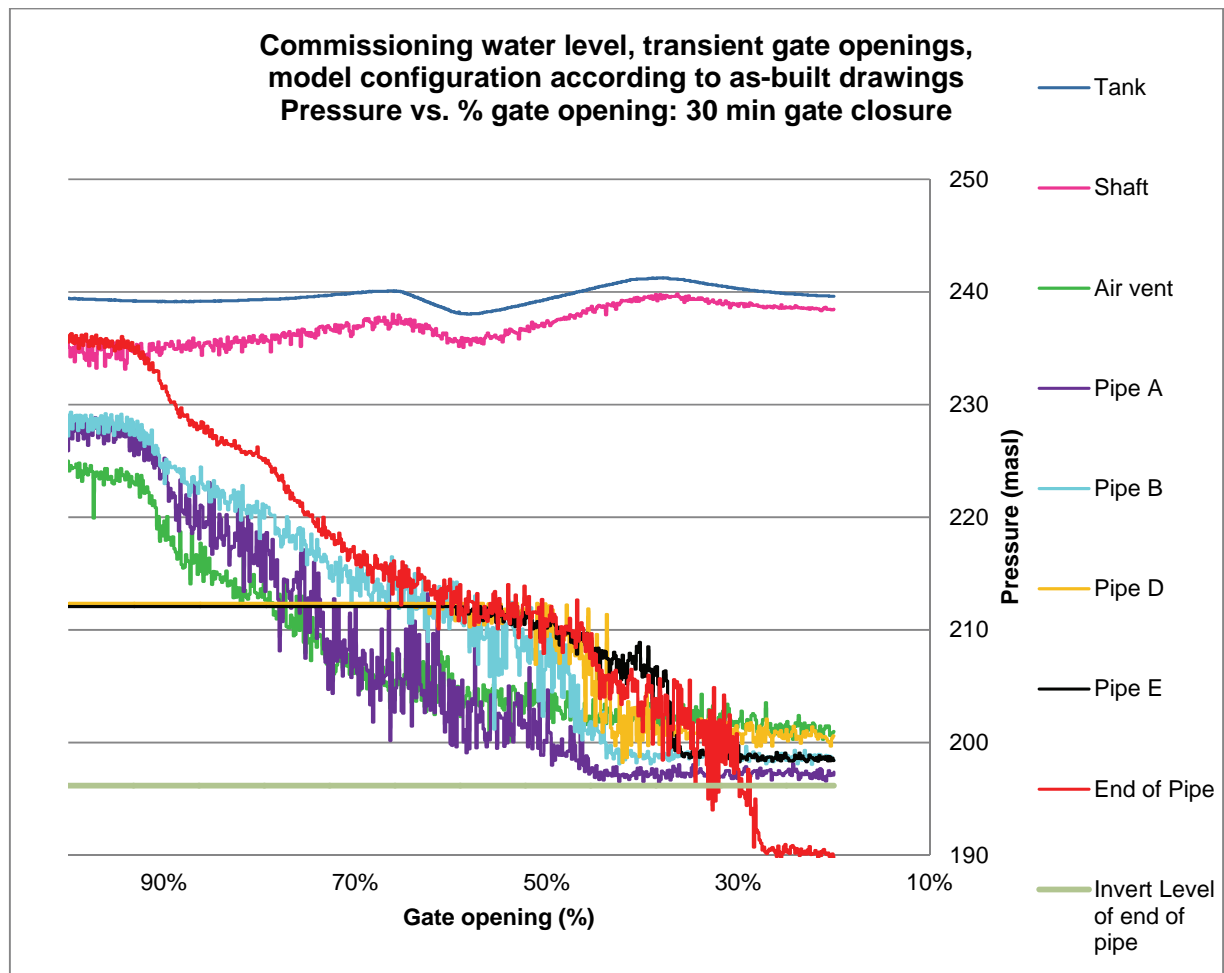


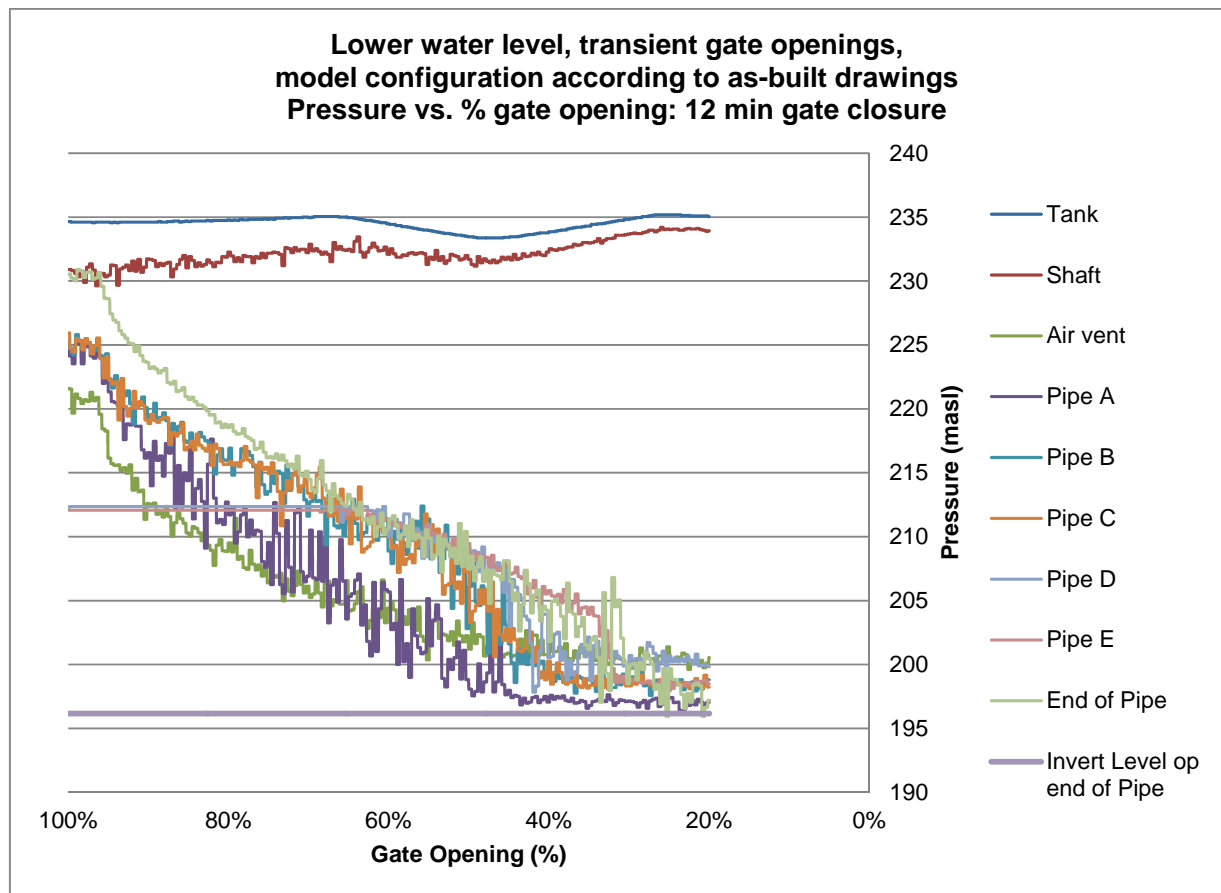


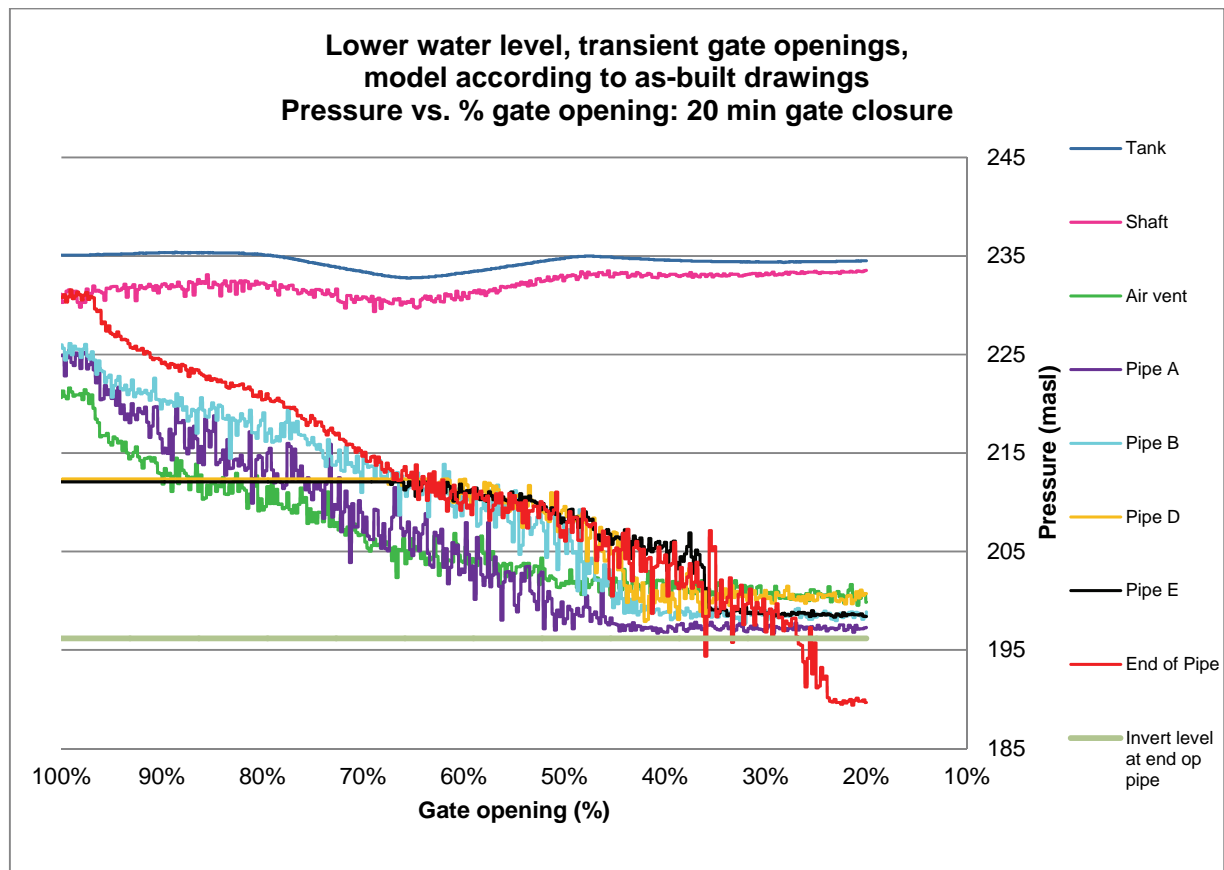
## APPENDIX E2: Pressures – Closing Gate Simulations; Commissioning Water Level; As-Built

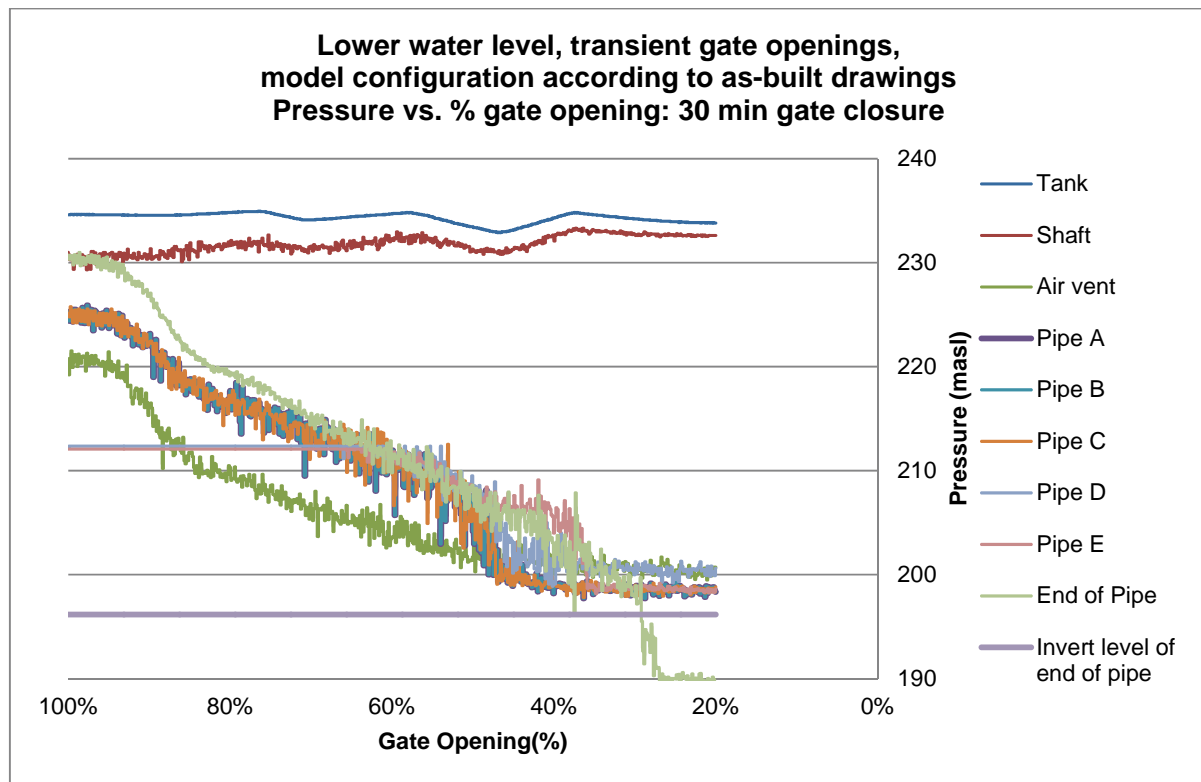




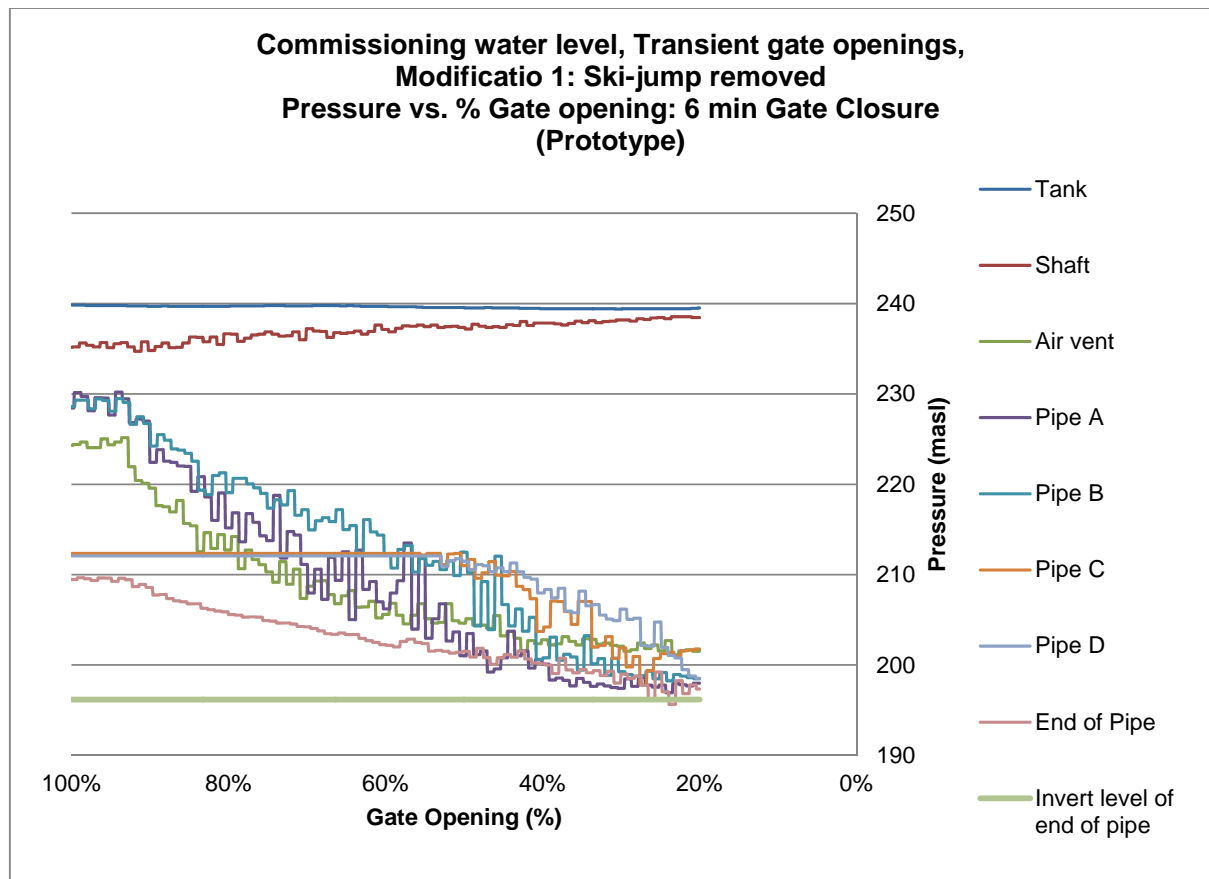


**APPENDIX E3: Pressures – Closing Gate Simulations; Lower Water Level; As-Built**



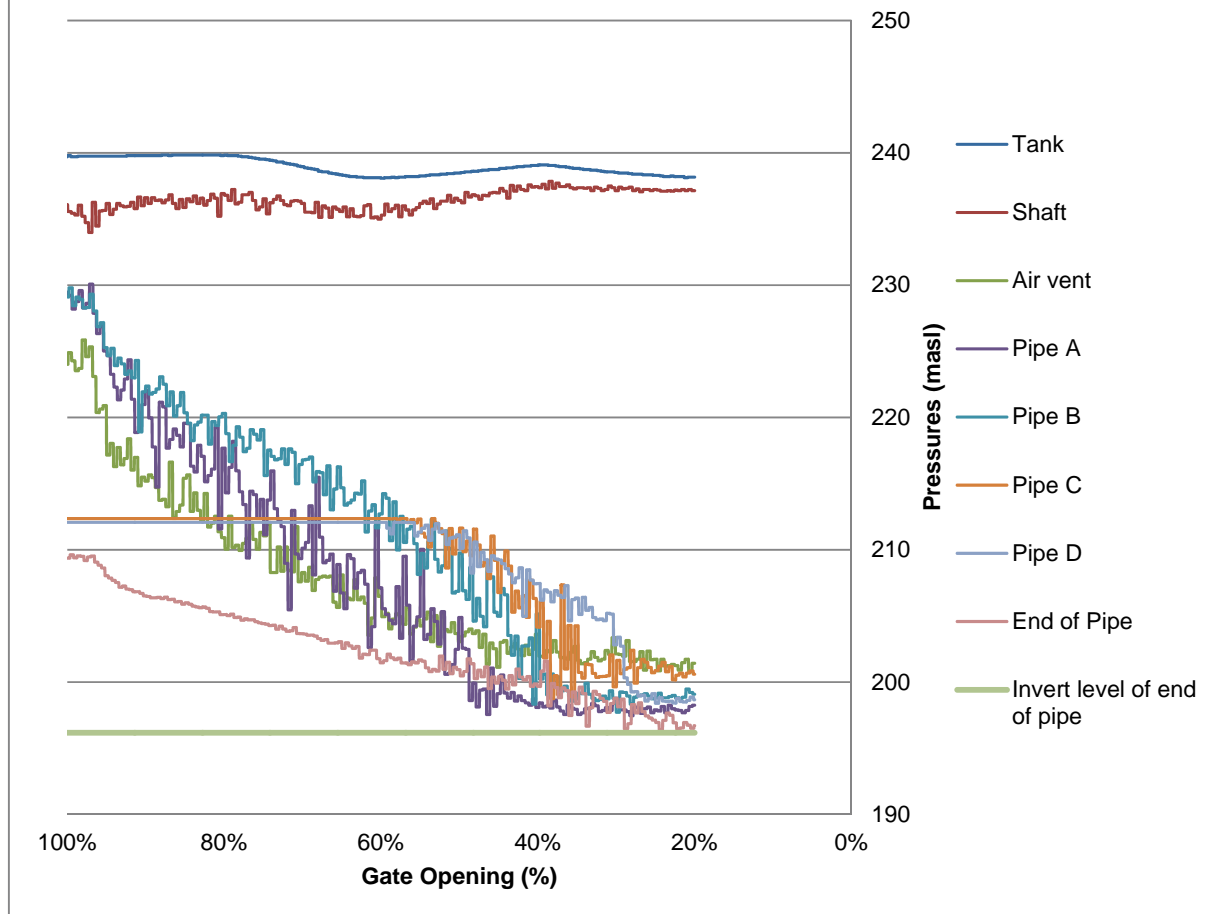


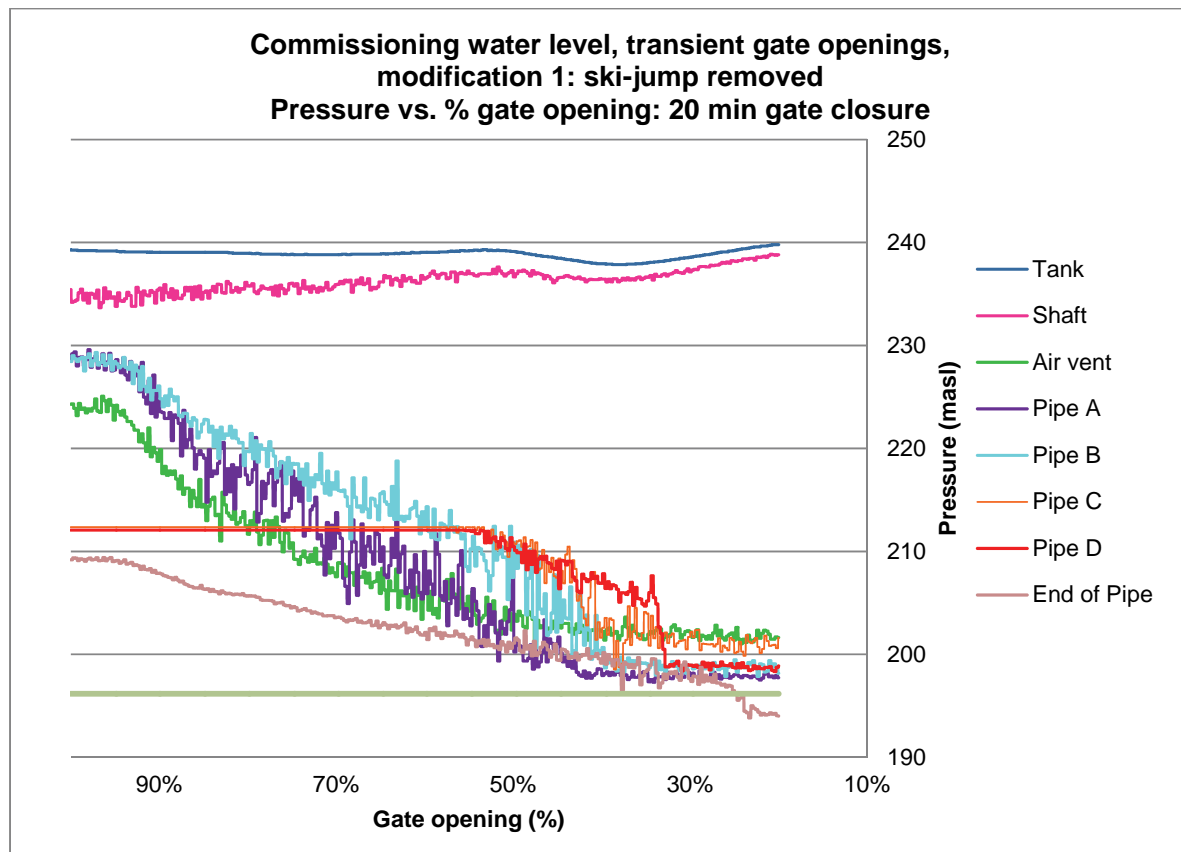
## APPENDIX E4: Pressures – Closing Gate Simulations; Commissioning Water Level; Modification 1

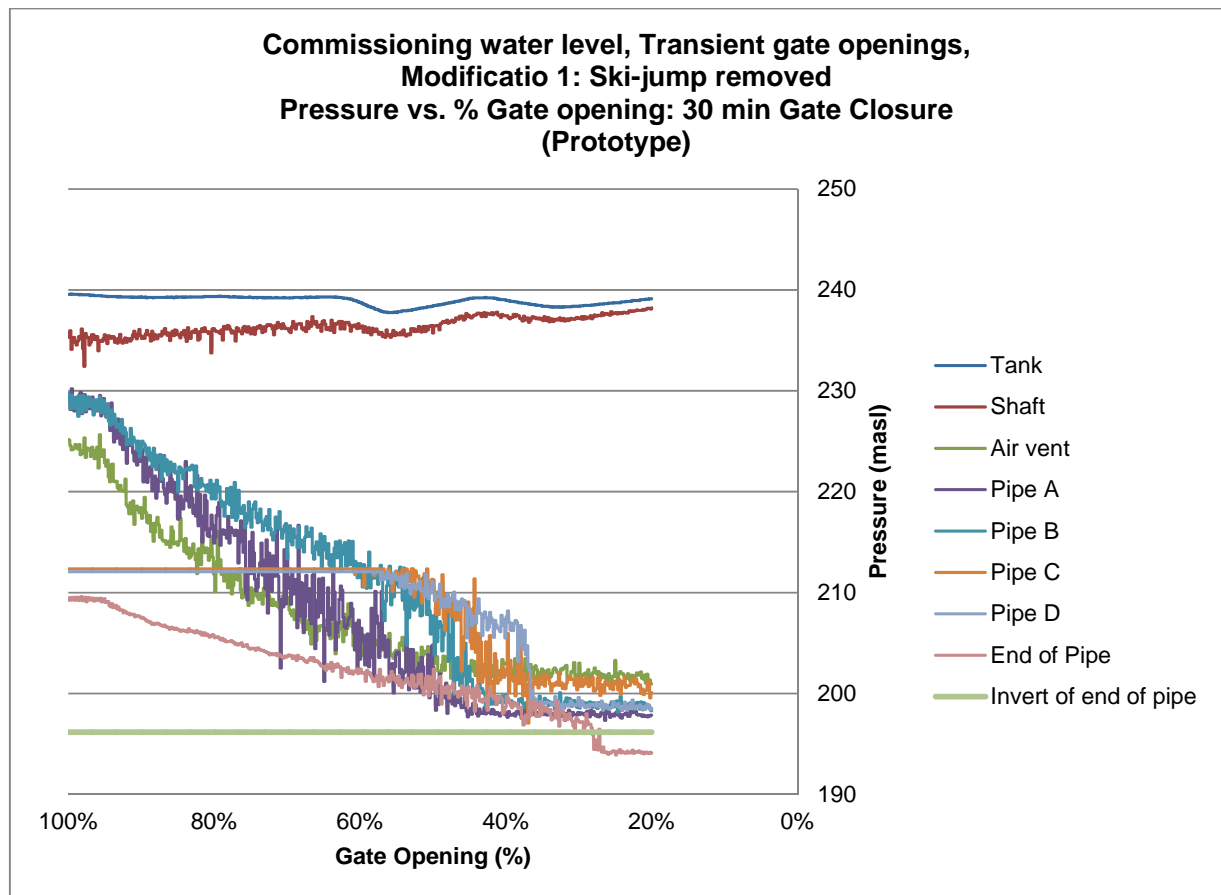




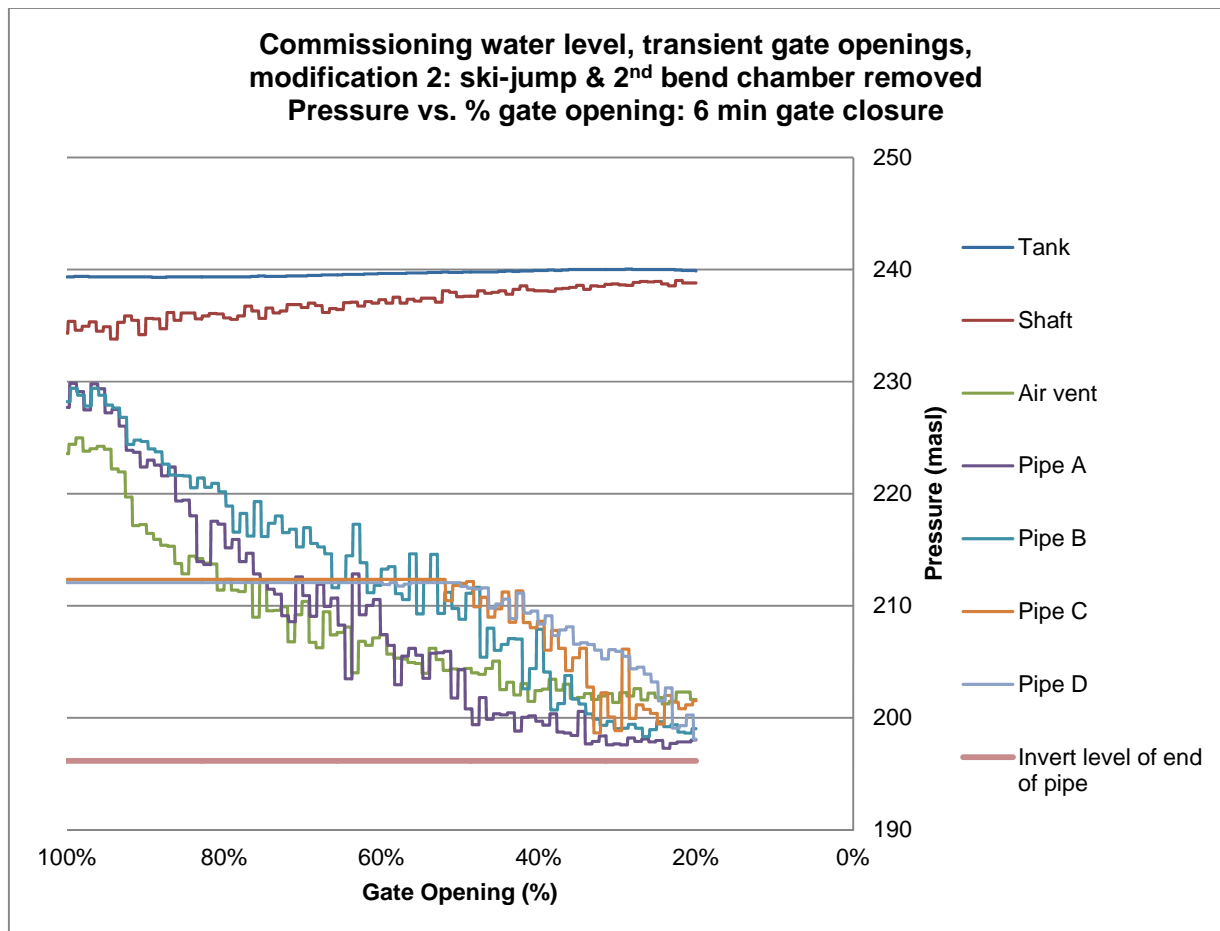
**Commissioning water level, Transient gate openings,  
Modification 1: Ski-jump removed  
Pressure vs. % Gate opening: 12 min Gate Closure  
(Prototype)**

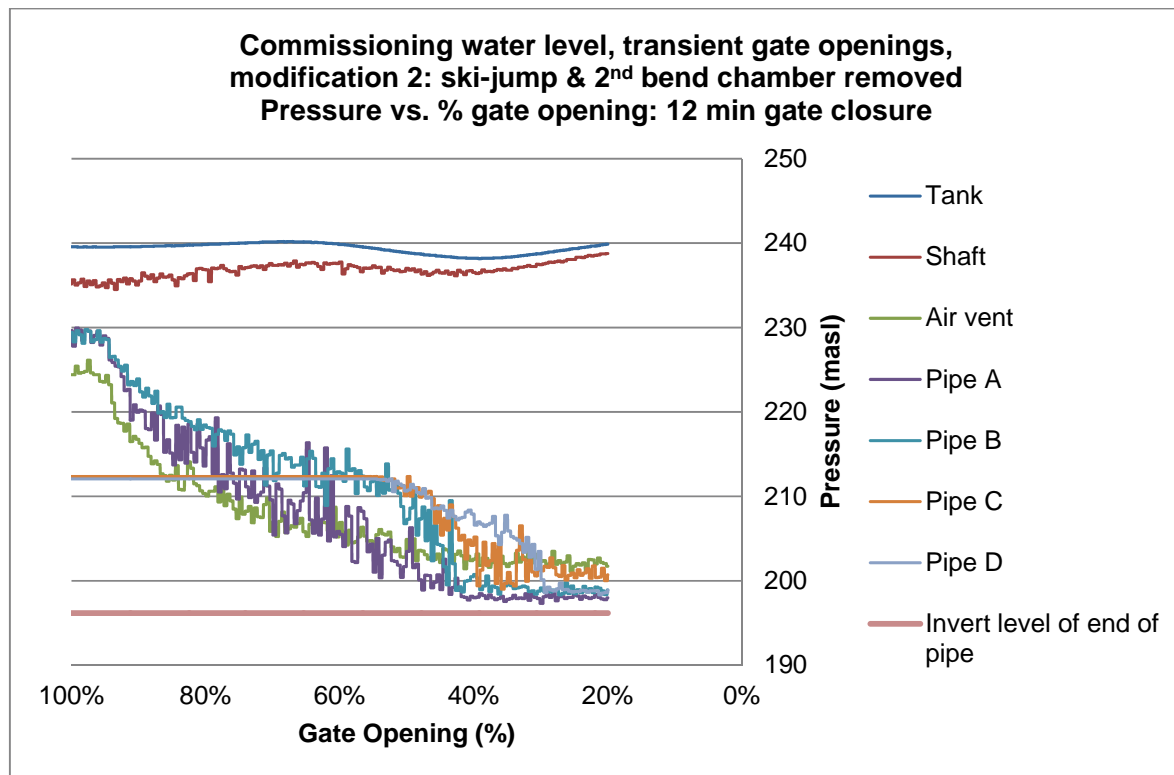


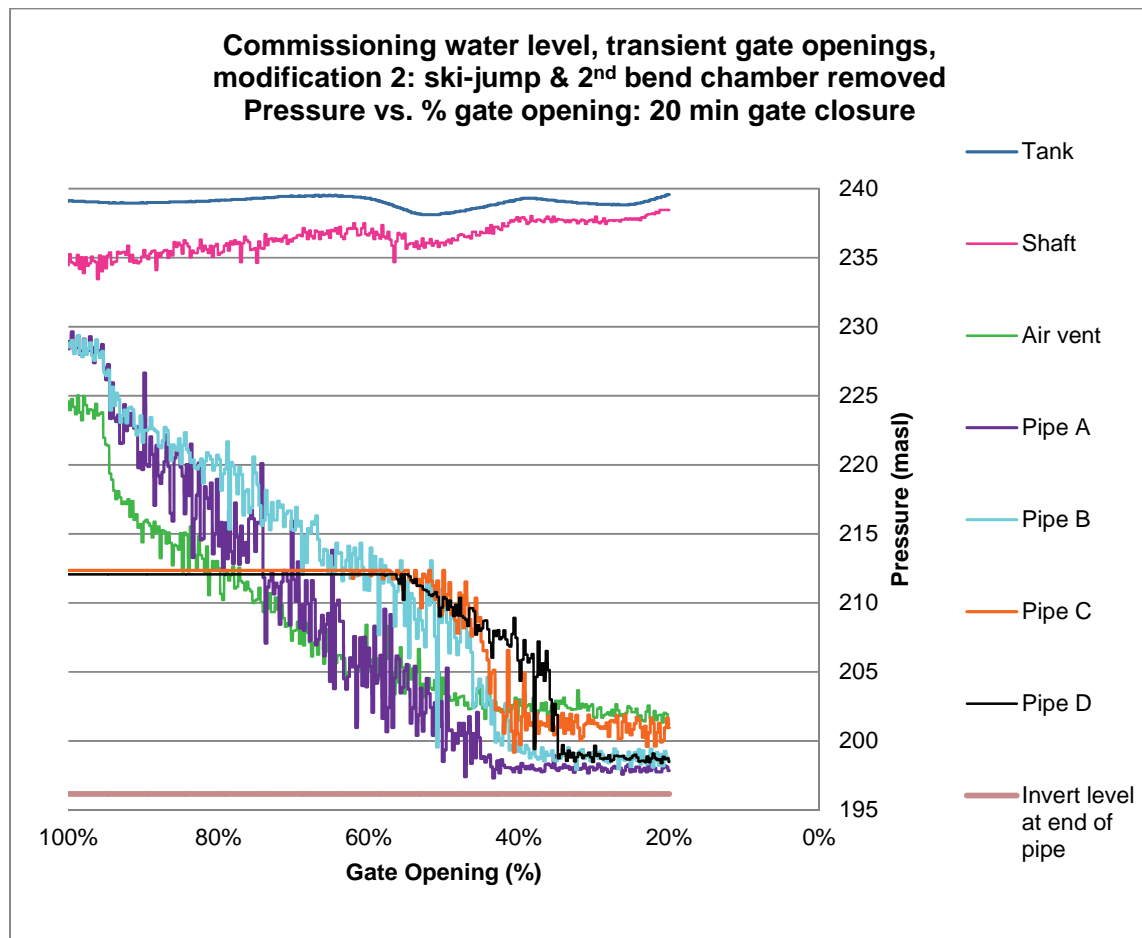


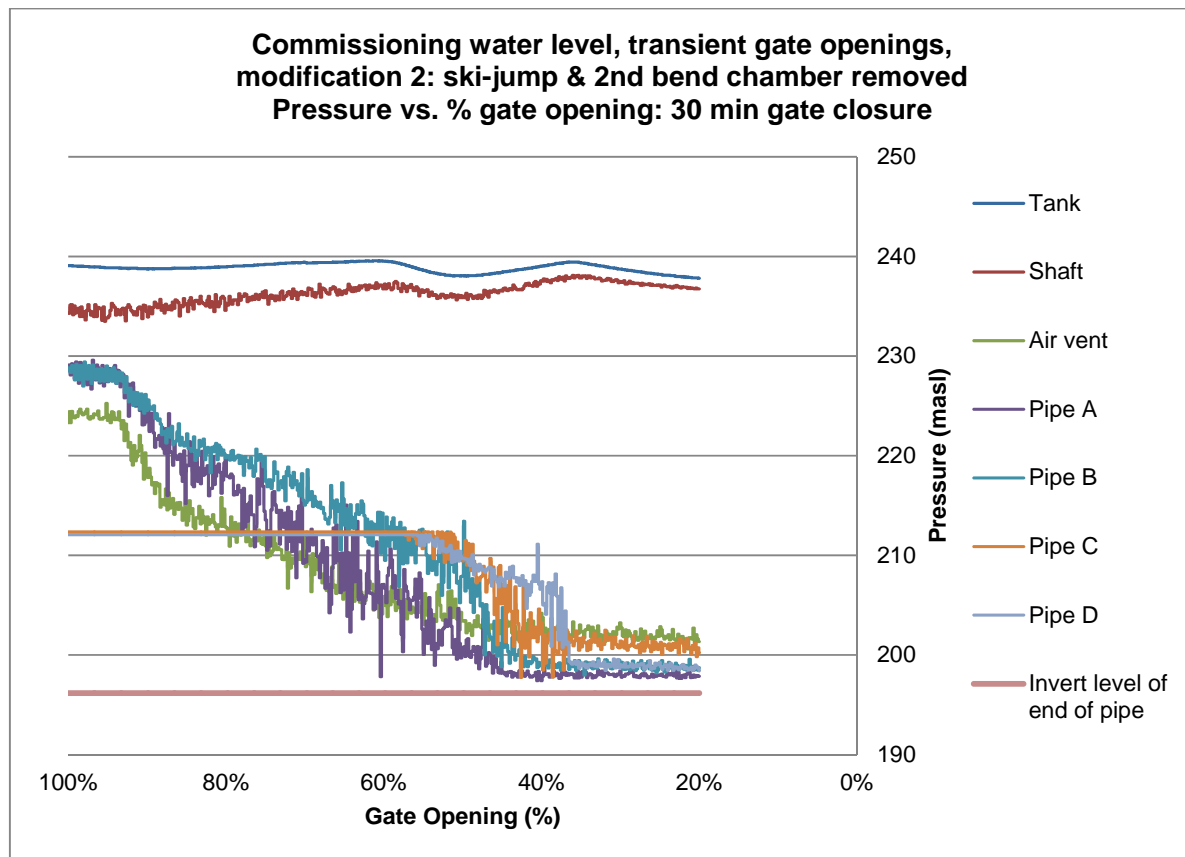


## APPENDIX E5: Pressures – Closing Gate Simulations; Commissioning Water Level; Modification 2



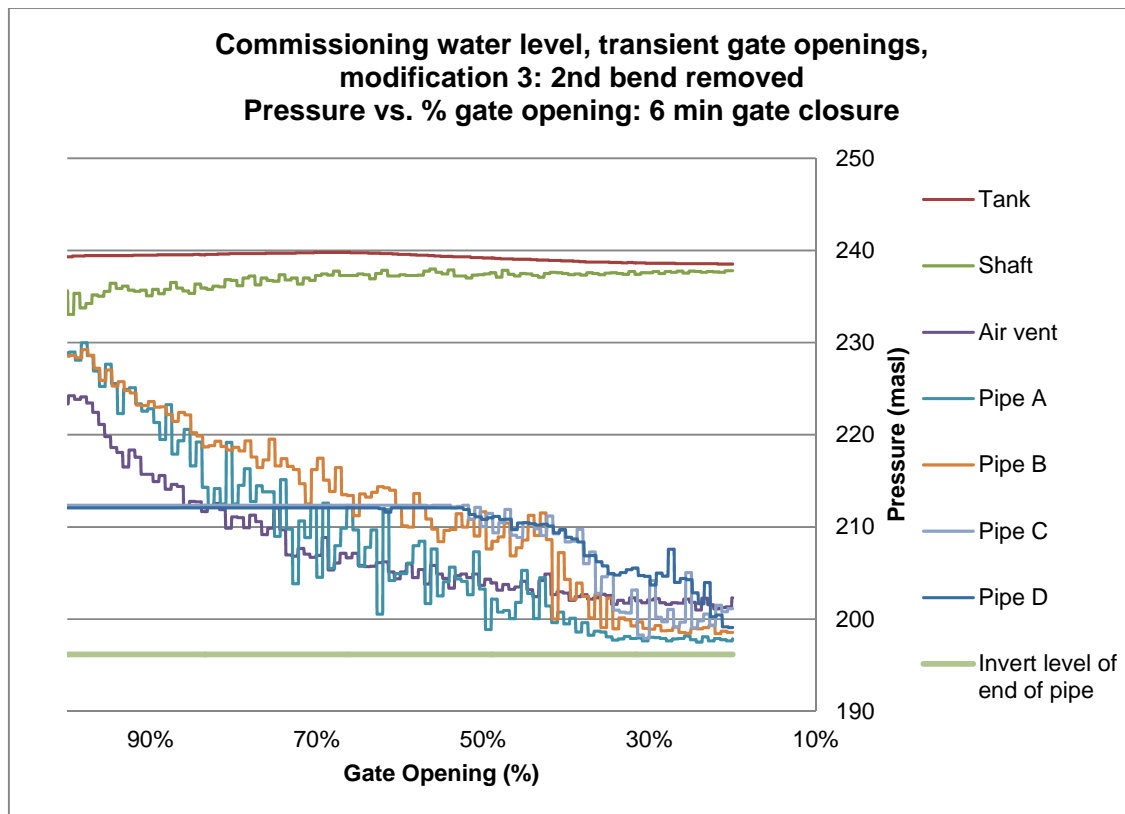


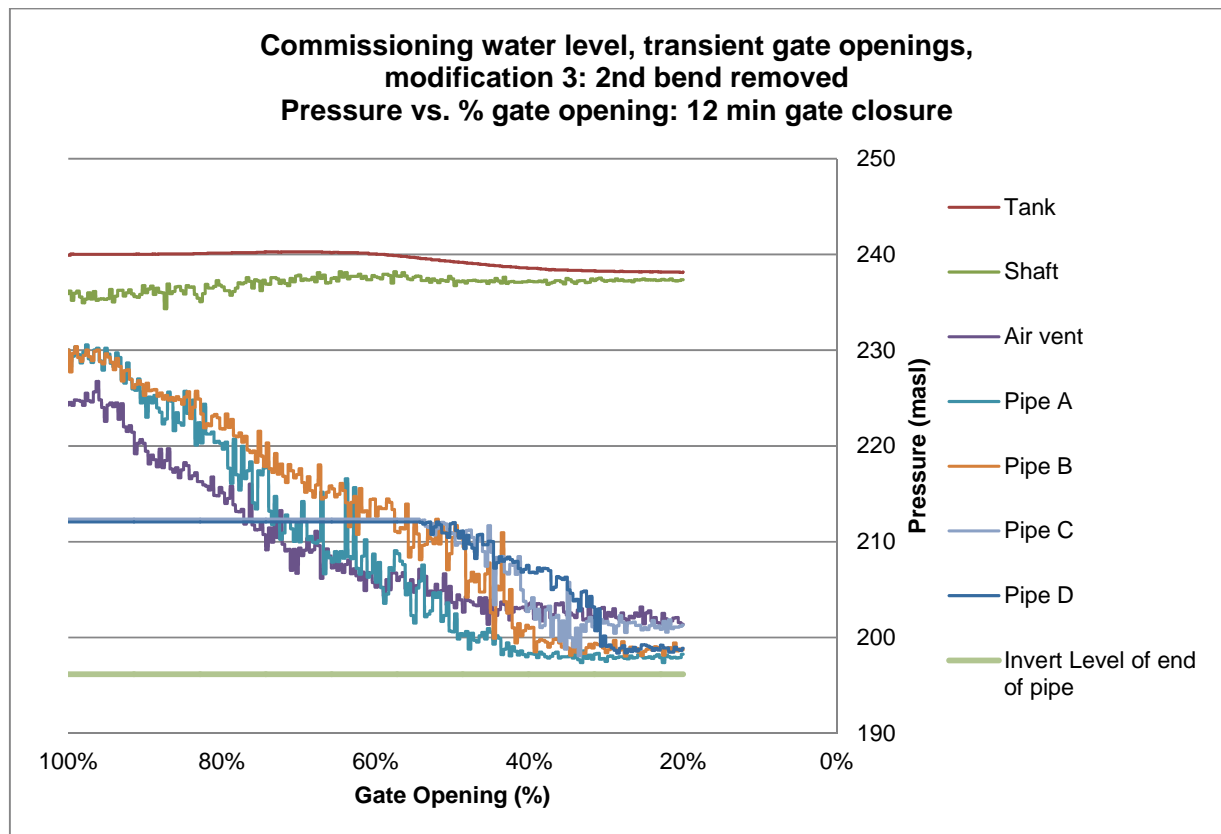


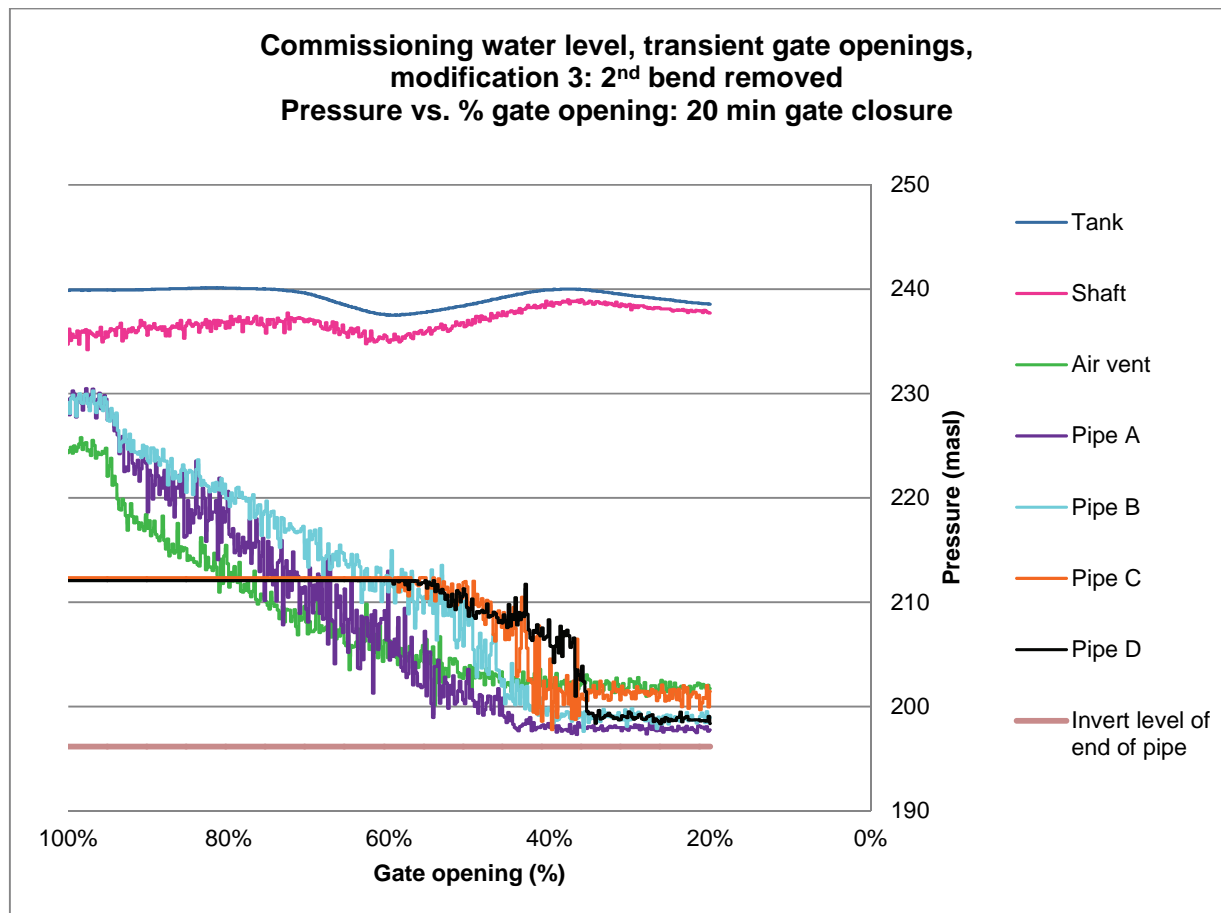


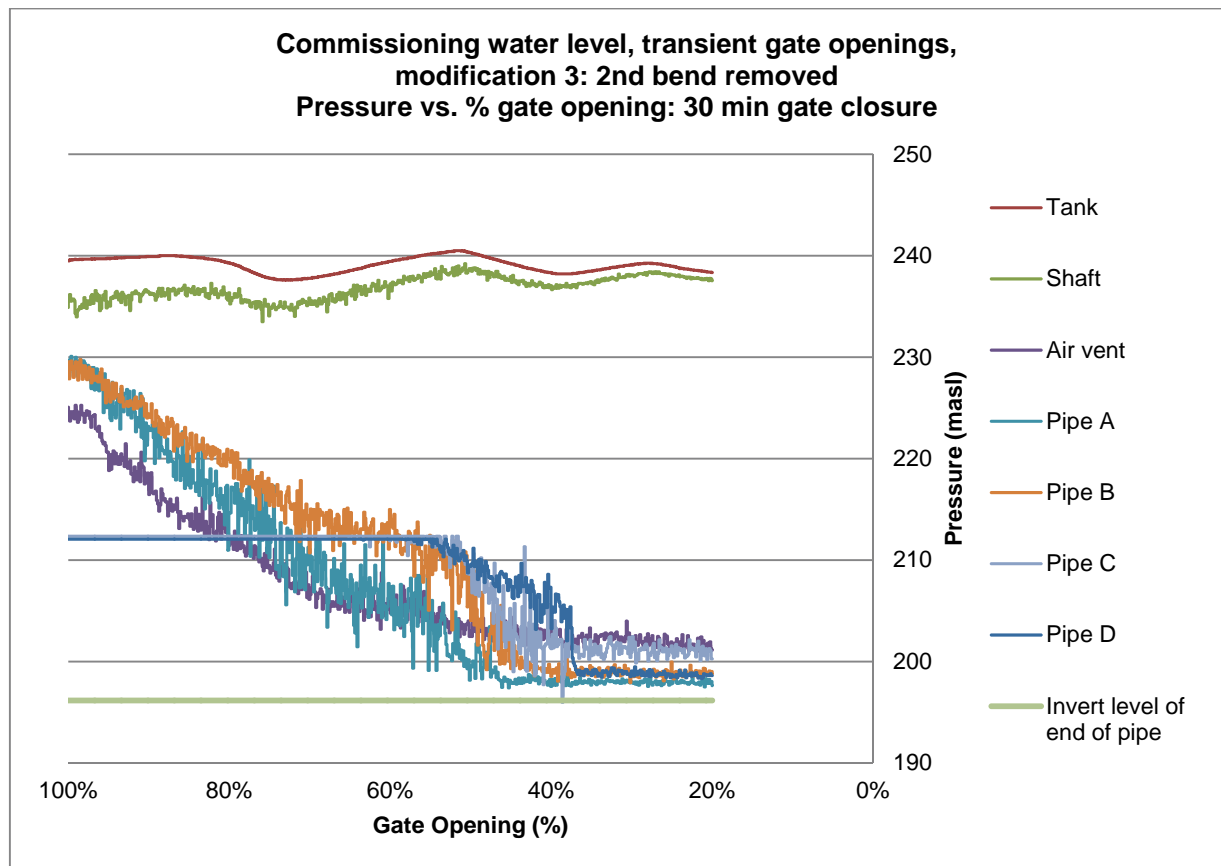


## APPENDIX E6: Pressures – Closing Gate Simulations; Commissioning Water Level; Modification 3

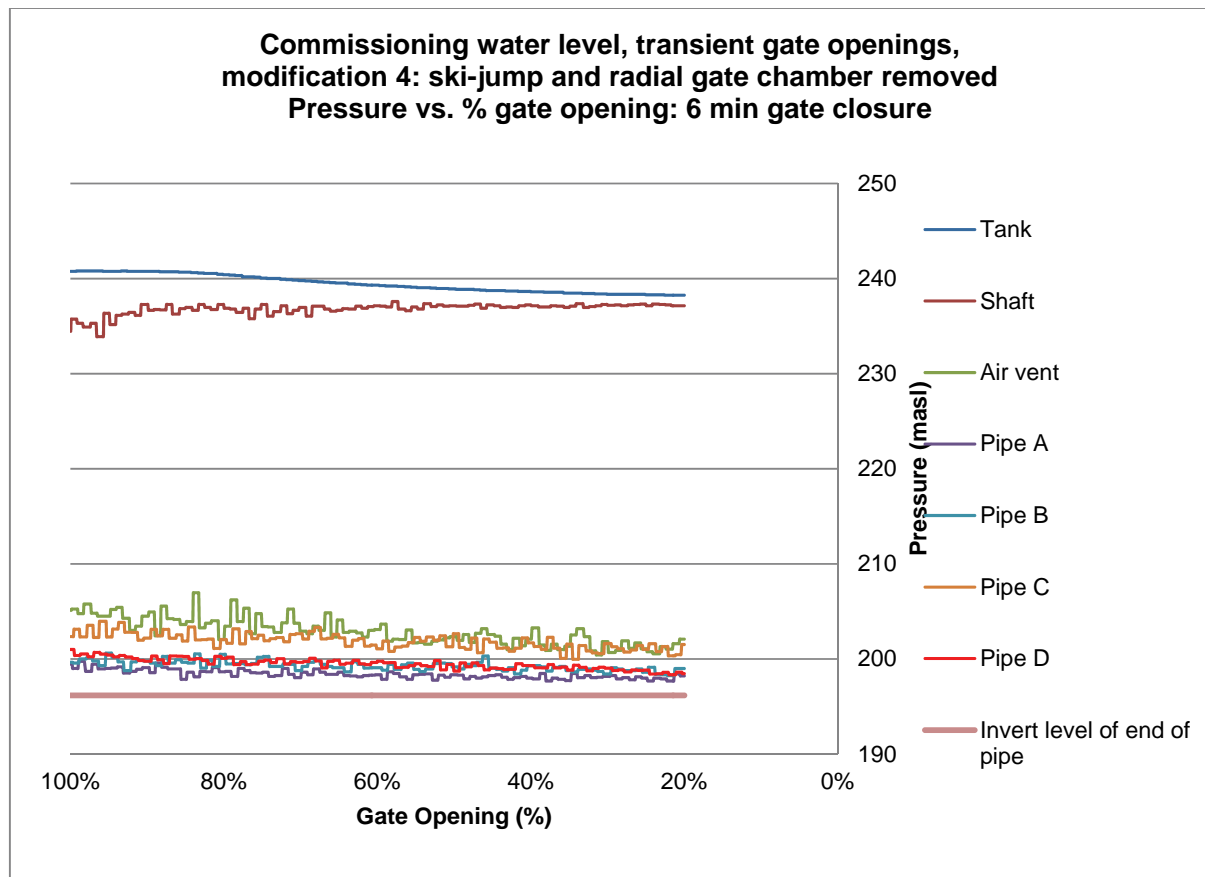


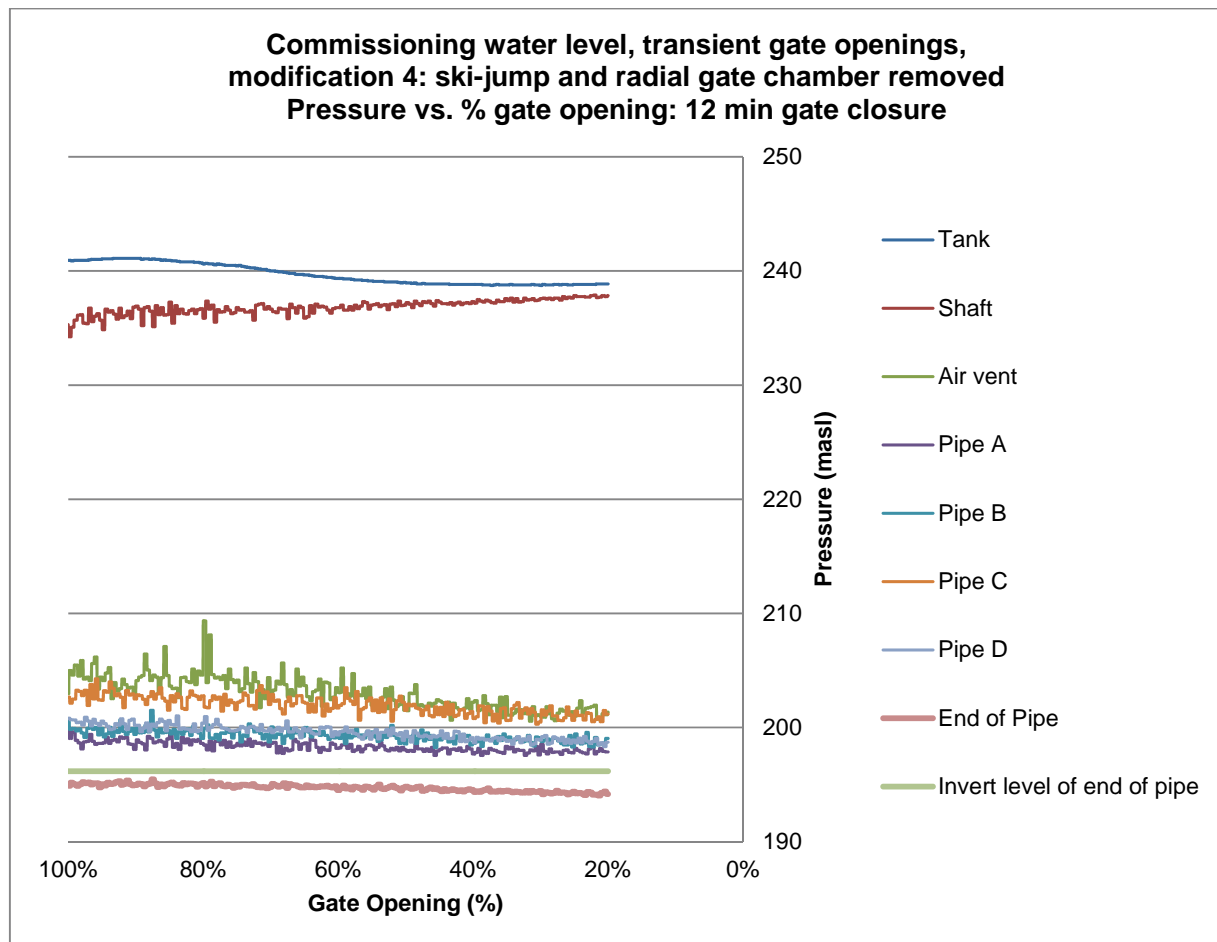


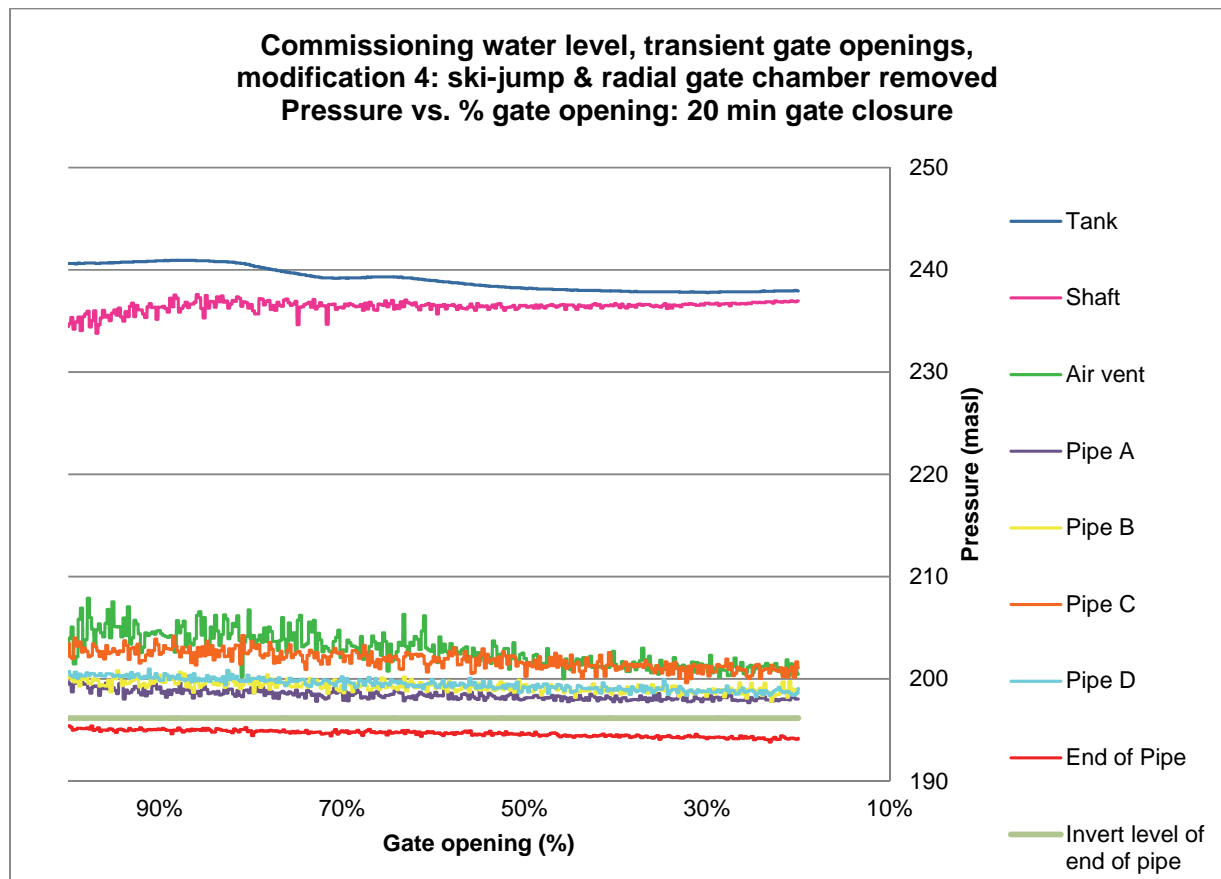


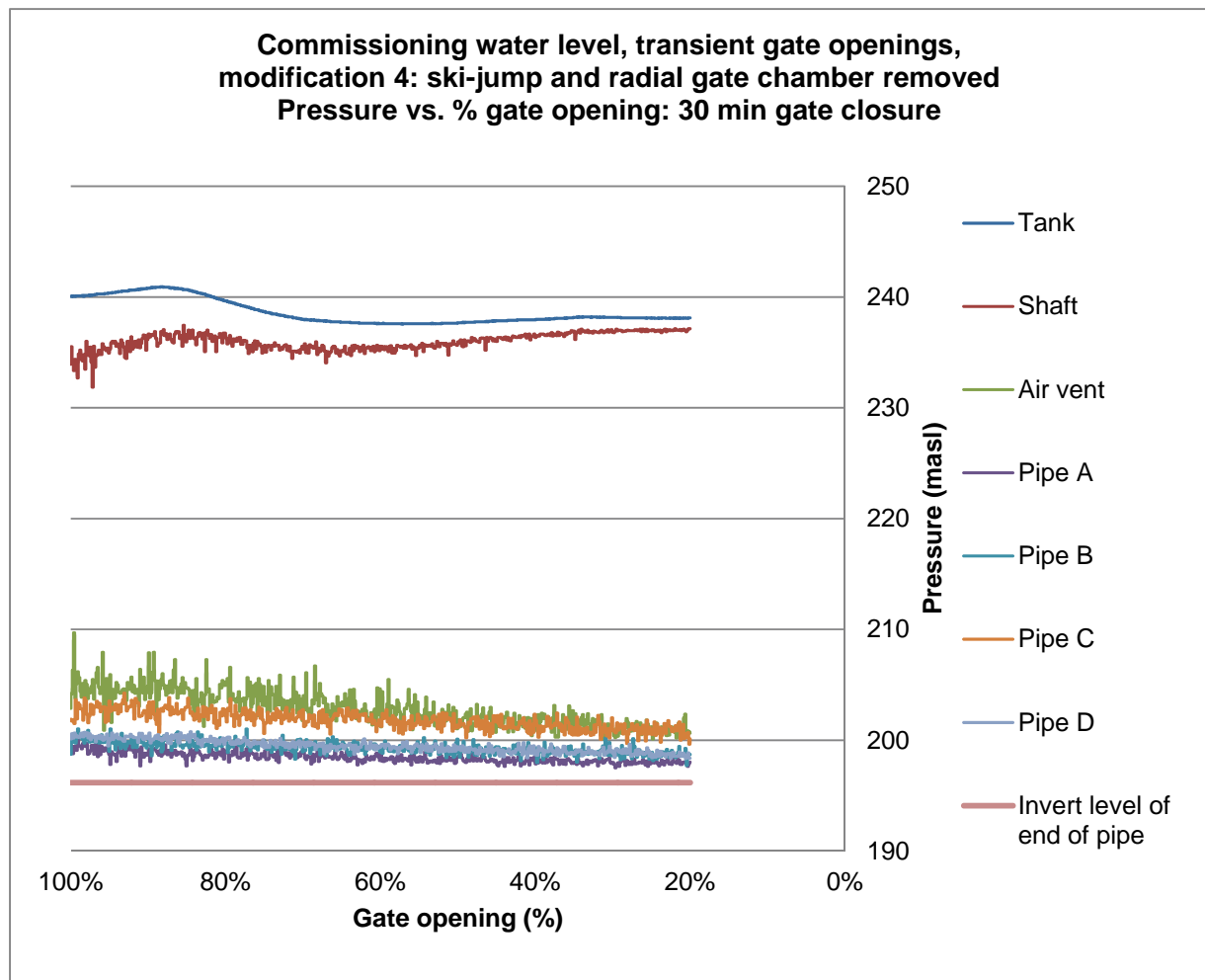


## APPENDIX E7: Pressures – Closing Gate Simulations; Commissioning Water Level; Modification 4











## APPENDIX F: STAGE DISCHARGE CURVE

Department of Water Affairs

HYRATAB V159 Output 26/10/2011

Site G1H077

Bergriver Dam W-Component

Rating Table 1.01

28/05/2008 to Present

Interpolation = Log CTF = 0.0000

Converting  
Into 101  
103Corrected Surface Water Level in Metres  
Uncorrected Surface Discharge in Cubic Metres/Second

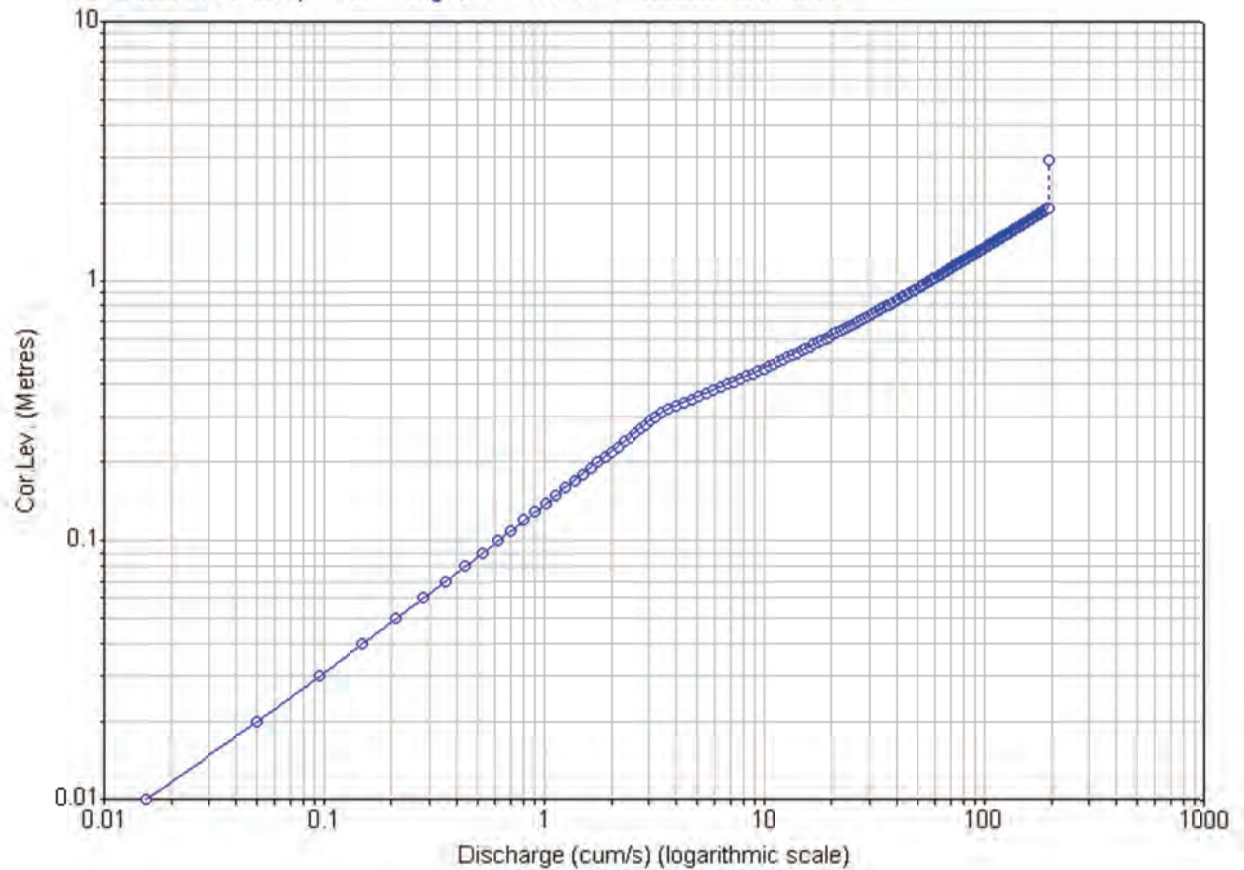
G. H.	0	0.01	0.02	0.03	0.04	0.05	0.06	0.07	0.08	0.09
0.00	0.0	0.0155	0.0497	0.0951	0.149	0.211	0.280	0.355	0.435	0.521
0.10	0.611	0.707	0.806	0.910	1.02	1.13	1.25	1.37	1.49	1.62
0.20	1.75	1.88	2.02	2.16	2.30	2.44	2.59	2.74	2.90	3.06
0.30	3.22	3.43	3.69	4.00	4.33	4.69	5.08	5.48	5.91	6.35
0.40	6.81	7.29	7.79	8.30	8.82	9.36	9.92	10.5	11.1	11.7
0.50	12.3	12.9	13.5	14.2	14.9	15.5	16.2	16.9	17.6	18.3
0.60	19.1	19.8	20.6	21.3	22.1	22.9	23.7	24.5	25.3	26.1
0.70	27.0	27.8	28.7	29.6	30.4	31.3	32.2	33.1	34.1	35.0
0.80	35.9	36.9	37.8	38.8	39.8	40.8	41.8	42.8	43.8	44.8
0.90	45.8	46.9	47.9	49.0	50.1	51.1	52.2	53.3	54.4	55.5
1.00	56.7	57.8	58.9	60.1	61.2	62.4	63.6	64.8	66.0	67.2
1.10	68.4	69.6	70.8	72.1	73.3	74.6	75.8	77.1	78.4	79.6
1.20	80.9	82.2	83.6	84.9	86.2	87.5	88.9	90.2	91.6	93.0
1.30	94.3	95.7	97.1	98.5	99.9	101	103	104	106	107
1.40	109	110	111	113	114	116	117	119	120	122
1.50	124	125	127	128	130	131	133	135	136	138
1.60	139	141	143	144	146	148	149	151	153	154
1.70	156	158	159	161	163	164	166	168	170	171
1.80	173	175	177	179	180	182	184	186	188	190
1.90	192	194	194A	194A	194A	194A	194A	194A	194A	194A
2.00	194A	194A	194A	194A	194A	194A	194A	194A	194A	194A
2.10	194A	194A	194A	194A	194A	194A	194A	194A	194A	194A
2.20	194A	194A	194A	194A	194A	194A	194A	194A	194A	194A
2.30	194A	194A	194A	194A	195A	195A	195A	195A	195A	195A
2.40	195A	195A	195A	195A	195A	195A	195A	195A	195A	195A
2.50	195A	195A	195A	195A	195A	195A	195A	195A	195A	195A
2.60	195A	195A	195A	195A	195A	195A	195A	195A	195A	195A
2.70	195A	195A	195A	195A	195A	195A	195A	195A	195A	195A
2.80	195A	195A	195A	195A	195A	195A	195A	195A	195A	195A
2.90	195A	196A	196A							

----- Notes -----  
 All rated data has been coded as reliable  
 except where the following tags are used...  
 A ... Above Rating

## Department of Water Affairs

HYDRAS V159 01/12/2011

Site G1H077 Bergriver Dam W-Component  
VarFrom 101 Corrected Surface Water Level in Metres  
VarTo 103 Uncorrected Surface Discharge in Cubic Metres/Second  
Table 1.01 Interpolation = Log CTF = 0.0000 28/05/2008 to Present



## ***APPENDIX G: EXTRA TEST RESULTS***

On 9 February 2012 an extra set of tests were performed on modifications of the Berg River Dam to determine:

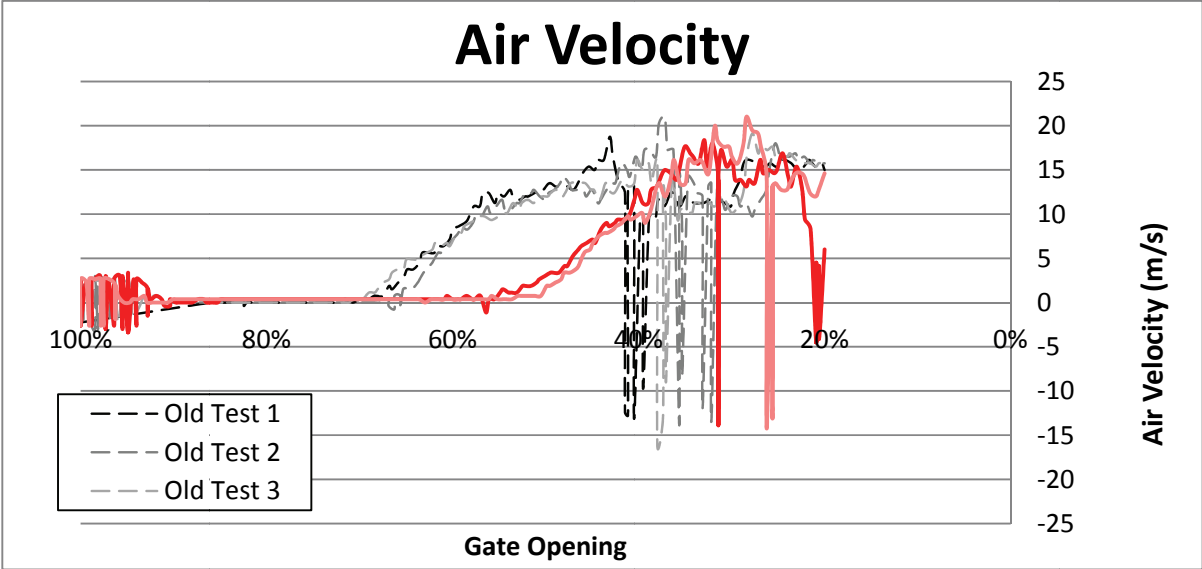
1. Whether the flow behaviour would be affected if the radial gate was closed to restrict the maximum outflow to 204 m<sup>3</sup>/s (as opposed to fully open as for the rest of the tests).
2. Whether vortices could form at the commissioning level if the water was stirred, and what would happen if the gate was closed with vortices upstream of the gate.
3. If the provision of an extra pipe, 450 mm in diameter, at the constriction in the radial gate chamber would reduce blowback in the airshaft.

These tests are presented in turn below. Videos and photos taken during these tests are available on request.

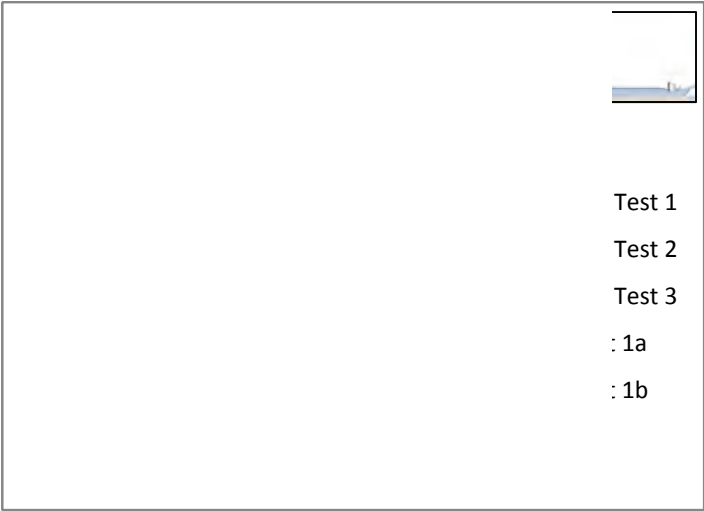








Results:

The air velocity and pressure results are show below, compared to the as-built configuration (“old tests”).



Pressures



<div></div> <div>Test 1 Test 2 Test 3 : 1a : 1b</div>	<div></div> <div>: 1 : 2 : 3</div>
<div></div> <div>Test 1 Test 2 Test 3 : 1a : 1b</div>	<div></div> <div>: 1 : 2 : 3</div>
<div></div> <div>Test 1 Test 2 Test 3 : 1a : 1b</div>	<div></div> <div>t 1 t 2 t 3</div>

**Conclusions:**

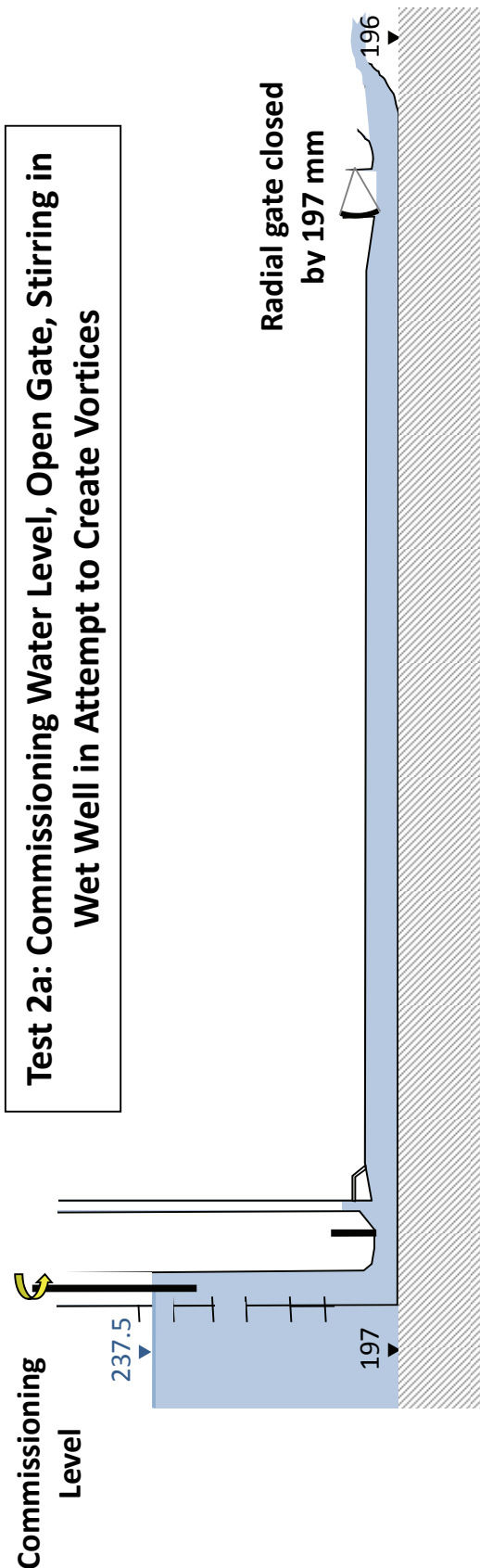
Air velocities are similar to those of the as-built tests, with blow back occurring slightly later.

Pressures are marginally higher than those of the as-built tests.

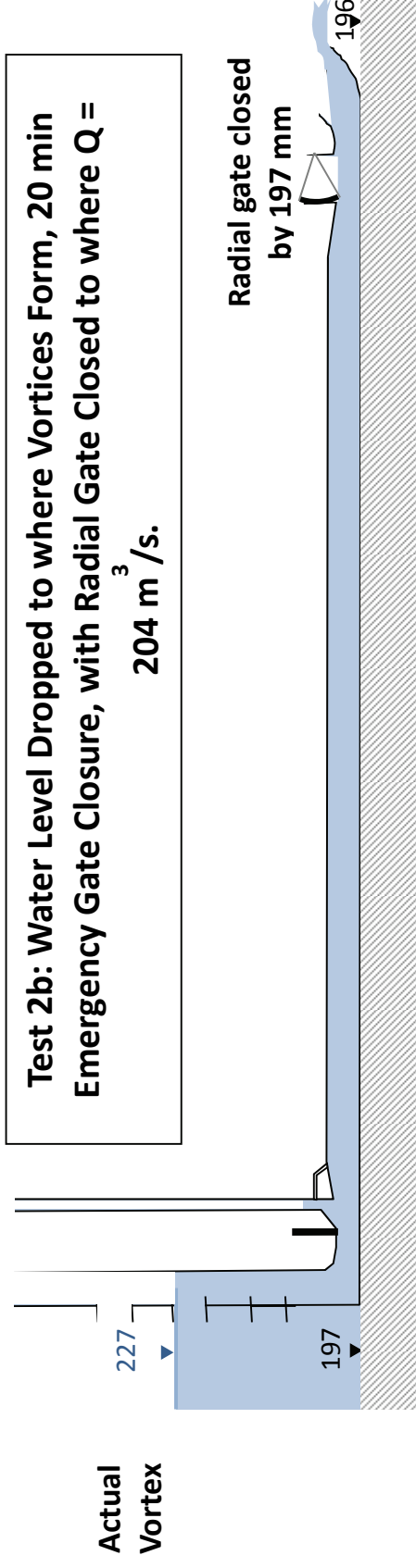
The slightly closed radial gate does not have a significant effect on the flow. Therefore, due to the time involved in moving the radial gate, the gate remained partially closed for the rest of the tests.

**Test 2: Vortex Formation Test**

Configuration:



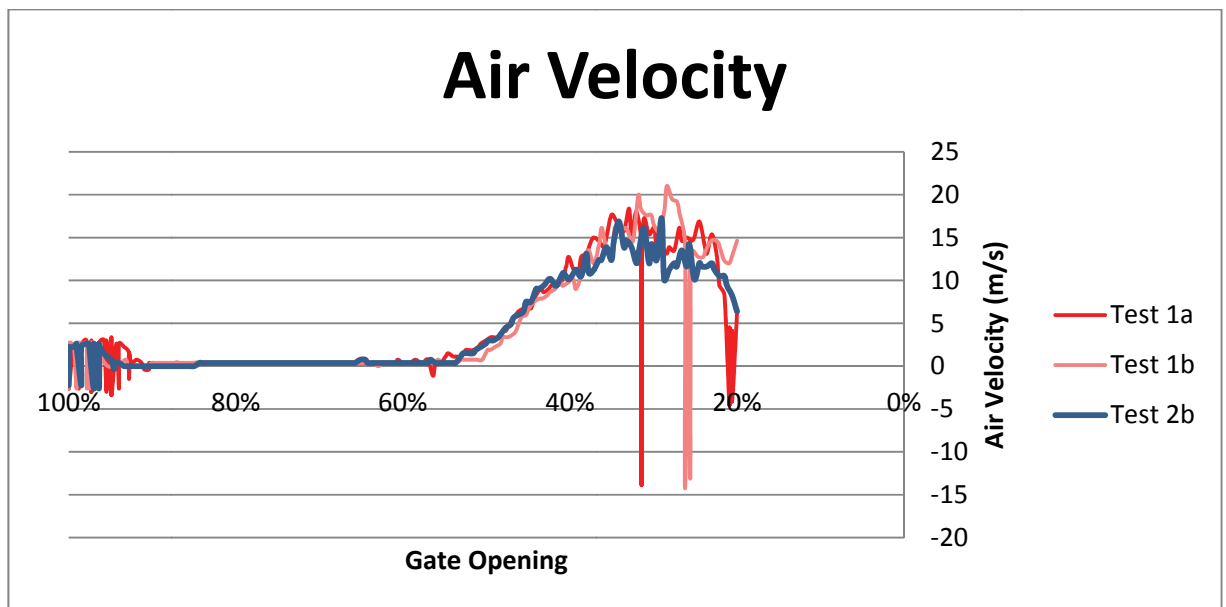




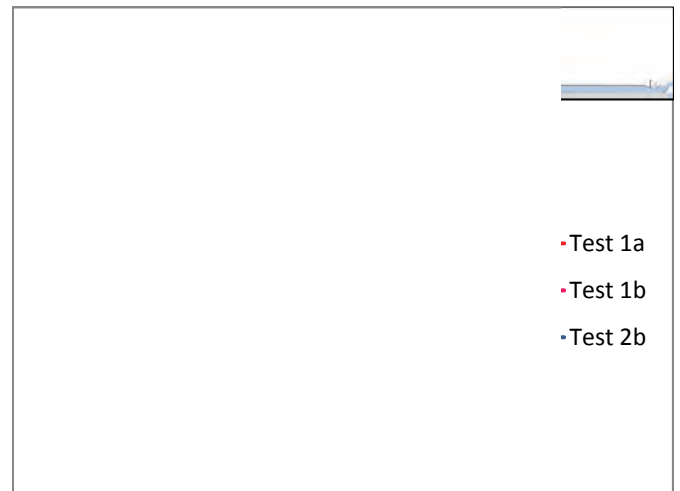
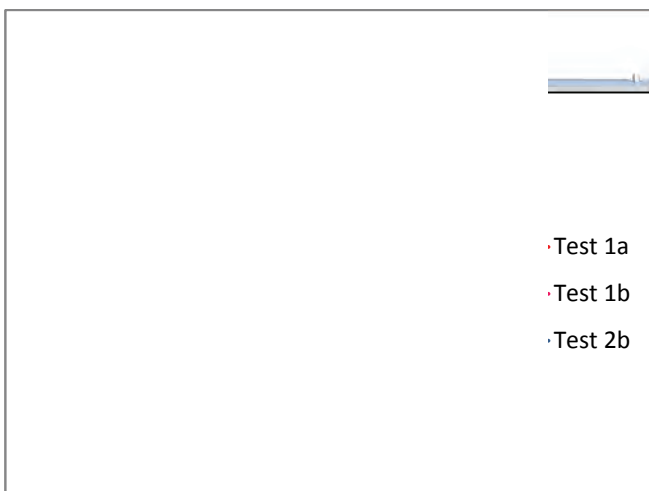
**Results:**

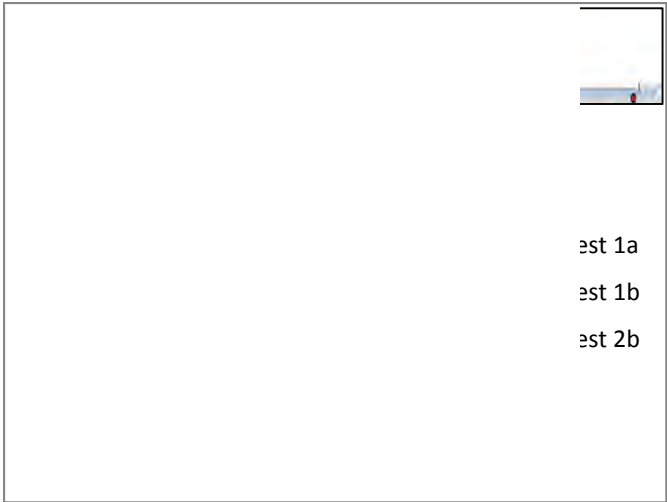
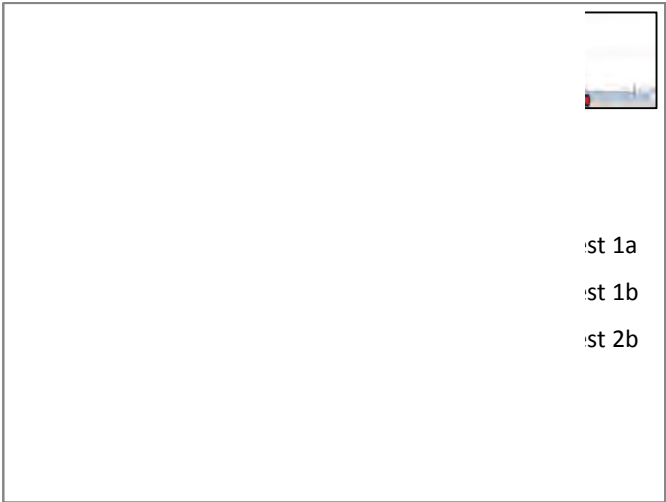
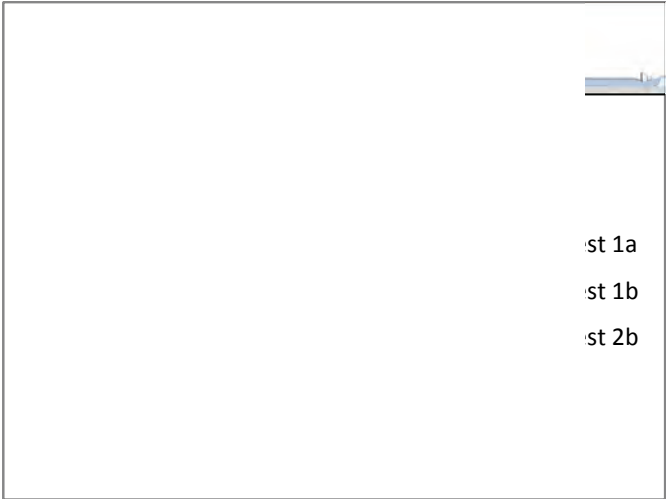
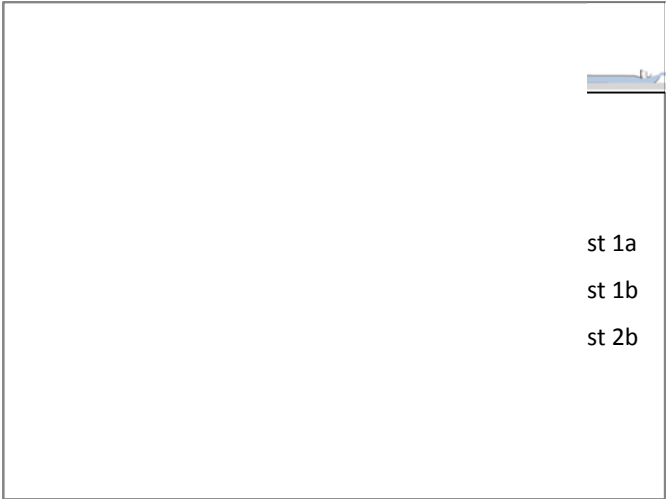
For Test 2a no vortices formed.

The air velocity and pressure results for Test 2b are shown below compared to those of Test 1.



### Pressures





**Conclusions:**

Vortices do not form at the commission level, even when the water is vigorously stirred.

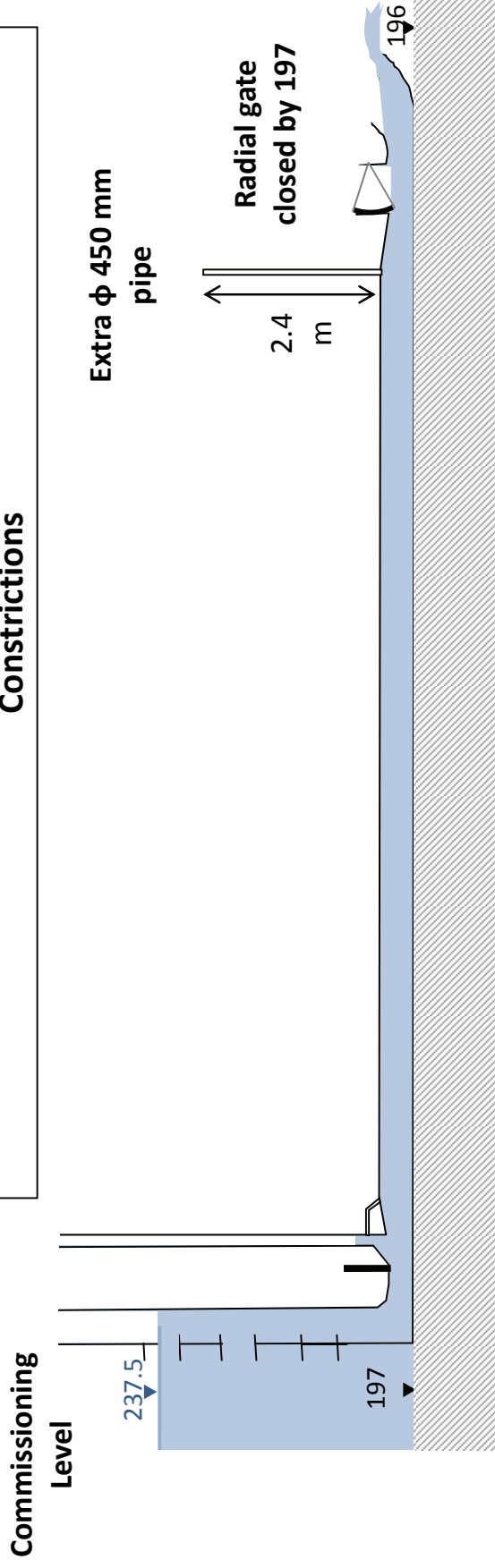
The vortex forming level is 227 masl, 10.5 m below the commissioning level.

When the gate is closed at the vortex forming level, the air is transported down the conduit and does not exit through the air shaft. For such a low water level, no blowback was observed.

### Test 3: Extra Air Vent

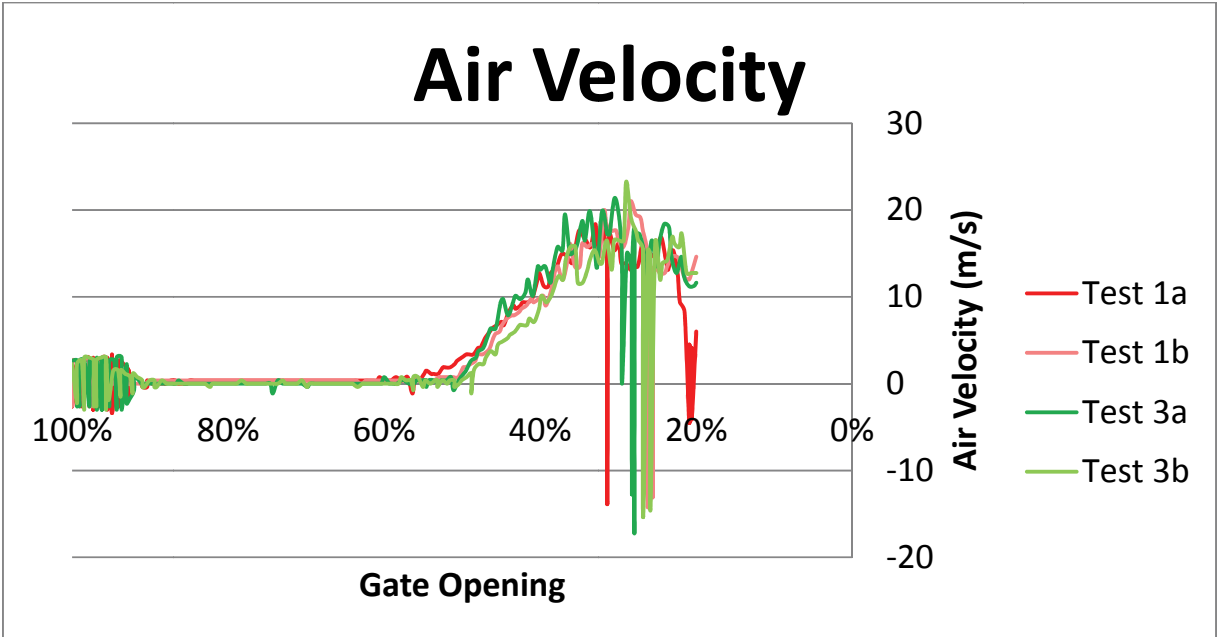
#### Configuration:

**Test 3: Commissioning Water Level, 20 min Emergency Gate Closure, with Radial Gate Closed to where  $Q = 204 \text{ m}^3/\text{s}$  & Extra Air Outlet Pipe before Constrictions**

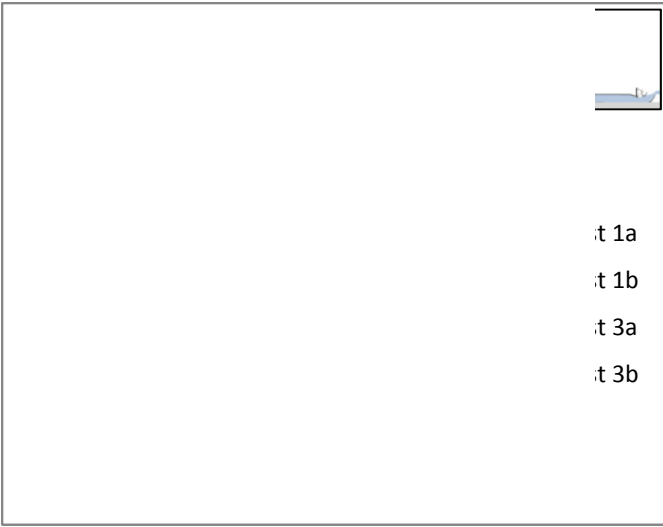


#### Results:

The air velocity and pressure results for 2 tests on this configuration are shown below compared to the results of Test 1 (same configuration without the extra vent).




Pressures






est 1a  
est 1b  
est 3a  
est 3b




t 1a  
t 1b  
t 3a  
t 3b



est 1a  
est 1b  
est 3a  
est 3b



: 1a  
: 1b  
: 3a  
: 3b



est 1a  
est 1b  
est 3a  
est 3b



: 1a  
: 1b  
: 3a  
: 3b

**Conclusions:**

The air velocities and pressures recorded for the tests with the extra air vent are almost identical to those on the same configuration without it.

The extra air vent is ineffective at reducing the blowback in the air shaft.